STUDIES ON THE ELECTRON ACCEPTORS OF ~~AN EPR INVESTIGATION INTO HIGHER PLANT~~ PHOTOSYSTEM TWO ~~ELECTRON ACCEPTORS~~

A Thesis submitted by

SIMON JOHN BOWDEN

For the degree of Doctor of Philosophy

Department of Biology
University College London

November 1991

ABSTRACT

The differences in temperature dependent behaviour and microwave power saturation characteristics between the g=1.9 and g=1.8 $Q_A^-Fe^{2+}$ signals are described. The dependence of these behaviourial differences on the presence or absence of bicarbonate is emphasised.

By studying the EPR signals of $Q_A^-Fe^{2+}$, $Q_A^-Fe^{2+}TBTQ^-$ and the oxidised non-haem iron *I* have found that detergent solubilisation of BBY PS2 preparations with the detergent OGP, at pH 6.0, results in loss of bicarbonate binding. New preparations, including a dodecylmaltoside prepared CP47, CP43, D1, D2, cytochrome b_{559} complex, are described which at pH 7.5 retain native bicarbonate binding. These preparations provide a new system for studies into the "bicarbonate effect" because bicarbonate depletion can now be achieved without displacement by another anion.

The new OGP particles have been used to investigate both the split pheophytin signal and the two step redox titration phenomenon associated with this signal. The low potential step of the titration was concluded to be independent of the Q_A/Q_A^- mid-point potential but was found to be linked to the ability to photoreduce pheophytin; once the low potential component, suggested here to be the fluorescence quencher Q_L, was reduced, pheophytin photoreduction increased. A model is described to explain the two step titration and, from analysis of the signal splitting in +/- HCO_3^- samples, a possible structural role for bicarbonate is proposed.

I have probed the structure of the PS2 electron acceptor region with the protease trypsin. The Q_A iron-semiquinone, oxidised non-haem iron and cytochrome b_{559} EPR signals were all found to be susceptible to trypsin damage, while oxygen evolution with ferricyanide was enhanced by protease treatment. The protective effect of calcium ions against trypsin damage was demonstrated and a possible Ca^{2+} binding site in the Q_A binding region identified.

ACKNOWLEDGEMENTS

Firstly I would like to thank my supervisor Dr Jonathan Nugent for his considerable help and guidance through the highs and inevitable lows of postgraduate research. Thanks also to Professor Mike Evans for his help with all things computer related.

I express my appreciation for the friendship extended to me by all past and present members of the UCL photosynthesis group, particularly Andrew Corrie, Christopher Lockett, Ian Davis, Jonathan Hanley and also Fenton Beed.

Last, but of course not least, thanks to Andrea for EVERYTHING.

This work was funded by the U.K. Science and Engineering Research Council.

Table Of Contents

List Of Tables And Figures

ABBREVIATIONS

Arg	arginine
ATP	adenosine triphosphate
BBY	Berthold, Babcock and Yocum (1981) PS2 membrane preparation
(B)Chl	(bacterio)chlorophyll
CP	chlorophyll protein
DCBQ	2,5-dichloro-1,4-benzoquinone
DCMU	3-(3,4-dichlorophenyl)-1,1-dimethylurea
DM	n-dodecyl ß-D-maltoside
DMBQ	2,6-dimethylbenzoquinone
DMSO	dimethylsulphoxide
E_{mn}	mid-point potential at pH n
EPR	electron paramagnetic resonance
ESR	electron spin resonance
EXAFS	extended X-ray absorption fine structure
FCCP	carbonyl cyanide p-(trifluoromethoxy)phenylhydrazone
fs	femtosecond
Gln	glutamine
Hepes	4-(2-hydroxyethyl)-1-piperazineethanesulphonic acid
His	histidine
kDa	kilodaltons
Leu	leucine
LHC	light harvesting complex
Mes	2-(N-morpholino)-ethanesulphonic acid
mT	millitesla
NAD^+	nicotinamide adenine dinucleotide

$NADP^+$	nicotinamide adenine dinucleotide phosphate
OEC	oxygen evolving complex
OGP	n-octyl ß-D-glucopyranoside
OTP	n-octyl ß-D-thioglucopyranoside
o-phen	1,10-phenanthroline
PAGE	polyacrylamide gel electrophoresis
p-BQ	p-benzoquinone
PEG	poly(ethylene glycol)
(B)Ph	(bacterio)pheophytin
PQ	plastoquinone
ps	picosecond
PS1	photosystem one
PS2	photosystem two
Q_A	primary quinone electron acceptor
Q_B	secondary quinone electron acceptor
Q_H	high potential fluorescence quencher (Q_A)
Q_L	low potential fluorescence quencher
RC	reaction centre
SDS	sodium dodecyl sulphate
TBTQ	(tribromotoluquinone) 2,3,5-tribromo-6-methyl 1,4-benzoquinone
TEMED	tetramethylenediamine
Tris	tris-(hydroxymethyl)-aminomethane
Triton	octyl phenoxy poly(oxyethanol)
Trp	tryptophan
Tyr	tyrosine

1.0 INTRODUCTION

1.1 Photosynthesis

All organisms require energy and those organisms which developed a way of generating chemical energy from light energy had a clear advantage in the evolution of life. The production of chemical energy from light is called photosynthesis and provides energy without the oxidation of valuable organic compounds. Refinements to the system have led to the storage of reducing potential to fix carbon dioxide, thereby also removing the need for an organic source of carbon for biosynthesis. Most photosynthetic organisms can in fact lead a wholly photoautotrophic lifestyle and only certain types of photosynthetic bacteria remain photoheterotrophic.

The light driven reactions at the heart of photosynthesis are dependent on special pigments which absorb light in the region of 400-1000 nm. The most important pigments are the cyclic tetrapyrrole chlorophylls and bacteriochlorophylls. The four pyrrole nitrogen atoms are coordinated to a magnesium atom and in Chl a and b the molecule is made very hydrophobic by the esterification of phytol ($C_{20}H_{39}OH$) to one of the acid side chains (see Fig.1.1 for chlorophyll structure). When these pigments absorb electromagnetic radiation of the correct wavelength an electronically excited **singlet** state is induced in the molecule. The excitation energy can then be passed on to a neighbouring pigment molecule with high efficiency,

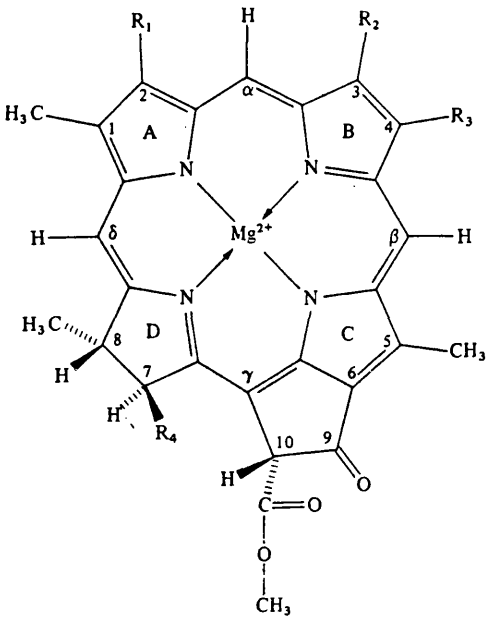

Textual No.	Chlorophyll Species	R_1	R_2	R_3	R_4	Loss of C-7 & C-8 hydrogens giving a 7,8 double bond
I	a	$-CH=CH_2$	$-CH_3$	$-CH_2CH_3$	X (see below)	No
II	b	$-CH=CH_2$	$-CHO$	$-CH_2CH_3$	X	No
III	c_1	$-CH=CH_2$	$-CH_3$	$-CH_2CH_3$	$-CH=CH.COOH$	Yes
IV	c_2	$-CH=CH_2$	$-CH_3$	$-CH=CH_2$	$-CH=CH.COOH$	Yes
V	d	$-CHO$	$-CH_3$	$-CH_2CH_3$	X	No

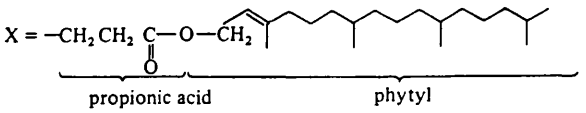

Figure 1.1 The cyclic tetrapyrrole structure of chlorophyll. The four nitrogen atoms of the pyrroles are coordinated to a magnesium atom making chlorophyll a magnesium porphyrin. These molecules are very efficient photoreceptors because of their polyene structure of alternating single and double bonds. [Diagram from Goodwin and Mercer: An Introduction To Plant Biochemistry, 2nd Edition, Pergamon Press]

through a radiation-less transfer dependent on the proximity and orientation of the two interacting molecules. The absorbance spectrum of the receiving pigment must have a certain degree of overlap with that of the donor molecule. During transfer, a small amount of energy is lost so that the light absorbed by the neighbour is of a slightly longer, less energetic, wavelength.

As an alternative to energy transfer the singlet state may undergo **photochemistry**. In the excited state the chlorophyll molecule (P^*) is a powerful reducing agent and will react with a suitable cofactor (A) if one is available.

$$P + \text{light energy} \longrightarrow P^* + A \longrightarrow P^+ + A^-$$

The transfer of an electron by P^* is the primary photochemical event in the conversion of light energy to chemical energy in photosynthesis.

In photosynthetic organisms the components responsible for charge separation are bound to a protein framework, ensuring their correct orientation for efficient electron transfer. The cofactor and protein unit is known as the **reaction centre.** The electron is distanced from the oxidised special chlorophyll P via further electron transfer steps, stabilising the separation by reducing the probability of a backreaction. A second electron transfer system exists to reduce P^+ and allow repeated turnovers of the reaction centre. The electrons for this are provided either by oxidation of a suitable electron donor or by cyclic electron flow around the reaction centre.

The primary function of photosynthesis is the production of energy. From Mitchell's chemiosmotic hypothesis, ATP synthesis is known to be coupled to a proton electrochemical potential generated across a membrane (the energy transducing membrane). The reduction/oxidation (redox) reactions of electron transfer often involve protonation events. Therefore reaction centres are always orientated in such a way that mobile electron carriers, such as quinones, can be reduced on one side of the membrane and oxidised on the other, effectively acting as proton transporters. This leads to a net movement of protons across the membrane creating the electrochemical potential that is utilised by ATP synthetase to generate energy in the form of ATP.

The second function of the light reactions of photosynthesis is the storage of reducing potential, in the form of NAD(P)H, for the fixation of carbon dioxide in complex organic compounds. This is achieved by the reduction of $NAD(P)^+$ in reactions either directly or indirectly related to photochemical electron transfer. Certain types of reaction centre can use $NAD(P)^+$ as the terminal electron acceptor in the transfer chain (direct reduction). Other organisms use the process of "reverse electron transfer" to generate NADH at the expense of ATP (indirect reduction). Both methods require a source of electrons (often called the hydrogen donor) and so the general equation for the photoautotrophic reaction is:

$$2H_2A + CO_2 \dashrightarrow (CH_2O) + 2A + H_2O$$

where H_2A represents the universal electron donor.

The number of charge separation events occurring in a reaction centre is high (up to 200 per second) due to the employment of **light harvesting** systems which efficiently funnel light energy to the reaction centre. This ensures that the reaction centre special chlorophyll is always supplied with excitation energy even at low light intensities. The light harvesting systems are large protein complexes that bind numerous pigments in highly ordered arrays. These arrays have very specific spacial arrangements optimised for the most efficient transfer of energy between pigment molecules. An absorption event by an outer pigment will lead to a series of energy transfers as the light follows a "random walk" around the pigment molecules. The slight increase in wavelength upon energy transfer results in pigments absorbing at longer light wavelengths being situated nearest the reaction centre special chlorophyll. P is a low energy trap so that random walks end at the special chlorophyll.

1.2 Photosynthetic Organisms

Photosynthetic organisms can be divided into two groups: the oxygenic, which evolve O_2 through the oxidation of water and the anoxygenic, which only perform photosynthesis under anaerobic conditions.

1.2.1 Anoxygenic Photosynthesis

This group can be roughly subdivided further depending on whether or not oxygen is toxic to the organism. The imprecise nature of the classification stems from relationships that were originally based on pigment content rather than functional correlations.

Organisms which are sensitive to O_2, and so tend to be obligate aerobes, include the Chromataceae (purple sulphur bacteria) and the Chlorobiaceae (green sulphur bacteria). They are photoautotrophic, capable of oxidising sulphur compounds and NAD^+ reduction for carbon dioxide fixation. In general, green sulphur bacteria possess a reaction centre capable of direct reduction of NAD^+ while the purple sulphur bacteria employ reverse electron transport.

The second group of organisms are facultative aerobes but their photosynthetic apparatus is only activated under anaerobic conditions. It includes the Rhodospirillaceae (purple non-sulphur bacteria) and the Chloroflexaceae (green non-sulphur bacteria). They have similar reaction centres, but different light harvesting systems, both using light to drive cyclic electron flow around the RC. The Chloroflexaceae are photoheterotrophic but the Rhodospirillaceae can be photoautotrophic, some using sulphur compounds (despite the name) while others utilise H_2 or organic substrates for indirect reduction of NAD^+ for use in CO_2 fixation.

All anoxygenic bacteria can be characterised by the

combination of pigment types and the wavelength of maximum absorption of the reaction centre special chlorophyll. In green bacteria it is the use of short wavelength absorbing bacteriochlorophylls c, d and e in their large light harvesting chlorosomes (up to 10,000 pigment molecules) which makes them appear green. Purple bacteria are so called because of their carotenoid component.

The previous groups of bacteria are all Gm -ve but a Gm +ve photosynthetic bacterium has been identified. Heliobacterium chlorum is a strict anaerobe characterised by the presence of a unique pigment, bacteriochlorophyll g, and containing a reaction centre similar to that of the green sulphur bacteria.

1.2.2 Oxygenic Photosynthesis

Whereas anoxygenic photosynthetic organisms use only one type of reaction centre, oxygenic organisms have developed a system that uses two types of reaction centre working in series. The first is Photosystem Two (PS2), a reaction centre similar to that of the purple non-sulphur bacteria. Molecular oxygen is released because PS2 generates an oxidising potential capable of water oxidation. The second reaction centre is Photosystem One (PS1) and is similar to that of green sulphur bacteria. PS1 creates a reducing potential capable of direct $NADP^+$ reduction. The two photosystems are linked by mobile electron carriers acting via a third membrane bound protein complex, cytochrome b_6f. The reaction centre special

chlorophyll, P, is always a Chl *a* molecule but there is considerable diversity in the pigment and protein structures used in light harvesting between different groups of oxygenic organisms.

The most primitive oxygenic system is that of the *Cyanobacteria*. Their "blue-green" appearance is due to the bilins (linear tetrapyrroles) in the phycobilisomes, the cyanobacterial light harvesting complexes bound to the cytoplasmic face of the thylakoid membrane. This type of light harvesting arrangement is also seen in the eukaryotic red algae, the *Rhodophyta*.

Other groups of oxygenic organisms use chlorophyll based antennae systems, including all higher plants and the *Chlorophyta* and *Chromophyta* green algae. Evolutionary origins of the use of chlorophyll in light harvesting systems are undetermined. Some clues have been provided by the study of a group of recently discovered organisms, the *Prochlorophyta*, which may be precursors of the higher plant/green algae system. They are oxygen evolving prokaryotes, closely related to *Cyanobacteria*, but they use chlorophyll *b* rather than phycobilins.

1.2.3 Evolutionary Relationships

The scheme presented by Mathis (1990) (adapted from Woese, 1987) for the evolutionary origins of the two photosystem arrangement found in *Cyanobacteria* suggests that the system arose from a genomic fusion between a purple bacterium and a Gm +ve bacterium. Woese's original

analysis included an evolutionary tree based on rRNA relationships but Mathis also took the structural and functional details of the various reaction centres into account. It was originally thought that PS1 was closest in evolutionary terms to the green sulphur bacteria but the new analysis proposes that a Gm +ve bacterium in fact gave rise to PS1 [Mathis, 1990].

Another important consideration is the development of the ability to oxidise water. The move towards water oxidation probably began with a mutation causing radical changes in the environment of the reaction centre special chlorophyll, probably shortening the wavelength of peak absorbance. Generation of the necessary oxidising potential requires the use of shorter wavelengths of light. This would have been followed by the less rapid development of a water oxidising "enzyme".

Recently Nitschke and Rutherford (1991) have expanded on the idea of a progenitor for all types of reaction centres, suggesting that the PS1 and PS2 "type" RCs have arisen by divergent evolution from a common ancestor.

The relationships between light harvesting systems, especially between the Prochlorophyta and chloroplasts, also need to be studied. Red algal chloroplasts may well have arisen from a symbiotic Cyanobacterium but origins of the use of Chl b in higher plant LHCII, at the possible expense of phycobilins, are unclear. Again genetic analysis has been used. Turner et al. (1989), looking at rRNA, concluded that the Prochlorophyta and the higher

plant chloroplast both arose from Cyanobacteria but are the result of divergent lines, the ability to synthesise Chl b having developed independently or through lateral transfer. They believe that evolutionary relationships should not be determined solely by comparisons of pigment composition. Morden and Golden (1989) compared the psbA gene which encodes an integral PS2 reaction centre subunit, taking into account the variation between species of an integral component of the photosynthetic apparatus (Mathis (1990) used a similar approach by adapting the genetic analysis to fit the functional relationship between reaction centres). Morden and Golden (1989) concluded that the higher plant chloroplast and the Prochlorophyta both arose from a Cyanobacteria derived progenitor that had the ability to synthesise Chl b. This is in disagreement with the analysis of Turner et al. (1989), but is more likely, since the independent evolution of Chl b use by two different organisms is less probable.

1.3 The Reaction Centre Of Purple Non-Sulphur Bacteria

The reaction centre structure of the purple non-sulphur bacterium Rhodopseudomonas (Rps.) viridis has been determined by X-ray crystallographic analysis to less than 3Å resolution [Deisenhofer et al., 1984 and 1985; Michel et al., 1986]. This was the first structure of an integral membrane protein complex to be solved and earned the researchers the Nobel prize for Chemistry in 1988

[Deisenhofer and Michel, 1989]. The reaction centre was found to consist of four proteins: L (light), M (medium), H (heavy) and a c-type cytochrome with four covalently linked haems. The L and M subunits form the core of the reaction centre, bound together in a heterodimer. An analysis of their structures showed them to be very closely related to each other so that an axis of approximate twofold symmetry runs through the centre of the reaction centre.

The heterodimer binds all the cofactors involved in primary photochemistry: the primary electron donor, P960, two accessory BChl b molecules, two bacteriopheophytins (BPh) and two quinones, so that the cofactors appear to form two functionally related branches (see Fig.1.2). P960 was already known to be a pair of BChl b molecules (the special pair) from spectroscopic studies and the crystal data showed the dimer to be bound by ligands from both L and M. After P960 excitation the electron is transferred along one "branch" to BPh_L and then on to the primary quinone electron acceptor, Q_A. The two reaction centre quinones are different, M binds a menaquinone (Q_A) and L binds ubiquinone (Q_B). The conformation of the reaction centre is such that it is the menaquinone bound to the M subunit that is closest to BPh_L and known as the primary quinone electron acceptor.

The electron transfer from Q_A^- is parallel to the plane of the membrane to the secondary quinone, Q_B, the ubiquinone of the L subunit. Q_B is a mobile two electron carrier that

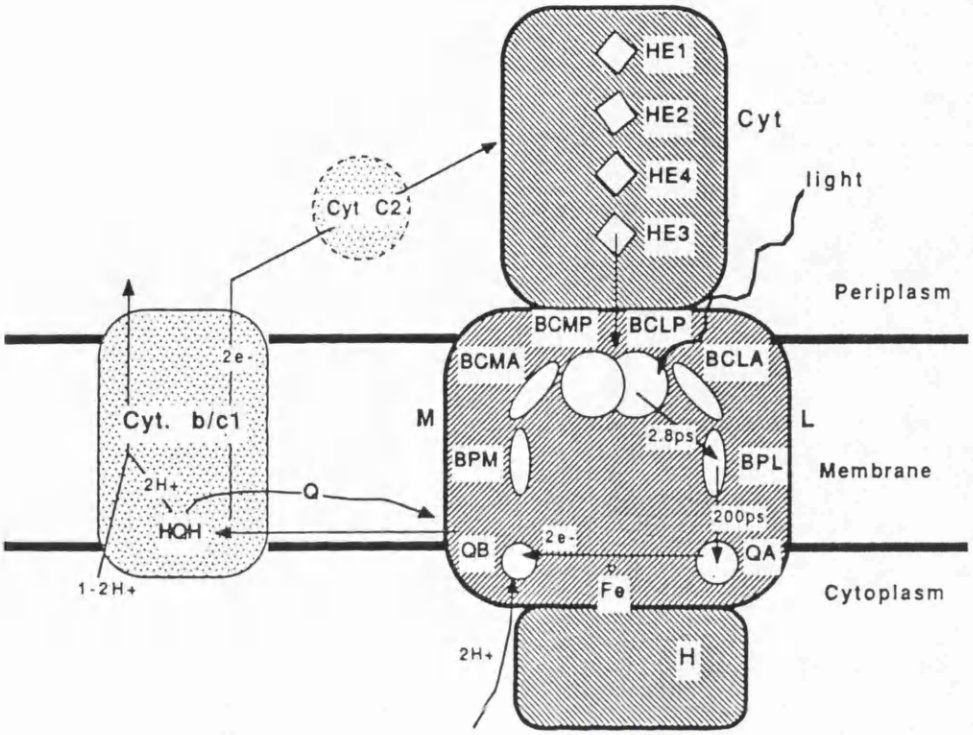

Figure 1.2 The reaction centre of the purple non-sulphur bacterium Rhodopseudomonas viridis. The reaction centre consists of four subunits: L, M, H and the multihaem cytochrome. Primary photochemistry takes place in the membrane bound LM heterodimer, which binds the special pair P960 (two BChl b molecules BCMP and BCLP), the accessory BChls BCMA and BCLA, the two BPhs BPM and BPL, the primary and secondary quinones Q_A and Q_B, and the non-haem iron. Arrows indicate the flow of electrons. Following two charge separations ubiquinol dissociates from the reaction centre so that electrons are cycled back to the RC via the membrane bound cytochrome b/c_1, the soluble cytochrome c_2 and the multihaem (HE1 to 4) cytochrome. [Diagram from Deisenhofer and Michel, 1989]

dissociates from the reaction centre in the doubly reduced quinol form.

A non-haem iron atom is bound between the quinones, the ligands of which are provided by four histidine residues, two each from L and M, and a glutamate residue found in a seven residue insertion in the M subunit (compared to the L subunit). The function of the iron is unclear but it could stabilise the reaction centre conformation or possibly influence the redox behaviour of the quinones.

The electrons are cycled via the membrane bound cytochrome b/c_1. Oxidation of Q_BH_2 by the cytochrome is associated with the movement of protons across the membrane to generate the electrochemical potential. A water-soluble cytochrome c_2 completes the chain back to the multihaem reaction centre cytochrome (see Fig.1.2) which reduces $P960^+$.

The structure of the reaction centre complex from Rhodobacter (Rb.) sphaeroides was solved not long after that of Rps. viridis (for review see Feher et al., 1989) and was found to be very similar. The main differences between the two systems are that P870 is a BChl a dimer, both Q_A and Q_B are ubiquinones and there is no bound multi-haem cytochrome, the soluble cytochrome c is thought to donate electrons directly to the special pair.

The preferential direction of electron transfer along the BPh_L/Q_A branch (as opposed to the use of BPh_M) appears to be determined by several factors. These are related to the

spacial arrangement of the cofactors and the environment around the reactants. For instance, in Rps. viridis one tetrapyrrole ring of the special pair is more planar than the other and the overlap of electron densities is greater between the dimer and accessory $BChl_L$ rather than with $BChl_M$ [Feher et al., 1989].

The accessory BChls are bound close to the special pair and $BChl_L$ may be involved in primary photochemistry as electrons are transferred to BPh_L. This step takes only a few picoseconds and may be explained by two mechanisms. The first alternative is that the accessory BChl actually forms a reduced intermediate so that it is in fact a two step transfer to bacteriopheophytin. The second is that $BChl_L$ bridges the gap between the special pair and BPh_L by enhancing the electron density overlap between the two through a "superexchange" mechanism. Work by Holzapfel et al. (1990) using femtosecond spectroscopy on Rb. sphaeroides has suggested that BPh_L does actually form an intermediate.

The H subunit of the reaction centre has a single transmembrane helix and a globular domain covering the cytoplasmic face of the reaction centre core. Removal of H leads to abnormal electron transfer between the quinones but the exact role of H in this process is still unresolved.

1.4 Structure And Function Of Higher Plant Photosystem Two

Eukaryotic organisms organise their photosynthetic apparatus in chloroplasts. These specialised organelles have a double membrane envelope enclosing the aqueous stroma (Fig.1.3), containing all the necessary components for the CO_2 fixing, dark reactions of photosynthesis. The actual energy transducing membrane is the third membrane, the thylakoid, which is arranged within the chloroplast in single (stromal) lamellae and in membrane stacks (grana). The distribution of the two photosystems between these two distinct regions of the thylakoid is heterogeneous, with PS1 found mainly in the stromal lamellae and PS2 in the grana. This lateral heterogeneity is concerned with the mechanisms controlling the rate of photosynthesis which operate by changing the distribution of light harvesting complexes between RCs. The cytochrome b_6f complex appears to be evenly distributed between both the stromal and granal regions [Anderson and Andersson, 1982].

Figure 1.4 shows the "Z" scheme and illustrates the path of electrons through the three protein complexes. The electrons are generated by water oxidation on the lumen side of PS2 and pass through the RC as a result of photochemistry to reduce the mobile carrier Q_B. Plastoquinol then dissociates from PS2 and is oxidised by the cytochrome complex which in turn reduces plastocyanin, a copper protein soluble in the lumen. Plastocyanin donates the electron to PS1, whose terminal acceptor is $NADP^+$.

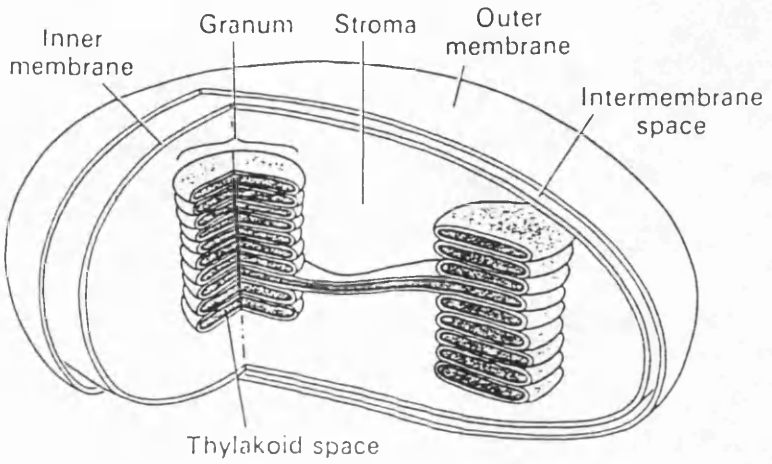

Figure 1.3 The chloroplast. These organelles have three separate membranes: the inner and outer envelope membranes and the thylakoid. The thylakoid is the energy transducing membrane and is divided into two distinct regions, the stromal lamellae and the granal stacks. It is the thylakoid, surrounded by the aqueous stroma, that binds the protein complexes involved in electron transport. [Diagram from Wolfe: Biology Of The Cell, 1972]

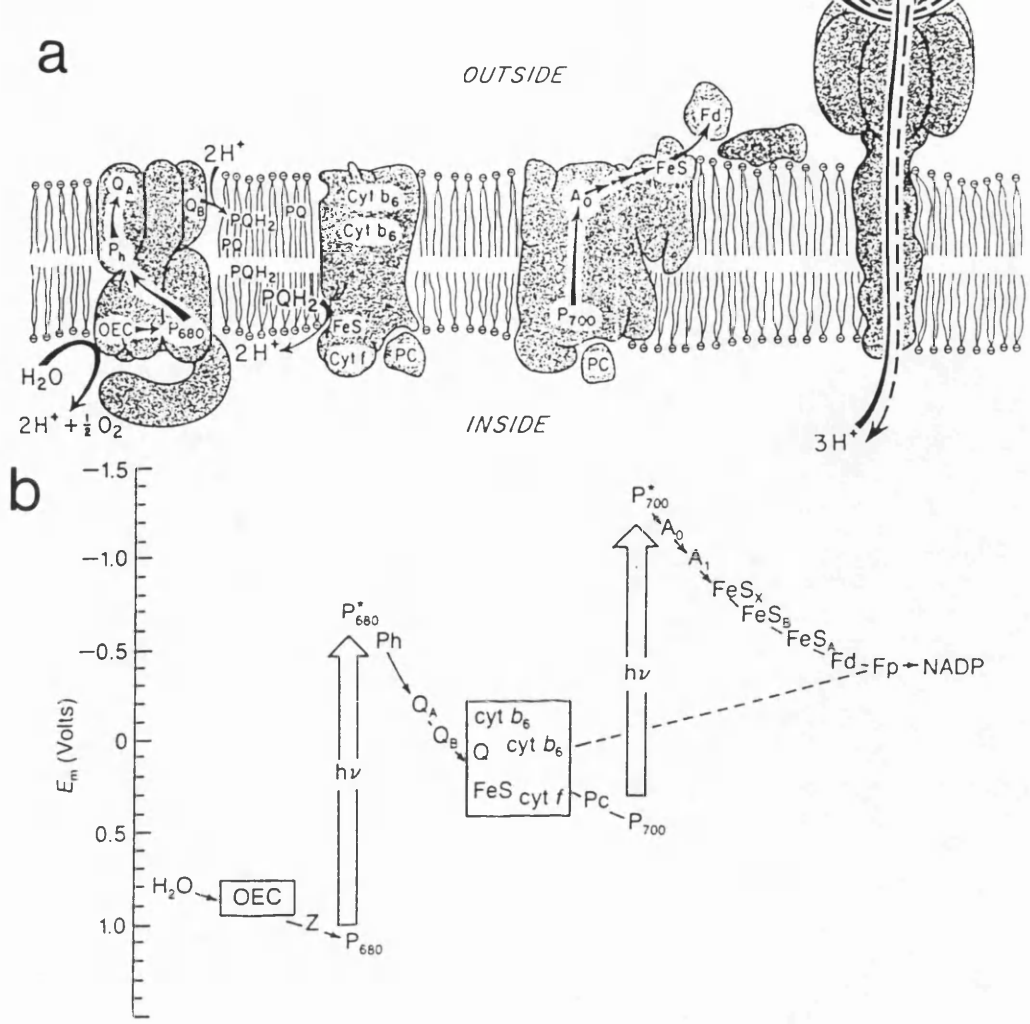

Figure 1.4 The Z-Scheme: a useful model for describing both the movement of electrons through the thylakoid protein complexes involved in electron transfer and the redox potential relationship between the cofactors. (a) Electrons are made available through water oxidation at the thylakoid lumen side of PS2 and are then moved across the membrane by a series of electron transfer events. The mobile electron carrier PQH_2 leaves PS2 and moves within the membrane to the cytochrome b_6f complex, where it is oxidised. The electrons are then transferred to the soluble e^- carrier plastocyanin (PC). PC donates an electron to $P700^+$, in PS1, that is subsequently transferred across the thylakoid and eventually used to reduce $NADP^+$. This diagram also shows where contributions are made to the proton gradient and the ATP-synthetase complex. (b) The cofactors involved in each electron transfer event are shown with their respective mid-point redox potentials. OEC, oxygen evolving complex; Z, tyrosine residue; P680, PS2 reaction centre special chlorophyll; Ph, pheophytin; Q_A and Q_B, primary and secondary quinones; cyt, cytochrome; FeS, Rieske iron-sulphur protein; Pc, plastocyanin; P700, PS1 reaction centre special chlorophyll; A_0 and A_1, early acceptors of PS1; FeS_X, FeS_B and FeS_A, are PS1 iron-sulphur centres; Fd, ferredoxin; Fp, ferredoxin-NADP reductase. [Diagrams from Ort and Good, 1988]

The possibility that the reaction centres from PS2 and purple non-sulphur bacteria were structurally and functionally similar was known prior to the elucidation of the reaction centre structure from Rps. viridis. When the amino acid sequences of L and M were compared with known PS2 subunits, very significant homology was apparent with the polypeptides known as D1 and D2 [Williams et al., 1983; Michel and Deisenhofer, 1988] (D standing for diffuse, a reference to their staining behaviour in PAGE analysis). D1 had already been identified as the site of herbicide action through photoaffinity labelling [Pfister et al., 1981], a known characteristic of the L subunit. However, direct evidence that D1 and D2 actually formed the reaction centre was missing. There were even proposals that the primary photoreactants resided on another subunit, the 47 kDa chlorophyll protein (CP47) [Nakatani et al., 1984]. The location of the PS2 reaction centre was firmly established when Nanba and Satoh (1987) isolated a reaction centre complex consisting of D1, D2 and cytochrome b_{559}, which could photoaccumulate reduced pheophytin. They determined the pigment composition of their complex to be 5 chlorophylls, two pheophytins and one ß-carotene.

A basic folding model for the structure of the D1/D2 heterodimer, based on homology studies with L and M, is now accepted. It relies on the location of functionally significant amino acid residues involved in cofactor binding and herbicide resistance and residues such as prolines or glycines found to be of structural importance

at the ends of helices [Trebst, 1986; Michel and Deisenhofer, 1988]. Like L and M, D1 and D2 are proposed to have five transmembrane helices (I to V). The Q_B and Q_A binding sites are formed in the regions between helices IV and V of D1 and D2 respectively. Among the conserved residues are the histidine ligands to the special pair chlorophylls and four possible His ligands to the non-haem iron. The region corresponding to the M subunit insertion containing the fifth non-haem iron ligand, Glu M232, is missing.

The assignment of the reaction centre to the D1/D2 heterodimer and its close structural relationship with the purple non-sulphur bacteria is therefore beyond doubt. However large differences do exist, which show the reaction centre, and PS2 as a whole, to be functionally distinct. Most notable of these is the ability of PS2 to oxidise water. Each structural and functional aspect of PS2 will be described in detail in the following sections (see Table 1.1 for a list of PS2 subunits and Figure 1.5 for PS2 structure).

1.4.1 P680 And Pheophytin

The primary electron donor of PS2 (P680) was first identified by Doring *et al*. (1969) using flash spectroscopy. They obtained an absorbance spectrum with bleaching at 682 and 435 nm that was attributed to Chl *a*. The use of a pigment with a shorter wavelength of maximum absorbance for the reaction centre special chlorophyll is

Table 1.1 **The Subunits of Photosystem Two**

SUBUNIT	DESCRIPTION	GENE
Plastid encoded polypeptides		
D1 32 kDa	Reaction centre subunits	psb A
D2 34 kDa		psb D
cyt.b_{559} 9 kDa α	Function unknown	psb E
cyt.b_{559} 4 kDa ß		psb F
4 kDa	copurified with RC	psb I
CP43	Chl a binding proteins	psb C
CP47		psb B
9 kDa	phosphoprotein	psb H
4 kDa	unknown	psb K
2 (5?) kDa	unknown	psb L
24 kDa	possible subunits identified	psb G
unknown	from genome analysis	psb J
Nuclear encoded polypeptides		
33 kDa	lumen extrinsics associated	psb O
23 kDa	with the OEC	psb P
17 kDa		psb Q
CP29		cab
CP26	inner LHC components	genes
CP24		
≈25 kDa	peripheral LHC II	cab genes
10 kDa	closely associated with	psb R
22 kDa	PS2 core	psb S

Several other small polypeptides may also be associated with PS2. A recent study by Nagatsuka et al. (1991) has identified several possible candidates.

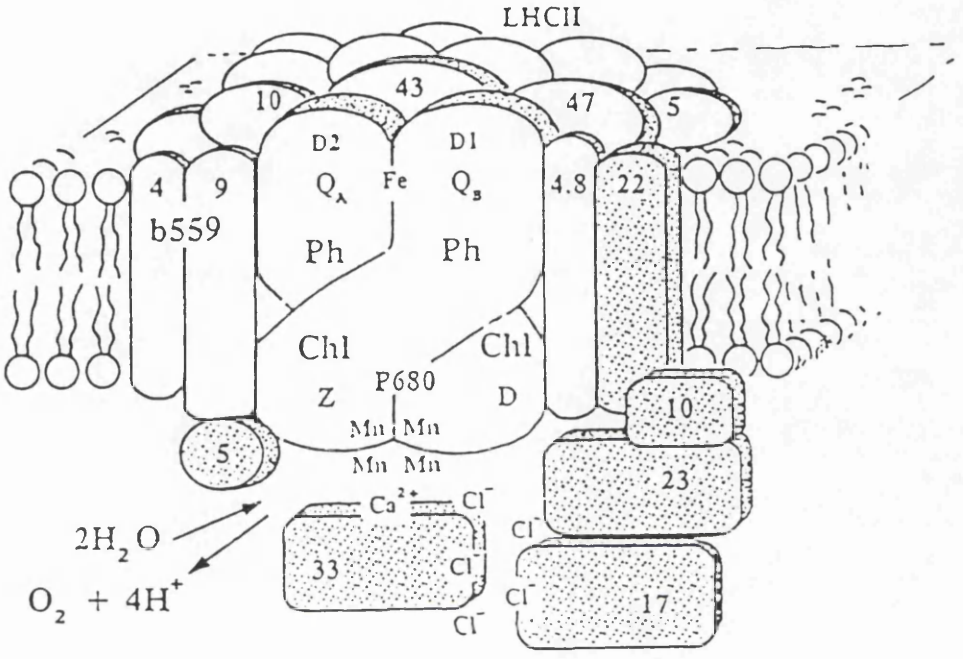

Figure 1.5 The structure of Photosystem Two. At the core of the complex is the reaction centre, a heterodimer of the D1 and D2 subunits. The cofactors shown bound to the reaction centre are: P680, the special chlorophyll; two possible accessory chlorophylls; the tyrosine residues D and Z; two pheophytin molecules; Q_A and Q_B, the primary and secondary quinones and the non-haem iron. The manganese of the oxygen evolving complex (OEC) is shown here bound by both D1 and D2. Also included are the 33, 23 and 17 kDa extrinsic polypeptides associated with the OEC, the two subunits of cytochrome b_{559}, the chlorophyll proteins CP43 and CP47, the light harvesting complex (LHCII) and several other subunits of unknown function. [Diagram supplied by Prof. J. Barber]

the fundamental difference between PS2 and the purple bacterial system. $P680^+/P680$ has an oxidising mid-point potential greater than 1.0 V whereas $P960^+/P960$ (the BChl b dimer of Rps. viridis) is only 0.4 V.

The identification of P680 as a monomer or a dimer is still unresolved. Structural comparisons with the bacterial system show that the ligands are available to bind a dimer but electron paramagnetic resonance (EPR) studies on the P680 spin-polarised triplet ($^3P680$) signal show that P680 may be a monomer [Rutherford et al., 1981a]. Van Mieghem et al. (1991) propose that both the triplet and $P680^+$ positive charge are localised on a single chlorophyll orientated 30° out of the membrane plane, but whether this chlorophyll is a monomer or one half of a weakly coupled pair is unknown. These observations could conceivably result from the migration of excitation energy to a monomer Chl near to P680.

$^3P680$ arises from a charge recombination between $P680^+$ and Ph^-, the reduced primary electron acceptor (also known as I, the intermediate) which was identified as a pheophytin molecule [Klimov et al., 1977]. Instead of recombination to a singlet state the electron returns to a higher energy orbital. This results in a molecule with two unpaired electrons that create a characteristic EPR signal by the interaction of the two magnetic dipoles. At liquid helium temperatures the triplet has a high quantum yield (nearly 100%) and is relatively long-lived, with a half-life of ≈1.1 ms [van Mieghem et al., 1989], measured at 9

K. ^{3}P680 is seen in samples where electron transfer beyond pheophytin is blocked, ie. in chemically reduced samples (the redox potential poised between -350 and -610 mV with sodium dithionite) or where the next acceptor, the primary plastoquinone (Q_A), is absent. The latter situation is encountered in the reaction centre preparation of Nanba and Satoh which has no bound plastoquinone. A radical type EPR signal can also be observed arising from $P680^+$ [Hoganson and Babcock, 1989; Nugent et al., 1989]. The signal is narrower (≈0.8 mT) than the other chlorophyll radical (≈1.1 mT) that can be observed in PS2 [de Paula et al., 1985]. This narrowing may be characteristic of a dimer but environmental factors are also known to cause linewidth variations. Therefore the assignment of P680 to a monomer or a dimer through analysis of the radical signal is also inconclusive.

The primary charge separation in PS2 ($P680^* + Ph \dashrightarrow P680^+ + Ph^-$) takes place in a few picoseconds, 3.0 ± 0.6 ps [Wasielewski et al., 1989]. In bacteria the accessory BChls are thought to be involved in this reaction but no corresponding His residues have been identified in PS2 which could act as ligands to any accessory or "voyeur" Chls. The optical experiments of Wasielewski et al. (1989) used a 500 fs time resolution and failed to find evidence for an intermediate formed before pheophytin reduction. Despite this fact the reaction centre is known to bind at least 3 extra chlorophylls as well as the P680 monomer/dimer [Nanba and Satoh, 1987]. Their proximity to

P680 cannot be determined although at least one is known to donate electrons to $P680^+$ [de Paula et al., 1985; Thompson et al., 1988].

The reaction centre binds two pheophytin molecules [Nanba and Satoh. 1987], probably one on each of the D1 and D2 branches. However, only one is involved in primary charge separation and by analogy with the bacterial system this is believed to be the pheophytin bound to D1. The mid-point redox potential of this cofactor was determined by Rutherford et al. (1981b) to be ≈-604 mV by measuring the changes in triplet yield as the potential was varied.

The choice of a pheophytin molecule as the primary acceptor has been investigated recently in a site-directed mutagenesis study in Rb. sphaeroides [Kirmaier et al., 1991]. Leu M214 was replaced by a His residue which resulted in the incorporation of a BChl molecule as opposed to a BPh. The quantum efficiency of the mutant was reduced to 60% of the wild type as the forward rate of electron transfer was diminished. This increased the life-time of the reduced primary acceptor and consequently raised the probability of a P^+BCHl^- recombination. The high quantum yield of the wild type is maintained because (bacterio)pheophytin combines a faster rate of forward electron transfer with a slow backreaction.

1.4.2 The Primary And Secondary Quinones (Q_A And Q_B)

The reactions of the "electron acceptor side" of PS2 have similarities with the bacterial system but both Q_A and

Q_B are plastoquinones, instead of either ubiquinone or menaquinone. Q_A was first identified as an efficient fluorescence quencher when present in an oxidised state [Duysens and Sweers, 1963]. It was subsequently termed X-320 because the light minus dark difference spectrum was found to have an absorbance maximum at 320 nm. van Gorkom (1974) eventually matched the reduced minus oxidised absorbance spectrum to that of a plastosemiquinone.

The reduction of Q_A is associated with an increase in the membrane potential that can be monitored through an electrochromic effect on the absorbance spectrum of pheophytin. The effect is expressed as a change in the absorbance at 548 nm (C-550) and was found to be dependent on the presence of ß-carotene [Cox and Bendall, 1974]. Redox titrations measuring C-550 or monitoring fluorescence determined the midpoint potential at pH 7.0 of the Q_A/Q_A^- couple to be around 0 mV.

Q_A is reduced by Ph^- 350 ± 100 ps after P680 oxidation [Eckert et al., 1988]. In the bacterial reaction centre a tryptophan residue (M250) plays a major role in the electron transfer from pheophytin to Q_A [Michel and Deisenhofer, 1988]. In PS2 the quinones are located in analogous binding sites and D2-254 is recognised as the corresponding Trp residue. Intermediate electron acceptors between Q_A and pheophytin have been proposed which will be discussed later in detail (section 3.4). These suggestions are related to PS2 heterogeneity, the behaviourial differences observed within PS2 populations (review:

Govindjee, 1990).

Under normal conditions Q_A is not doubly reduced. Instead it transfers the electron to the secondary quinone Q_B which is a two electron carrier. In the doubly reduced protonated form, Q_BH_2, the mobile carrier dissociates from the RC and moves within the membrane to be oxidised and regenerated by the cytochrome b_6f complex. Q_A and Q_B are both plastoquinones so the differences in their behaviour can only be a product of the intrinsic differences in their protein binding environments.

The rate of electron transfer from Q_A^- depends on the reduced state of the secondary quinone. A value of 100-200 μs is observed for the first reduction but this is increased slightly to 300-500 μs for the reduction of the semiquinone [Crofts and Wraight, 1983]. These relatively slow kinetics are possible because $P680^+$ is reduced by the primary donor (Z) on the nanosecond time scale, while a $P680^+Q_A^-$ backreaction is considerably slower with a half-time of 150 μs.

In bacteria the Q_B semiquinone is stabilised in the binding site by protonation of the reaction centre [Takahashi and Wraight, 1990]. Reduction of Q_B^- is believed to be coupled to protonation of the doubly reduced quinone [Crofts and Wraight, 1983]. Q_B reduction and protonation:

1. $$Q_A^- + Q_B \dashrightarrow Q_A + Q_B^-$$

2. $$Q_A^- + Q_B^- + 2H^+ \dashrightarrow Q_A + Q_BH_2$$

The protons are thought to arrive in the binding site through a chain of protonatable side chains from the

"outside". In the bacterial system several candidates for this role have been suggested and site-directed mutagenesis studies have been carried out to test this theory. Paddock et al. (1989,1990) replaced Glu L212 and Ser L223 with glutamine and alanine respectively and Takahashi and Wraight (1990) have substituted asparagine for Asp L213, both groups working on Rb. sphaeroides. Mutation of these residues provided evidence for the theory as all the mutants expressed reduced rates of electron transfer to Q_B^- or slower proton uptake, or both. On the evidence of their experiments Paddock et al. (1990) now propose that two proton transfer chains are active and that proton uptake involves two separate steps. In PS2 a comparable system of transfer chains may exist but there have been other mechanisms proposed claiming that Q_B^{2-} protonation is intimately related to the "bicarbonate effect" (see section 1.4.4).

The protein loops in PS2 between transmembrane helices IV and V in D1 and D2 are significantly longer than the equivalent regions in L and M. This has made structural predictions of the quinone binding sites difficult. The secondary quinone binding site is known to be the site of action for many herbicides which act by blocking electron transfer beyond Q_A by displacing Q_B. Analysis of herbicide resistant mutants has helped to determine important residues in the binding site and has aided the production of folding models [Trebst et al., 1990]. Fig.1.6 shows all the residues currently thought to be important in herbicide

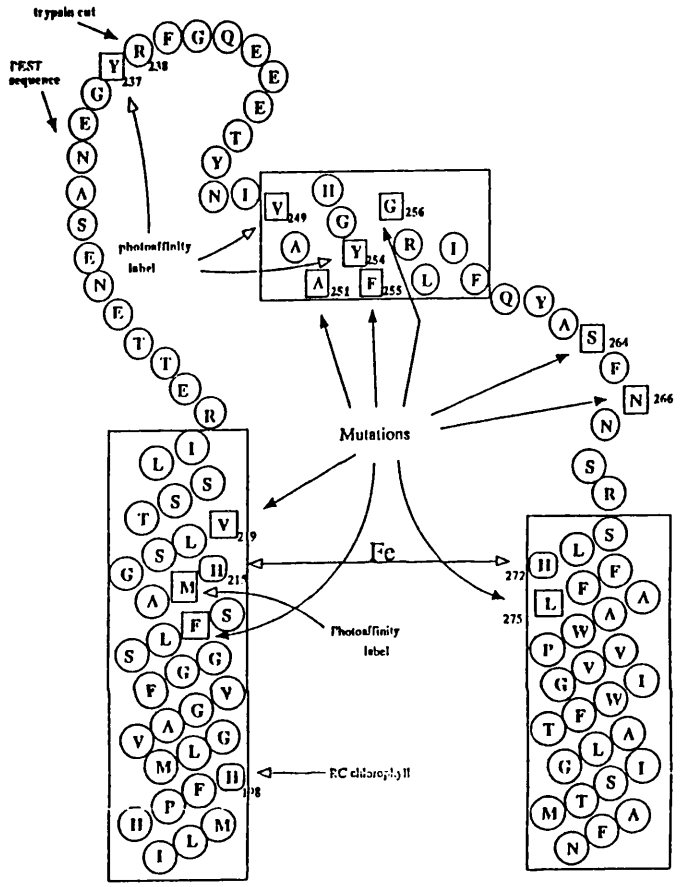

Figure 1.6 Folding model of the D1 Q_B binding region. The model has marked all the mutations known to be involved in herbicide resistance, possible chlorophyll and non-haem iron histidine ligands, the proposed trypsin cut site [Trebst et al., 1988], residues identified from photoaffinity labelling studies and a possible PEST sequence involved in protease recognition and D1 turnover. [Diagram from Trebst et al., 1990]

binding/resistance, non-haem iron ligands and those labelled in photoaffinity studies. The model also has marked a possible PEST sequence (sequences high in the amino acids proline, glutamate, serine and threonine, thought to be recognition sites for the proteases responsible for intracellular protein turnover). D1 is known to be rapidly turned over and this may be the recognition site for the protease responsible. D1 turnover is thought to be related to the process of photoinhibition, whereby damage occurs to the reaction centre under high light stress conditions.

1.4.3 The Non-Haem Iron

Petrouleas and Diner (1986) identified the non-haem iron of the electron acceptor complex of PS2 as the previously recognised fluorescence quencher Q_{400}, understood to be located between Q_A and the site of DCMU inhibition [Bowes et al., 1979]. This demonstrated that the iron could participate in redox reactions. The E_{m7} of the Fe^{2+}/Fe^{3+} couple was determined to be +400 mV with a pH dependence of 60 mV per pH unit in the range 6-8.5, indicating that reduction of Q_{400}^{+} is associated with proton binding.

The iron can be oxidised by dark incubation with potassium ferricyanide. Fe^{3+} can then be reduced by a single reaction centre turnover. At low temperatures where the electron cannot normally move beyond Q_A this makes it possible to send two electrons through the reaction centre,

as first Fe^{3+} is reduced then Q_A.

Alternatively, a process of reductive-oxidation can be used to oxidise the iron by the addition of high potential quinones (E_{m7} of the Q^-/Q^{2-} couple >+400 mV). In these samples a single turnover at room temperature generates the quinol as the exogenous quinone becomes doubly reduced by one electron from photochemistry and another from non-haem iron oxidation in the sequence:

1. $$Q_A^- + Q_B \dashrightarrow Q_A + Q_B^-$$

2. $$Q_B^- + Fe^{2+} + 2H^+ \dashrightarrow Q_BH_2 + Fe^{3+}$$

The non-haem iron is not thought to be directly involved in redox reactions in the course of normal PS2 activity as the mid-point potential of plastoquinone is too low for the semiquinone to oxidise Fe^{2+}. The iron is paramagnetic in the oxidised state so the artificially generated EPR signal has been used as a sensitive probe into the electron acceptor complex. The signal has two peaks at g=8 and 5.6. Changes in the spectrum occur when the Q_B binding site is occupied either by herbicides [Diner and Petrouleas, 1987a] or quinone analogues [Zimmermann and Rutherford, 1986a; Petrouleas and Diner, 1987; Hallahan *et al.*, 1991]. The spectral variations arise from interactions with the proposed non-haem iron ligands. In *Rps. viridis* Michel *et al*. (1986) found that the herbicide o-phenanthroline (o-phen) binds with a hydrogen bond to His L190, one of the non-haem iron ligands (identified as D1-His-215). Terbutryn was found to bind to the opposite side of the binding site. In PS2 the Q_AFe^{3+} EPR spectrum of o-

phen treated samples is greatly altered to a g=6 axial spectrum while terbutryn treatment causes little, if any, alteration. Therefore g-value changes depend on the proximity of the binding species to the non-haem iron.

Analysis of the Fe^{3+} EPR signal has led to proposals as to the identity of the iron ligands in PS2. Aasa et al. (1989) compare the iron ligation to that found in transferrins and speculate that tyrosines and bicarbonate may be involved as well as histidines. The possibility that bicarbonate is a ligand has been more directly approached by the experiments of Diner and Petrouleas (1990) who argue that HCO_3^- provides either a bidentate or monodentate ligand. The study of Semin et al. (1990) using Mössbauer spectroscopy shows that formate washing induces a bicarbonate reversible change in the spectrum of the non-haem iron, a result that can also be interpreted in favour of the existence of a bicarbonate ligand to the iron.

The physiological role of the non-haem iron is still uncertain. In bacteria the iron can be replaced by other divalent metal ions with no effect on the rate of electron transfer between the quinones; complete removal of the metal atom only reduces the rate by a factor of 2-3. The iron may function in stabilising transition states involved in electron transfer or it may influence the redox potential/behaviour of the quinones. The ligands are thought to be provided by both D1 and D2 so the iron may also help maintain the conformation necessary for efficient PS2 function.

1.4.4 The Bicarbonate Effect

The discovery of the carbon dioxide requirement in the Hill reaction (the evolution of oxygen by illuminated thylakoids in the presence of an artificial electron acceptor) is attributed to Warburg and Krippahl (for a review see Blubaugh and Govindjee, 1988a). They demonstrated that the reaction was inhibited by CO_2 removal and stimulated by its re-addition. Carbon dioxide was shown not to be the source of the oxygen evolved as O_2 evolution did not reduce the concentration of CO_2. Therefore the effect on the Hill reaction was not substrate related. Experiments by Good (1963) found that this inhibition could be imitated by the addition of small anions such as formate (HCO_2^-) and acetate ($CH_3CO_2^-$). His conclusion was that bicarbonate (HCO_3^-) was the active species and not CO_2. Formate is now routinely used in bicarbonate depletion studies of PS2 because it is thought to displace HCO_3^- from its binding site(s).

Bicarbonate depletion was shown by Jursinic *et al.* (1976) to increase the half-time of Chl *a* fluorescence decay, indicating that Q_A^- oxidation was slowed. This points to a blockage in Q_A to Q_B electron transfer so the site of bicarbonate action was implied to be somewhere between the two quinones. A study on the reliance of fluorescence decay with flash number [Govindjee *et al.*, 1976] found that Q_A^- oxidation was slowest only after the third flash, suggesting a link between bicarbonate and Q_B^{2-} protonation. In inhibited samples the first two flashes

may still be able to drive two electrons through the reaction centre but subsequent turnovers would be blocked as Q_B^{2-} remains unprotonated and unable to leave the binding site.

The observed dual role of bicarbonate, as a possible non-haem iron ligand [van Rensen et al., 1988; Michel and Deisenhofer, 1988; Blubaugh and Govindjee, 1988a; Diner and Petrouleas, 1990] (see section 3.1.3) and proton source for Q_B, leads to speculation that there are multiple binding sites. Blubaugh and Govindjee (1988b) interpreted their data to show the existence of two high-affinity binding sites. A "pool" of bicarbonate bound to a low affinity site(s) buried within the membrane has also been suggested [Stemler, 1977]. In the model presented by Blubaugh and Govindjee (1988a) for the mechanism of the bicarbonate effect, the first of the high-affinity binding sites is assigned to a bidentate ligand to the non-haem iron. The second high-affinity site is proposed to be an arginine residue on D1 (Arg-257) and the bicarbonate bound here would be intimately involved in protonation of the secondary quinone. The pK_a of HCO_3^-/CO_3^{2-} is ≈10 but binding to the Arg residue could stabilise the negative charge and lower the pK_a. The pH of the stroma is approximately 8 during photosynthesis so bicarbonate could act as proton donor [van Rensen et al., 1988]. Blubaugh and Govindjee propose that as Q_B is reduced, a nearby histidine residue (His-252) becomes protonated by the bound bicarbonate. His-252 may be the side chain observed to undergo a pK_a

increase as Q_B^- is generated [Crofts et al., 1984]. This would provide a flow of protons directly into the Q_B binding site as the bicarbonate bound to Arg-257 is regenerated from the low-affinity pool. Takahashi and Wraight (1991) also propose a role for bicarbonate in Q_B protonation. They identified an aspartate residue possibly involved in Q_B protonation in Rb. sphaeroides and mutated it to an asparagine. The effect of the mutation was similar to that of bicarbonate depletion in higher plants so they proposed that HCO_3^- plays a role similar to that of the aspartate residue in protonation.

Diner (1988) suggests that the second binding site may be a lysine residue (D2-Lys-264) near one of the proposed non-haem iron histidine ligands, D2-His-268. Bicarbonate would be involved in carbamate formation. In a site-directed mutagenesis study the lysine was mutated to either Arg, Gln or Leu and in all cases electron transfer between the quinones was slowed significantly. This does not prove the carbamylation theory but gives some support to the hypothesis.

Bicarbonate has also been suggested to affect protein phosphorylation. Sundby et al. (1989) observed that HCO_3^- addition to chloroplasts, or isolated thylakoids, caused a stimulation of the level of phosphorylation of a 25 kDa light harvesting component. This may indicate a role for bicarbonate in the control mechanism regulating the size of the light harvesting complex. Bicarbonate addition also reduced the level of phosphorylation of the 9 kDa

phosphoprotein. However the function of this subunit is unknown. Sundby (1990) also identifies bicarbonate depletion as a possible cause of photoinhibition. A "pool" of bicarbonate would normally be maintained to ensure rapid replacement of HCO_3^- used in proton donation to Q_B^{2-}. Depletion of this proton store would lead to increased photoinhibition as electron flow via Q_B is blocked.

1.4.5 The Tyrosine Residues D And Z

Although D and Z are separate redox components of PS2 their corresponding radicals give rise to identical EPR signals (signal II) distinguishable only by their kinetics. Signal II_{vf} (very fast) and signal II_f (fast) are light induced forms of the signal assigned to Z^+ and signal II_s (slow) is a dark stable signal from D^+. The signal is centred at g=2 with a linewidth of 1.9 mT and has characteristic hyperfine peaks that are partially resolved. The kinetically different EPR signals demonstrate that D and Z have chemically identical structures but are functionally distinct.

The signals were first thought to arise from plastohydroquinone cations [O'Malley and Babcock, 1984] but analysis of the quinone content of the reaction centre revealed that there were actually fewer quinones than there were proposed quinone cofactors [de Vitry et al., 1986; Takahashi and Katoh, 1986]. D and Z were finally identified as tyrosine residues by Barry and Babcock (1987, 1988, see also Barry et al., 1990) who grew Cyanobacteria

on deuterated compounds and found that isotopic labelling of tyrosine altered signal II. They created a model for the arrangement of the methylene protons in the tyrosine and using this were able to simulate a signal II type EPR spectrum.

D is known to interact with the oxygen-evolving complex (OEC) through deactivation/advancement of the S-states (the five sequential redox stages in the process of water oxidation). In the dark the OEC relaxes to the S_1 state either by advancement from S_0 as an electron is donated to D^+ ($t_{½}$ = 20 or 50 mins at room temperature depending on the type of preparation [Styring and Rutherford, 1987]), or by deactivation from S_2 as D is oxidised ($t_{½}$ < 1 min at 0 °C [Nugent et al., 1987; Kawamori et al., 1987; Styring and Rutherford, 1987; Inui et al., 1989]). S_3 also oxidises D but the further deactivation from S_2 to S_1 in these centres must occur by another, slower, mechanism. The manganese complex at the core of the OEC is thought to be most stable in the S_1 state. For D to be involved in the above reactions the mid-point potential of D/D^+ must be between that of S_0/S_1 and S_1/S_2. The E_m has been estimated to be +720-760 mV from a study of equilibrium constants [Vass and Styring, 1991]. A role for D has also been suggested in photoactivation [Styring and Rutherford, 1987; Vermaas et al., 1988] which is the light driven process of Mn^{2+} oxidation and assembly in the OEC as water oxidation is activated (review: see Tamura and Cheniae, 1987).

D has now been identified as D2-Tyr-160 by site-directed mutagenesis studies in the cyanobacterium Synechocystis sp. PCC 6803 [Vermaas et al., 1988; Debus et al., 1988a]. The mutant was found to have a reduced rate of photoautotrophic growth (doubling time increased from 12 to 40 hrs) although the number of PS2 complexes remained comparable to the wild type [Vermaas et al., 1988]. This suggests that the interactions of D with the OEC play an important, but not essential, part in normal PS2 photosynthetic activity.

Z is the transient electron carrier linking the OEC with P680 [Babcock et al., 1983]. Time resolved EPR spectroscopy [Hoganson and Babcock, 1988] and optical experiments [Gerken et al., 1988] have shown that Z is the only intermediate in the step between $P680^+$ and water oxidation and is a tyrosine radical. Z is oxidised by $P680^+$ on the nanosecond time scale but the exact speed depends on the S-State in which the OEC is poised. In S_0 and S_1 the $t_{1/2}$ = 20 ns but in S_2 and S_3 the reaction is slower and biphasic (possibly due to different protonation states of PS2) with kinetics of 40 and 280 ns [Meyer et al., 1989]. The reduced reaction times must be due to coulombic effects of the accumulated charges in the OEC on Z. The E_m of the Z/Z^+ couple is estimated at +950-990 mV [Vass and Styring, 1991]. The EPR signal II_{vf} arises from Z^+ as the normal water oxidation cycle operates and Z^+ is reduced by the OEC. The $t_{1/2}$ for Z^+ reduction is again S-state dependent, taking 30 μs, 100 μs, 300 μs and 1.0-1.2 ms

respectively for the four S-state transitions between S_0 and S_4 (review: Babcock et al., 1989). Signal II_f is a slower kinetic variation observed when the OEC is inactivated and Z^+ has a longer life-time.

Site-directed mutagenesis studies have also been carried out on Z, identifying D1-Tyr-161 as the tyrosine residue [Debus et al., 1988b; Metz et al., 1989]. The mutant cannot grow photosynthetically although PS2 is assembled normally. This demonstrates the essential role of Z and also that the symmetry related tyrosine residue D cannot substitute for Z. This type of experiment is important because it provides evidence that current structural predictions are reasonably accurate because the residues studied were first suggested from D1/D2 reaction centre folding models.

1.4.6 The Oxygen Evolving Complex

The release of molecular oxygen from the oxidation of water is a four electron process:

$$2H_2O \dashrightarrow 4H^+ + 4e^- + O_2$$

The electrons available from this reaction are used to reduce $P680^+$. Therefore a coupling mechanism must exist to accommodate the multiple electron chemistry of water oxidation with the single electron reactions of primary photochemistry. This is achieved in the oxygen evolving complex (OEC) by the use of a charge storage system based on manganese. For each electron donated to $P680^+$ (via Z) a "positive hole" is left in the OEC. When sufficient

oxidising equivalents are accumulated, O_2 is evolved. Kok et al. (1970) proposed that five sequential redox states exist in the OEC (the 5 S-states) after they discovered that the flash-induced release of oxygen exhibited a periodicity of four. It is now well established that each flash (a single PS2 turnover) advances the OEC to the next S-state as an electron is donated to Z^+. When S_4 is reached O_2 is immediately evolved and the system circulates back to S_0 to begin another charge accumulation sequence (see Fig.1.7).

The OEC is located on the thylakoid lumen side of PS2 and is associated with three extrinsically bound proteins, the 17, 23 and 33 kDa extrinsic polypeptides. Removal of the 17 and 23 kDa subunits (with a 2 M NaCl wash) reduces the rate of oxygen evolution but activity can be recovered by addition of Cl^- and Ca^{2+}. Removal of the 33 kDa subunit (a 1 M Tris pH 8.8 wash) has a more drastic effect on O_2 evolution but some activity is restored by 200 mM Cl^- [Miyao et al., 1987]. This demonstrates that calcium and chloride ions are important cofactors necessary for oxygen evolution and that the extrinsic subunits enhance their binding in the OEC [Nakatani, 1984]. Details of the essential role played by these ions are unclear but have been the subject of much investigation (for reviews see Yocum (1991), Ca^{2+}, and Coleman (1990), Cl^-).

The OEC is thought to bind four Mn atoms per reaction centre [Yocum et al., 1981] although recently Witt (1991) proposed that the stoichiometry is actually six per RC, in

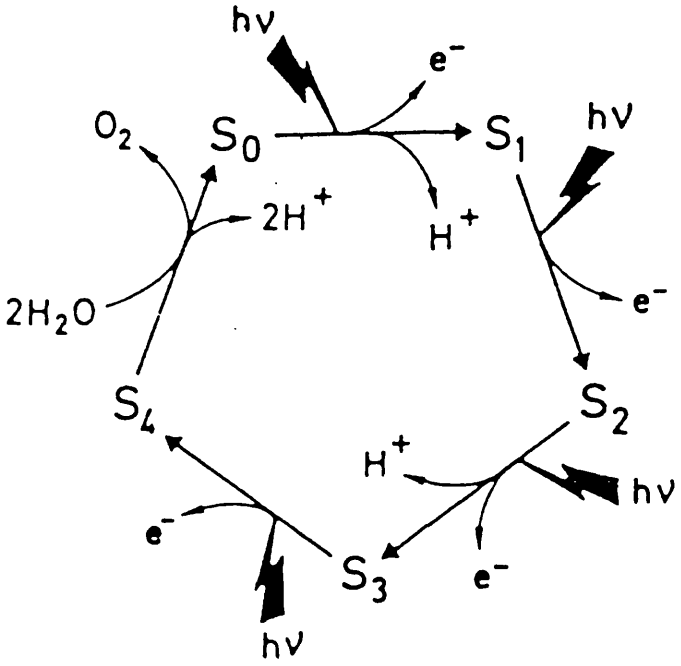

Figure 1.7 The S-state cycle of oxygen evolution. This is a kinetic model used to explain the accumulation of positive charges in the oxygen evolving complex (OEC) necessary to accommodate the four electron chemistry of water oxidation with the single electron reactions of primary photochemistry. As electrons are donated by the OEC to $P680^+$ (via Z) the cycle is advanced to the next S-state. Once S_4 is reached oxygen is evolved and the system cycles back to S_0 so that the accumulation of four oxidising equivalents can begin again. [Diagram from Rutherford, 1989]

two trimers. The exact location of the Mn complex is undetermined but the most probable site is the lumen side of the D1/D2 heterodimer [Rutherford, 1989]. The symmetry of the reaction centre could be maintained if the Mn complex is bound by ligands from both D1 and D2, as in the model of Dismukes (1988) (see Fig.1.8a). Alternatively the reaction centre symmetry could be broken with the Mn complex bound entirely by D1, possibly in the loop region between transmembrane helices I and II [Svensson et al., 1990]. However, there is no conclusive evidence in favour of one or the other of these options. The model of Dismukes (1988) relies on a primary structure analysis to identify the most likely carboxylate ligands for the manganese. The second option is again supported by sequence analysis but also by the different microwave power saturation characteristics of the D^+ and Z^+ EPR signals [Warden et al. 1976]. Z^+ is harder to saturate at high microwave powers indicating a stronger magnetic interaction with the Mn complex and hence Z is inferred to be closer to the complex than D (Z being D1-Tyr-161, part of transmembrane helix III). Svensson et al. (1990) analysed several D1 and D2 primary structures and concluded that the lumen exposed region of D1 was more conserved than that of D2. They also identified a number of strictly conserved carboxylate residues and histidines, possible manganese ligands, in the D1 loop between transmembrane helices I and II. They took these observations as evidence for the model described in Figure 1.8b.

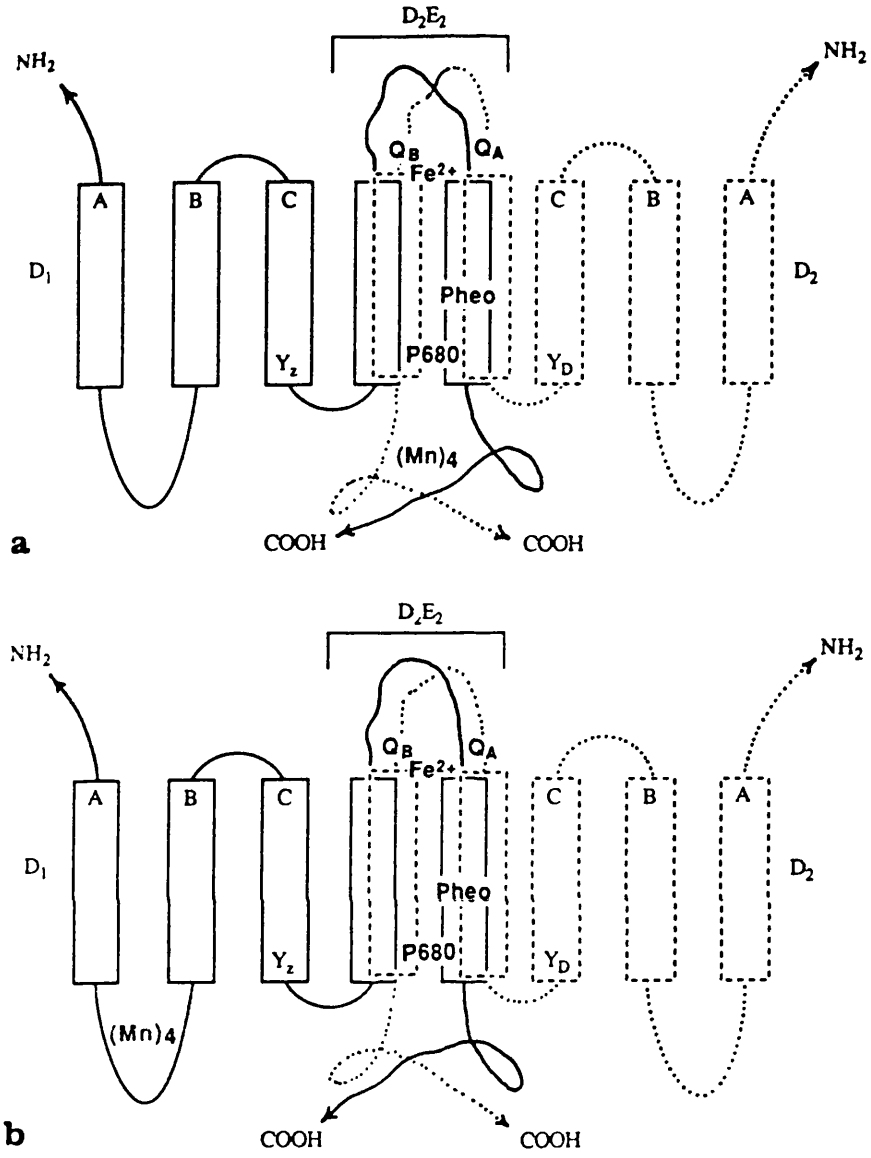

Figure 1.8 The location of the OEC manganese complex. Water oxidation is achieved through a charge accumulation system based on manganese. The exact location of this manganese complex is currently unknown but two possible models are described here. The five transmembrane helices of both D1 and D2 are shown. (a) The reaction centre symmetry could be maintained with the Mn complex bound by ligands from the C-termini of D1 and D2, or (b) the symmetry could be broken with the complex bound entirely by D1, possibly in the loop region between helices I and II. [Diagram from Babcock et al., 1989]

The exact nature of the manganese charge accumulation system, in terms of structure and valence state, is currently the biggest unresolved question in water oxidation studies. A variety of techniques have been used to study this problem.

Three EPR signals arising from the S_2 state have been identified, the multiline [Dismukes and Siderer, 1981], the g=4.1 signal [Zimmermann and Rutherford, 1984] and a g≈2 signal [Pace et al., 1991]. The multiline can be generated either by flash illumination of a PS2 sample at 273 K or illumination at 200 K. This results in a single charge separation event advancing the dark adapted samples, poised in S_1, to S_2. The multiline EPR signal seen in these samples is centred at g=2 and has at least 19 hyperfine lines. Dismukes and Siderer (1981) proposed that the signal was characteristic of a mixed-valence cluster of exchange coupled Mn ions. Illumination of a sample below 160 K generates a different signal, the g=4.1 signal, at the expense of the multiline signal [de Paula et al., 1985]. Both these S_2 EPR signals could arise from different conformations of a tetranuclear Mn complex [Zimmermann and Rutherford, 1986b] or from a bi(or tri)nuclear mixed-valence Mn cluster (giving rise to the multiline signal) in combination with a monomeric Mn^{4+} ion (the origin of the g=4.1 signal) [Hansson et al., 1987]. Recently however, EPR data has been obtained which argues against the latter possibility [Kim et al., 1990]. Pace et al. (1991) suggested that a ground state arising from a $Mn^{3+}Mn^{4+}$

heterodimer is responsible for the multiline and that the g=4.1 signal is observed when this heterodimer is coupled to a $Mn^{3+}Mn^{3+}$ dimer. Rutherford et al. (1991) are more in favour of a tetramer or a trimer/monomer arrangement being responsible for the EPR behaviour.

The Mn valence states and oxidation events in the S_0 to S_3 steps have been studied by UV-absorbance. Mn may be oxidised during each of the S-state transitions up to S_4 [Kretschmann et al., 1988]. Dekker et al. (1984) proposed that Mn^{3+} ---→ Mn^{4+} oxidation occurs on each of the three transitions up to S_3, but Lavergne (1987) suggested that the S_0 to S_1 transition is different and more likely to involve a Mn^{2+} ---→ Mn^{3+} oxidation. Data concerning the S_3 to S_4 step are difficult to obtain because S_4 immediately decays to S_0.

There is some evidence that the S_2 to S_3 transition may not involve manganese oxidation. Extended X-ray absorption fine structure (EXAFS) [Guiles et al., 1990] and EPR [Styring and Rutherford, 1988] experiments have provided data in favour of this proposal. Of particular relevance is an investigation by Boussac et al. (1989) into the effect of calcium depletion on the S-states. They concluded that calcium depletion blocks charge accumulation after S_3 and identified a new EPR signal appearing upon S_3 formation in these samples, probably arising from an oxidised organic radical in the OEC. Oxidation of this component, as opposed to manganese, was postulated to be the physiological step in the S_2 to S_3 transition. Boussac et al. (1990) identified the radical as oxidised histidine.

1.4.7 Photoinhibition

Photoinhibition is the blockage of normal PS2 electron transfer by exposure to high light conditions. The problem is complex and currently the molecular mechanism of the phenomenon is unclear, although it is related to the observation that *in vivo* the reaction centre subunit D1 rapidly turns over [Ohad *et al*., 1990]. The native rate of D1 turnover probably indicates that PS2 is susceptible to photoinhibition even during exposure to "normal" light intensities but D1 degradation is increased following photoinhibition treatment.

Aro *et al*. (1990) demonstrated that D1 degradation is temperature dependent, indicating an "enzymatic" breakdown. Photoinhibition treatment at temperatures below 7 °C inhibited electron transport but D1 degradation did not occur until the temperature was raised. Turnover is also light independent identifying photoinhibition as a two step process. Firstly there is the light induced blockage of e^- flow that acts as a trigger for the second step, the protease degradation of D1. Virgin *et al*. (1991) attempted to identify the protease responsible by using specific inhibitors. In isolated PS2 core particles they characterised the enzyme as a serine protease and concluded that one of the integral subunits in this complex is responsible for the proteolytic activity. Shipton and Barber (1991) suggested that D1 itself incorporates the protease activity, so that degradation is in fact autoproteolytic. Cleavage of D1 was found to be inhibited

by certain herbicides [Gaba et al., 1987] and a 23.5 kDa N-terminal breakdown product was identified in vivo [Greenberg et al., 1987]. This points to the Q_B binding site as the primary cleavage point.

The other important question in photoinhibition is the identity of the photoinduced lesion that inhibits electron flow. This problem has been studied in both oxygen evolving and non-O_2 evolving (eg. Tris washed or Cl^- depleted) PS2 preparations. When the OEC is fully functional the lesion appears to occur at the electron acceptor side of PS2. Styring et al. (1990) suggest that double reduction of Q_A is the first step in photoinhibition while Eckert et al. (1991) report that photoinhibition blocks the capacity to perform a stable charge separation between $P680^+$ and Q_A^-. The stress conditions causing photoinhibition could generate highly reactive radicals, possibly oxygen related, that may damage the cofactors or D1 itself. Sopory et al. (1990) found that free radical scavengers did indeed inhibit D1 degradation so a role for oxygen in this type of photoinhibition has not been ruled out.

When the OEC is inhibited, prior to photoinhibition treatment, D1 becomes more susceptible to degradation and the lesion seems to occur at the electron donor side of the reaction centre, possibly blocking e^- flow from Z to $P680^+$ [Eckert et al., 1991]. Jegerschöld et al. (1990) and Shipton and Barber (1991) speculated that under these conditions it is the accumulation of $P680^+$ and/or Z^+ that

triggers D1 degradation. This type of photoinhibition is oxygen independent [Jegerschöld and Styring, 1991] demonstrating that there are two different light dependent mechanisms for triggering D1 degradation. The relevance of these *in vitro* observations to the *in vivo* situation is uncertain and is as yet unresolved.

Hundal *et al*. (1990) studied the effects of photoinhibition in intact thylakoids. They concluded that disassembly of the PS2 core followed photoinhibition and that subunits migrated out of the grana into the stromal lamellae. Once there, reassembly of the core was proposed to occur with the insertion of a new D1 polypeptide.

It is likely that PS2 possesses protective mechanisms designed to cope with sudden increases in light intensity and dissipate excess excitation energy. Thompson *et al*. (1988) propose that a cyclic flow around PS2 via cytochrome b_{559} could serve such a protective function.

1.4.8 Cytochrome b_{559}

Cytochrome b_{559} was identified as an intrinsic component of the PS2 complex by Knaff and Arnon (1969) but its function remains unclear. The structure of cytochrome b_{559} has also been difficult to elucidate but it is now generally believed that the haem cross-links two different subunits, α and ß. The α-subunit was first isolated by Widger *et al*. (1984) as a 10 kDa polypeptide. The α-subunit gene, *psb*E, encodes an 83 residue, 9.16 kDa protein. Analysis of the chloroplast genome revealed that

adjacent to psbE there was a second gene encoding a 39 residue polypeptide that was transcribed with psbE in a bicistronic mRNA, psbF [Herrmann et al., 1984]. Each polypeptide has only a single histidine residue located within a ≈25 residue hydrophobic domain. The two proteins are co-purified in a 1:1 ratio [Widger et al., 1985] so the psbF protein was assumed to be a second type of cytochrome subunit, the ß-subunit. Babcock et al. (1985) used a variety of spectroscopic techniques to determine the spin state and ligand arrangement of the haem. They found that the haem iron is low-spin in both the oxidised and reduced states and suggested that the fifth and sixth ligands are histidine nitrogens. From this data the haem was suggested to be ligated in a αß heterodimer. However there are thought to be two copies of cytochrome b_{559} per PS2 complex [de Paula et al., 1985] so the cytochrome could exist as α_2 and $ß_2$ homodimers or a $(\alpha ß)_2$ tetramer. The heterodimer arrangement is the most likely because of the co-purification of the two subunit types and the transcription of the genes in a bicistronic mRNA. A double haem tetramer can be discounted because reaction centre preparations may have only one cytochrome b_{559} [Gounaris et al., 1990]. This suggests that one of the two cytochromes is more intimately connected with the reaction centre than the other which could reflect the heterogeneous behaviour observed for the cytochrome b_{559} population (see below). This raises another question as to how two structurally identical PS2 components are incorporated into two different binding

environments.

The protease accessibility and antibody experiments by Tae et al. (1988) on the α-subunit found evidence for a single transmembrane helix and indicated that the subunit is orientated with the C-terminus exposed to the lumen and the N-terminus on the stromal side. This would place the haem histidine ligand towards the stromal side of the membrane. In an αß heterodimer the ß-subunit must therefore have a similar orientation.

Cytochrome b_{559} is thought to be involved in some form of cyclic electron flow around PS2 because it has been shown to be both photooxidised by $P680^+$ [Knaff and Arnon, 1969] and photoreduced by plastoquinol [Whitmarsh and Cramer, 1978]. Arnon and Tang (1988) proposed that cytochrome b_{559} takes part in Q_BH_2 oxidation and the translocation of protons into the lumen as it cycles electrons back into the reaction centre. Alternatively cytochrome b_{559} may be involved in the protection of PS2 against photoinhibition. In PS2 samples where cytochrome b_{559} is already oxidised, illumination at cryogenic temperatures (below 150 K) generates a Chl cation. Thompson and Brudvig (1988) suggested that cytochrome b_{559} oxidation by $P680^+$ occurs via this Chl molecule. They speculate that photooxidation of this neighbouring Chl is a low quantum yield event that occurs during normal photosynthetic activity. In an optical study [Thompson et al., 1988] Chl oxidation was thought to occur in 3-15% of reaction centres, depending on the S-state. The presence

of a long lived Chl radical could be the first step in photoinhibition. Their model proposed that the cytochrome prevents photoinhibition by reducing Chl^+ and accepting electrons from Q_BH_2 in a cyclic flow.

It is believed that the two copies of cytochrome b_{559} per PS2 have different redox potentials. These different forms can be observed by EPR. In PS2 preparations the low potential (LP) haem is normally oxidised in the dark by the ambient redox potential, producing a g_z resonance at g=2.93. The high potential (HP) haem is the primary electron donor to $P680^+$ when PS2 is illuminated at 77 K and has a photooxidised g_z resonance at g=3.06 [Malkin and Vänngård, 1980; Nugent and Evans, 1980]. Treatments that remove extrinsic subunits of the OEC, such as 1 M Tris or 2 M NaCl washing, are known to alter the mid-point potentials of the cytochrome(s). A third cytochrome b_{559} potential has been identified, the intermediate potential (IP) [Horton and Croze, 1977]. Thompson et al. (1989a) proposed that in BBYs there is one HP haem (375 mV) and one IP haem (230 mV), a similar situation existing in thylakoids. Removal of the 17 and the 23 kDa extrinsic PS2 subunits converts this to one IP haem (170 mV) and one LP haem (5 mV). EPR studies of the cytochrome usually associate a drop in mid-point potential with a decrease in g-value. Babcock et al. (1985) suggest that the HP is maintained by deviations of the histidine ligand imidazole rings from a parallel orientation. When this orientation is relaxed the mid-point potential is lowered. However, Thompson et al.

(1989a) did not observe significant g-value changes that would arise from such a relaxation. They proposed that the HP is caused by a hydrophobic environment around the haem and that removal of extrinsic subunits increases solvent exposure and lowers the potential.

The significance of these different potentials is still obscure. It may be that the heterogeneity is caused by damage occurring during PS2 preparation.

1.4.9 Light Harvesting Components

PS2 has three different categories of chlorophyll binding proteins as well as the D1/D2 reaction centre. They can be grouped according to their function, Chl a/b ratio and relationship with the reaction centre.

The first group consists of the Chl a binding proteins CP47 and CP43 (Chlorophyll Protein + molecular weight in kDa) and can be called the **proximal antenna** [Hansson and Wydrzynski, 1990]. They are closely associated with the reaction centre and are included in the complex known as the PS2 core. Primary structure analysis indicated that they are related to each other with each polypeptide possibly having six transmembrane helices. They each have sufficient histidine residues to bind approximately 15 chlorophylls although amino acid ligands may not be the predominant method of Chl binding in other light harvesting components [Kühlbrandt and Wang, 1991]. They probably transfer excitation energy directly to the reaction centre from the LHCII.

The second and third groups make up the **distal antenna** [Hansson and Wydrzynski, 1990], more commonly known as the **LHCII**. The exact structure and stoichiometry of the LHCII has been difficult to determine because all the subunits are related and are therefore of a similar size. The subunits bind both Chl *a* and *b* and are encoded by nuclear genes of the *cab* (Chl *a*/*b* genes) family [Green *et al.*, 1991].

The second group includes CP29 and CP26 (possibly CP24 as well) and can be called the **inner LHCII component** as they are closely associated with the PS2 core [Bassi and Dainese, 1990]. They are copurified with the PS2 core in oxygen evolving PS2 preparations [Barbato *et al.*, 1989] which lack the bulk of the LHCII, the **peripheral LHCII component**. CP29 and CP26 have a relatively high Chl *a*/*b* ratio of 3-5 and are thought to act as linkers between (or anchors for) the PS2 core and the peripheral LHCII. The number of inner LHCII components per P680 is disputed. Barbato *et al.* (1989) propose a stoichiometry of 3:3:1 for the CP29:CP26:P680 ratio while Dainese and Bassi (1991) suggest 1.5:1.5:1.

The third group of chlorophyll binding proteins, the peripheral LHCII, form the main body of the LHCII and consist of several different apoproteins, all approximately 25 kDa. The subunits are arranged in oligomeric complexes, probably trimers [Butler and Kühlbrandt, 1988], and have a Chl *a*/*b* ratio slightly greater than one. Kühlbrandt and Wang (1991) recently

presented a three dimensional structural model, to 6 Å resolution, of a peripheral LHCII trimer. The three monomers of the complex each have three transmembrane α-helices and bind fifteen chlorophylls, 8 Chl *a* and 7 Chl *b*.

The peripheral LHCII is involved in regulatory changes in the size of the light harvesting component in response to changing light intensities. It is proposed that there are two sub-populations of peripheral LHCII, the mobile and non-mobile complexes. When a low light adapted plant (one that has a large LHCII) is subjected to high light conditions the plastoquinone pool quickly becomes reduced. The increased level of plastoquinol is thought to activate a protein kinase which reversibly phosphorylates certain LHCII components, causing the migration of the mobile element of the peripheral LHCII out of the granal stacks and into the stromal lamellae [Anderson and Andersson, 1988]. A return to low light conditions involves the activation of a phosphorylase so that the mobile LHCII complexes are de-phosphorylated and are able to move back into the grana. These movements are known as the State I and State II transitions.

1.5 Aims Of This Thesis

I aim to examine:

1. The bicarbonate dependent behaviour of the Q_A iron-semiquinone EPR signal.
2. Loss of bicarbonate binding in PS2 preparations made with the detergent OGP and any possible relationship between this and Q_A loss from reaction centre preparations.
3. The split pheophytin signal, specifically the dependence of signal splitting on bicarbonate, and whether the redox titration behaviour of this signal is in any way related to HCO_3^-.
4. The susceptibility of the electron acceptor region to attack by trypsin.

These investigations were devised to advance current knowledge of the PS2 electron acceptors subsequent to the reaction centre special chlorophyll P680. Most of the work has been driven by a desire to study more closely the influence of bicarbonate over the quinone binding region.

2. MATERIALS AND METHODS

2.1 Types Of PS2 Preparation

2.1.1 Isolation Of PS2 Particles (BBYs) From Thylakoid Membranes

BBYs were prepared from either market spinach (Spinacea oleracea) or 14 day-old greenhouse grown pea seedlings (Pisum sativum var Feltham First) using the method of Berthold, Babcock and Yocum (1981) with modifications by Ford and Evans (1983).

In the case of spinach the leaves were first washed and the large leaf stems and ribs removed while the pea leaves required no pretreatment. The plant material was then ground in a Waring blender for 15 seconds in ice-cold 0.33 M sorbitol, 20 mM Mes-NaOH, 0.2 mM $MgCl_2$ pH 6.5 (grinding medium) with additional sodium ascorbate (5 mM). This mixture was filtered through 8 layers of muslin and the filtrate centrifuged at 3,000 g for 5 mins to obtain a chloroplast pellet. The pellet was resuspended in a hypotonic solution of 5 mM $MgCl_2$ for 60 secs to osmotically shock the chloroplasts and lyse the envelope, followed by addition of an equal volume of double concentration grinding medium. A thylakoid pellet was obtained by centrifugation at 3,000 g for 20 mins. This was resuspended in 20 mM Mes-NaOH, 25 mM NaCl, 5 mM $MgCl_2$ pH 6.3 (resuspending medium) and left on ice, in the dark, for a period of 2 hrs to promote thylakoid stacking.

Triton X-100 (20% (w/v) stock) and resuspending medium were then added so that the final detergent and chlorophyll concentrations were 5% (w/v) and 2 mg/ml. The mixture was inverted twice and left to digest for 25 mins then centrifuged at 40,000 g for 30 mins. The final BBY pellet was resuspended with the previous buffer plus 20% (v/v) glycerol (as the cryoprotectant) then stored at 77 K.

It is essential that buffers and samples are kept at ≈ 4 °C, and that each procedure, once the chloroplasts are obtained, is carried out under subdued lighting. These measures are necessary to obtain preparations with the greatest possible rates of oxygen evolution and to avoid photoinhibition.

2.1.2 Preparation Of OGP PS2 Core Particles

OGP PS2 core particles were prepared using a method based on that of Ghanotakis, Demetriou and Yocum (1987). BBYs were resuspended in 50 mM Hepes-NaOH, 0.4 M sucrose, 10 mM NaCl, 50 mM $NaHCO_3$ pH 7.5 to a chlorophyll concentration of 2.5 mg/ml. To this was added an equal volume of 50 mM Hepes-NaOH, 1.0 M sucrose, 0.8 M NaCl, 50 mM $NaHCO_3$, 75 mM octyl glucopyranoside pH 7.5. The digestion mixture was incubated for 12 mins on ice, in the dark, then diluted with 2 volumes 50 mM Hepes-NaOH, 1.0 M sucrose, 0.4 M NaCl, 50 mM $NaHCO_3$ pH 7.5, followed by 30 mins centrifugation at 40,000 g. The supernatant was dialysed for 60 mins against a buffer containing 50 mM Hepes-NaOH, 50 mM NaCl, 50 mM $NaHCO_3$ pH 7.5, then

centrifuged at 40,000 g for 60 mins. The resulting pellet was resuspended in 20 mM Hepes-NaOH, 15 mM NaCl, 5 mM $MgCl_2$, 50 mM $NaHCO_3$, 20% (v/v) glycerol pH 7.5 and stored at 77 K. The major differences between this method and that of Ghanotakis et al. (1987) are the raised pH, from 6.0 to 7.5, the addition of bicarbonate to every step and the omission of $CaCl_2$. Also, a greater OGP concentration was used with a two minute longer digestion. OGP PS2 core particles were also prepared at pH 6.0 using the same buffers as above but Mes was substituted for Hepes and $NaHCO_3$ was omitted.

2.1.3 Preparation Of Dodecylmaltoside PS2 Core Particles

The method employed for dodecylmaltoside (DM) digestion of pH 7.5 OGP PS2 core particles was similar to that developed by Dekker et al. (1989). The OGP prepared particles were resuspended in 0.5% (w/v) DM, 20 mM Hepes-NaOH pH 7.5, 20 mM NaCl, 10 mM $MgCl_2$, 1.5% (w/v) taurine, 50 mM $NaHCO_3$, to 0.5 mg/ml Chl then incubated for 60 mins before being mixed with 2 volumes of the above buffer minus detergent. The suspension was then loaded onto a fast flowing Q-sepharose column (Pharmacia ion exchange media). The column was washed extensively with 20 mM Hepes-NaOH pH 7.5, 20 mM NaCl, 10 mM $MgCl_2$, 1.5% taurine, 50 mM $NaHCO_3$, 0.03% (w/v) DM and 30 mM $MgSO_4$ until the eluate was colourless. The CP47, CP43, D1, D2, cytochrome b_{559} (DM PS2 core) complexes were eluted using the previous buffer plus 100 mM $MgSO_4$. The detergent digestion and column steps were

carried out in the dark at either 24 or 4 °C (see results section 3.3). The Dekker procedure is normally carried out at pH 6.5 without bicarbonate and includes a second Q-sepharose step to ensure effective purification and an adequate concentration of final particles. I found that a single column step was sufficient and that concentrated samples for EPR analysis could be rapidly obtained by employing a PEG precipitation method (modified from McTavish et al. (1989)). 0.325 g PEG 3350 per ml was added to the PS2 particles and the mixture stirred continuously for 30 mins. The suspension was then centrifuged for 20 mins at 40,000 g and the pellet resuspended in 20 mM Hepes-NaOH pH 7.5, 20 mM NaCl, 1.5% (w/v) taurine, 50 mM $NaHCO_3$, 0.03% (w/v) DM, 20% (v/v) glycerol and stored at 77 K.

2.1.4 Reaction Centre Preparations

D1/D2/cytochrome b_{559} reaction centre complexes were prepared by two methods, similar to those described by Dekker et al. (1989).

The first involves Triton X-100 digestion of DM PS2 core complexes. The core particles were adjusted to 0.3 mg/ml Chl, 4% (w/v) TX-100, 20 mM Hepes-NaOH, 50 mM $NaHCO_3$ pH 7.5 and incubated on ice for 15 mins. The digest was then loaded onto a Q-sepharose column equilibrated at 4 °C with 20 mM Hepes-NaOH, 50 mM $NaHCO_3$, 0.2% (w/v) TX-100, 30 mM NaCl pH 7.5 and washed for 2-3 hrs with the above buffer. The reaction centres were eluted with this buffer plus 190 mM NaCl and precipitated using the PEG method

described in the preparation of DM PS2 core complexes. The pellet obtained was resuspended in 20 mM Hepes-NaOH, 50 mM $NaHCO_3$, 0.2% (w/v) TX-100, 20% (v/v) glycerol pH 7.5 and stored at 77 K.

The second method uses dodecylmaltoside and the chaotrope lithium perchlorate. DM PS2 core complexes were adjusted to 1.5% (w/v) taurine, 20 mM Hepes-NaOH pH 7.5, 50 mM $NaHCO_3$, 20 mM NaCl (buffer A) plus 2 M $LiClO_4$, 0.5% (w/v) DM at 1 mg/ml Chl then incubated on ice for 15 mins. After this the digest was dialysed against buffer A for 2 hrs then diluted 1:3 with this buffer + 0.03% (w/v) DM. The mixture was loaded onto a Q-sepharose column equilibrated with buffer A + 0.03% (w/v) DM and 30 mM $MgSO_4$ and washed extensively. The reaction centres were eluted with 100 mM $MgSO_4$ and precipitated as above. The final pellet was resuspended in buffer A + 0.03 (w/v) DM and 20% (v/v) glycerol and stored at 77 K.

2.2 Oxygen Evolution Measurements

Measurements of oxygen evolving capacity were made with a Clark type oxygen electrode at 20 °C. For specific details of each assay, ie. chlorophyll concentration, electron acceptor used or any other specific additions, see the appropriate text or figure legend. All assays were performed in pH 6.3 resuspending medium (see BBY prep. section 2.1.1).

The sample was illuminated with a 650 W light source directed through a heat filter and the rate of oxygen

evolution measured using the amount of oxygen released in the first minute of illumination (μmol O_2/mg Chl/hr).

2.3 Trypsin Digestion Of PS2

Trypsin treatment of BBY PS2 samples was carried out at room temperature in the dark in 20 mM Mes-NaOH, 15 mM NaCl, 5 mM $MgCl_2$ pH 6.3. Chlorophyll and trypsin concentrations were 33 and 66 μg/ml respectively. After the specified time the reaction was stopped by the addition of 100 μg/ml trypsin inhibitor. Samples for EPR analysis were concentrated by centrifugation at 40,000 g and resuspended to 5 mg/ml in the above buffer plus 20% (v/v) glycerol. Oxidised non-haem iron samples were resuspended to 10 mg/ml in a 20 mM Hepes-NaOH, 15 mM NaCl, 5 mM $MgCl_2$ pH 7.5 buffer and incubated for 45 mins in the dark with 10 mM potassium ferricyanide before freezing. All dark adapted samples were frozen and stored at 77 K. Samples used for oxygen electrode experiments were digested in the electrode itself using the above concentrations. Oxygen evolution assays used either 3 mM potassium ferricyanide or 1 mM DMBQ as the electron acceptor and, where added, DCMU was used at a concentration of 7 μM.

2.4 Determination Of Chlorophyll Concentration

The concentrations of chlorophyll a and b in a sample were calculated by the method described by Arnon (1949) using the extinction coefficients given by MacKinney (1941) for chlorophyll extracted in 80% (v/v) acetone (pathlength

1 cm). The contributions to absorbance by each chlorophyll at 663 and 645 nm is given by:

$$A_{663} = 82.04 \text{ Chl } \underline{a} + 9.27 \text{ Chl } \underline{b}$$

$$A_{645} = 16.75 \text{ Chl } \underline{a} + 45.6 \text{ Chl } \underline{b}$$

A is the absorbance at the respective wavelength and Chl is the mg/ml concentration of each chlorophyll type. When the above simultaneous equations are solved:

$$\text{Chl } \underline{a} = 0.0127\ A_{663} - 0.00259\ A_{645}$$

$$\text{Chl } \underline{b} = 0.0229\ A_{645} - 0.00467\ A_{663}$$

A value for the total chlorophyll, both a and b, can be calculated using the absorbance at 652 nm:

$$\text{Chl} = 0.029\ A_{652}$$

In practice the chlorophyll from either 25 or 50 µls of sample was extracted in a total volume of 10 mls 80% acetone (v/v) and then filtered. Therefore a dilution correction factor of either 400 or 200 was necessary. All absorbance spectra and measurements were made using a Phillips PU 8740 UV/VIS scanning spectrophotometer.

2.5 Inactivation Of Oxygen Evolving Capacity

Inactivation of PS2 oxygen evolving capacity was achieved by removal of the extrinsic polypeptides and the manganese complex on the thylakoid lumen side. PS2 particles were centrifuged at 40,000 g for 30 mins and resuspended in 1 M Tris-HCl, 1 mM EDTA pH 8.8 to a

concentration of 1 mg/ml Chl, in the case of BBYs, or to 0.5 mg/ml Chl when using OGP PS2 core particles. The mixture was incubated on ice for 60 mins with occasional stirring then centrifuged as above and resuspended in the appropriate buffer, depending on the particle type. The supernatant from this spin was concentrated in dialysis tubing against solid PEG 15,000-20,000 and the extrinsic polypeptides removed were analysed using SDS-PAGE. The PS2 particles were subjected to a further centrifugation step and resuspended in a 20% (v/v) glycerol buffer if the particles were to be stored at 77 K.

2.6 Polyacryalamide Gel Electrophoresis

The analysis of the polypeptide composition of the different preparations in use was performed using SDS-PAGE with a method based on that of Chua (1980). Optimum separation was found using 15% acrylamide resolving gels with 6 M urea to improve resolution. The samples were solubilised by mixing 1:4 with 4% (w/v) SDS, 5% (v/v) mercaptoethanol, 0.1% (w/v) bromophenol blue, 6 M urea, 7.5% (v/v) glycerol, 100 mM Tris-HCl pH 6.8. These were left overnight at room temperature before use.

The gels were run at a constant current of 20 mA for several hours then stained overnight with 10% (v/v) glacial acetic acid, 10% (v/v) methanol, 0.1% bromophenol blue. Destaining was carried out using the same solution minus the dye and where gels were dried they were first equilibrated with this solution plus 5% (v/v) glycerol.

The gel compositions were as follows:

	RESOLVING	STACKING
40% acrylamide/1.07% bis-acryl	11.25 ml	1.5 ml
5X lower reservoir buffer	6 ml	--------
4X stacking gel buffer	--------	2.5 ml
10% (w/v) SDS	0.4 ml	0.1 ml
urea	10.8 g	3.6 g
TEMED	20 µl	10 µl
10% (w/v) ammonium persulphate	60 µl	100 µl
TOTAL VOLUME	30 ml	10 ml

40% acrylamide/1.07% bis-acrylamide (w/v) solution obtained from Sigma, 5X lower reservoir buffer 0.42 M Tris-HCl pH 9.18, 4X stacking gel buffer 54 mM Tris-H_2SO_4 pH 6.1 and 20X upper reservoir buffer 40 mM Tris-HCl, 40 mM borate, 2% (w/v) SDS pH 8.64. The ammonium persulphate was prepared fresh each time.

The samples were run alongside Sigma Dalton Mark VII-L molecular weight markers but identification of the bands obtained was primarily through comparison with known polypeptides (eg. RC components and PS2 extrinsic polypeptides) and the assignments of other researchers. The reaction centres were obtained from the photosynthesis group at Imperial College where the constituent subunits had previously been identified by Western blotting.

2.7 Redox Potentiometry

Redox potentiometry was carried out according to the method presented by Dutton (1978). The sample was stirred and kept under anaerobic conditions by continuous bubbling with O_2-free nitrogen and maintained at 10 °C using a Churchill thermostatic pump. To ensure the absence of oxygen the nitrogen was first passed through a 1% (w/v) sodium dithionite, 0.005% (w/v) methyl viologen, 100 mM Tris-HCl pH 8 solution in a Drechsel bottle and then a second flask of 100 mM Tris-HCl pH 9.

The redox potential (all potentials quoted are relative to the hydrogen electrode) was raised or lowered by microlitre additions of freshly prepared solutions of either 20 mM potassium ferricyanide or 0.6% (w/v) sodium dithionite (kept anaerobic) in 100 mM Tris-HCl pH 8. After any addition(s) the sample was left to equilibrate for at least 10 mins before an EPR sample was taken. Samples were frozen immediately in liquid nitrogen. The titrations were carried out in almost complete darkness with the only illumination coming from the green filtered safe light and electrode LED displays.

The redox potential was measured with a platinum electrode used in conjunction with a calomel reference electrode (P101 and K401 respectively, obtained from Radiometer, Copenhagen). The electrodes were calibrated using 1. a saturated quinhydrone solution in 100 mM potassium hydrogen phosphate pH 7 (E_{m7} +286 mV), pH dependent and 2. an equimolar solution (5 mM) of potassium

ferricyanide and potassium ferrocyanide in 100 mM Tris-HCl pH 8 (E_m +420 mV), pH independent. At 10 °C the E_h of the calomel electrode is +254.1 mV.

To ensure rapid and accurate measurements of the redox potential mediators were employed over the +100 to -350 mV range. These were:

	E_{m7} (mV)
thionine blue	+60
methylene blue	+11
indigotetrasulphonate	0
Janus green	-96
phenosaffranine	-255
saffranine T	-289
benzyl viologen	-311
diquot	-350

All mediators were used at a concentration of 20 μM. In certain titrations anthraquinone-1,5-disulphonate (-170) was also included (see results).

All titrations (sections 3.4.2/3) were carried out at pH 7.0 in a 100 mM Hepes-NaOH, 15 mM NaCl, 5 mM $MgCl_2$ pH 7.0 buffer. Where necessary 50 mM sodium bicarbonate or formate was added. The titrations were carried out on OGP PS2 preparations Tris-washed to inactivate the OEC and remove the possibility of Mn release during reduction. The data for the Q_A/Q_A^- titrations were obtained from the same samples used for the pheophytin split signal titrations. The dark $Q_A^-Fe^{2+}$ EPR signal was measured first and then the

split signal generated by 200 K illumination. The samples in section 3.4.1 were also Tris-washed but resuspended in the appropriate buffer depending on which OGP PS2 preparation was being used, either pH 6.0 or 7.5.

2.8 Electron Paramagnetic Resonance

2.8.1 EPR Theory

Electron paramagnetic resonance (EPR or ESR, electron spin resonance) spectroscopy is a sensitive technique used in the study of molecules with unpaired electrons, known as paramagnets.

The spin of an electron around its own central axis creates an associated magnetic field, termed the magnetic dipole moment, and it is this vector quantity that is utilised in EPR. The spins of an electron pair are opposed, creating magnetic dipole moments of equal magnitude but of opposite direction and therefore the net field is zero. However, molecules with unpaired electrons are paramagnetic because they have a net magnetic dipole moment that will interact with an externally applied magnetic field. The application of an external magnetic field splits the electrons into two subsets with quantum numbers $M_s = +/- \frac{1}{2}$ as the magnetic moments become orientated either parallel or antiparallel to the external field (see Fig.2.1). The latter alternative is a less favourable, high energy, state. Therefore, an energy difference exists between the two sub-populations and if electromagnetic

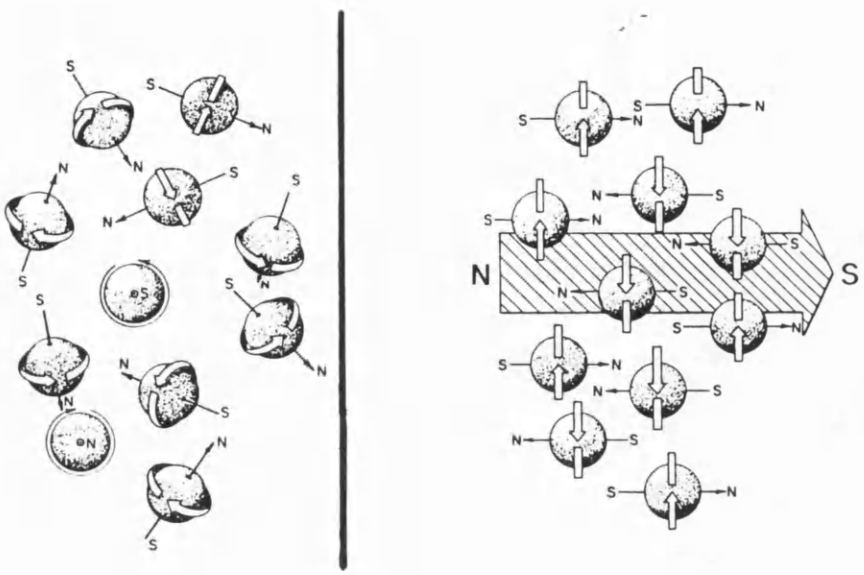

Figure 2.1 The behaviour of electrons in an externally applied magnetic field. In the absence of a magnetic field the orientation of the magnetic dipole moment of an electron is random. However, when an external magnetic field is applied to the system the electron magnetic dipole moment can take up one of two possible orientations, either parallel or antiparallel to the field. The former option is the low energy state, and therefore the most probable, while the latter is the high energy state and consequently will be less populated. The distribution of electrons in these sub-populations is determined by the Boltzmann distribution (see equation 3 section 2.8.1). [Diagram from Swartz, Bolton and Borg: Biological Applications of Electron Spin Resonance, Wiley interscience]

radiation of the correct quantum energy, ie. the correct frequency, is applied to the system it is possible to induce transitions between the two energy levels according to the relationship:

1. $$E = h.v$$

E = energy difference, h = Planck's constant (6.626×10^{-34} J s), v = the frequency of the radiation in hertz. In EPR the frequencies necessary to induce energy transitions and so meet the resonance condition are in the microwave region.

The magnitude of the energy difference between the two energy levels is dependent on the magnetic field H:

2. $$h.v = g.B.H$$

B = the Bohr magneton (9.27408×10^{-24} J/T), g = a value characteristic of the paramagnet being studied.

From equation 2 it is obvious that the frequency, and thus the energy splitting, will increase with increasing magnetic field (see Fig.2.2) and so resonance can be observed by either varying the frequency at a fixed magnetic field or vice versa. In practice the frequency is fixed and the microwave absorbance over a range of field values measured.

To obtain a net absorbance of microwaves there must be favoured occupation of the more stable low energy state. This is always the case where a system is in thermal equilibrium and is calculated as the Boltzmann distribution, given as a ratio:

3. $$N_{+\frac{1}{2}} / N_{-\frac{1}{2}} = 1 - (h.v/k.T)$$

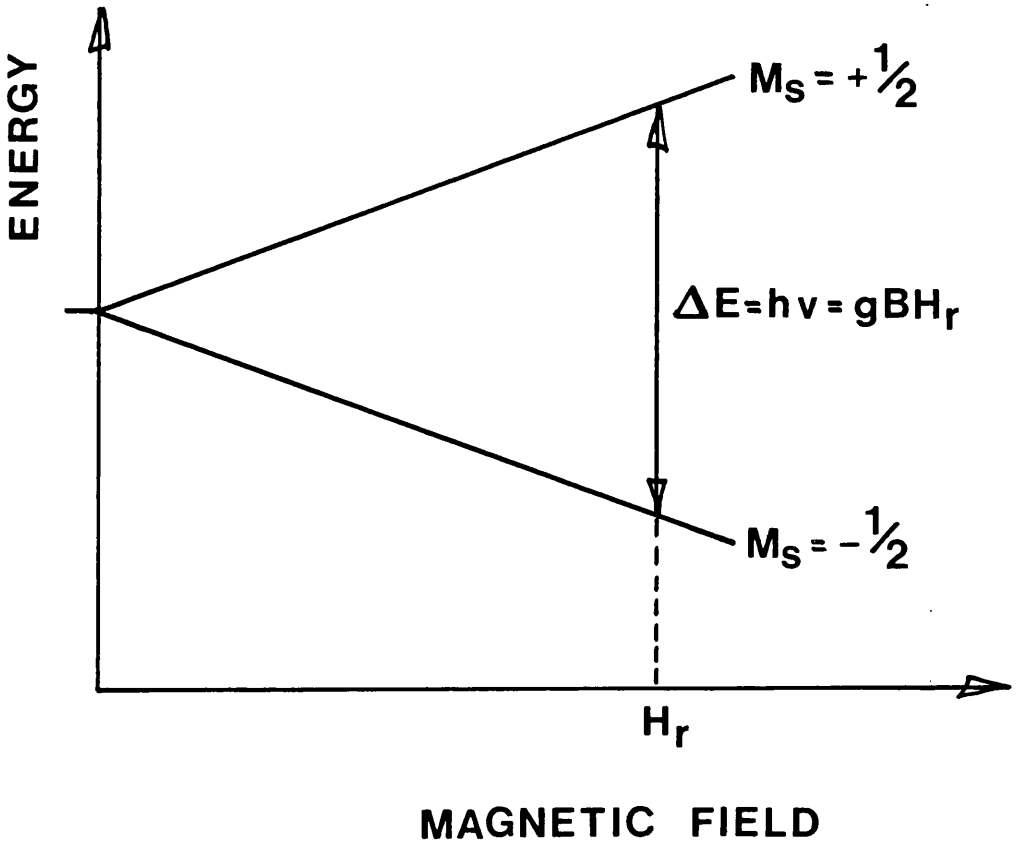

Figure 2.2 Electronic energy levels as a function of the magnetic field strength. The energy difference between the possible electron orientations increases with increasing magnetic field strength. Resonance can either be achieved by varying the magnetic field at a fixed microwave frequency of vice versa. E, energy difference; h, Planck's constant; v, frequency of radiation; g, g-value; B, Bohr magneton; H_r, magnetic field at resonance; M_s, electron spin quantum number. [Diagram from Swartz, Bolton and Borg: Biological Applications of Electron Spin Resonance, Wiley interscience]

N = number of electrons in each energy state, T = absolute temperature, k = Boltzmann's constant (1.381×10^{-23} J/K). At 5 K with a microwave frequency of 9.05 GHz the ratio is 0.9132 so the net absorbance is due to only a small proportion of the unpaired electrons. Low temperatures increase the population difference so a greater EPR signal intensity is obtained as the net microwave absorbance increases. This is one reason why the EPR signals in these studies are viewed at cryogenic temperatures because the signal intensity at a fixed frequency will increase proportionally with 1/T, but other factors are involved which help determine the actual temperature chosen.

In EPR the signal to noise ratio of the detection system is improved by the use of a field modulation technique that superimposes a low amplitude AC magnetic field on the DC field. A consequence of this is that the signal output is a first derivative of the microwave absorbance spectrum so an integration step is necessary to obtain absorbance peaks.

2.8.2 Relaxation Times And Power Saturation

The electrons in a spin system must be returned to the original Boltzmann distribution after microwave energy absorbance, otherwise the population difference that creates the net absorbance would quickly disappear after the initial energy input. This is normally avoided because mechanisms exist where $M_s+\frac{1}{2}$ electrons are allowed to "relax" to the low energy state. The energy released is

transferred to the lattice and dissipated through radiationless processes. The rate of spin relaxation is characterised by the spin-lattice relaxation time T_1 and the spin-spin relaxation time T_2. T_1 is a measure of the efficiency of energy transfer to the lattice and T_2 accounts for spin dephasing through interactions with neighbouring spin systems. If the microwave power is increased the spin system will eventually reach a point where the relaxation processes cannot return electrons to the low energy state fast enough. This is saturation and occurs as the Boltzmann distribution equals zero, so no EPR signal is observed. If log (I/√P) is plotted against log P (I = signal intensity, P = microwave power) then it is possible to calculate $P_{\frac{1}{2}}$, the power at half saturation (for example see Fig. 3.5a). This is important for optimising the conditions for signal observation where I is directly proportional to P and also for spin quantification studies.

At low temperatures the relaxation processes slow down so that the life-times of the high energy states are longer. Consequently the spin system will saturate at lower microwave powers. Increased life-times also effect the signal linewidth. The signals become narrower as the high energy states become more defined and the paramagnet comes into resonance over a reduced range of applied fields. At higher temperatures relaxation is faster and the high energy states become less well defined so that eventually the signal may become so broad that it cannot be detected. This is especially relevant where transition

metals are involved as the efficiency of relaxation is increased even at lower temperatures due to strong spin-orbit coupling. This can lead to extreme broadening of the signal so that temperatures as low as 4 K can be necessary to see a signal.

2.8.3 g-values

For a "free" electron the value of "g" is 2.00232 (using X-band microwaves resonance will occur around ≈ 320 mT) but this is only the case when the magnetic field experienced by the electron is solely due to the applied magnetic field. Often the electron is also subject to local magnetic fields generated within the molecule that add or subtract from the total field. This means that resonance will occur at higher or lower external fields away from the "free" electron value. To accommodate this a variable "g" factor is included in the resonance equation (eq^{n} 2) and so the g-value can be used as a marker for the position of a signal within an EPR spectrum. Variations in g-values arise from magnetic interactions with the parent and neighbouring nuclei and, in the case of transition metals, orbital contributions from the ligand electrons.

2.8.4 Experimental Details

EPR spectrometry was performed at cryogenic temperatures using a Jeol RE1X X-band spectrometer with 100 kHz field modulation and an Oxford Instruments ESR 9 liquid helium cryostat. Up until January 1990 a Jeol FE1X machine

was used which lacked the sensitivity of the RE1X model. Therefore spectra obtained before this date were subject to a reduced signal to noise ratio.

EPR samples were placed in calibrated quartz tubes of internal diameter 3 mm and stored at 77 K. In general the samples were dark adapted at 4 °C for at least one hour before freezing. More specific details about each sample and the EPR conditions used may be found in either the relevant text or figure legend.

Where it was necessary to illuminate samples several different methods were used: A. at 77 K, samples were placed in liquid nitrogen in a silvered dewar and illuminated from above by a 650 W light source for 10 minutes. B. at 200 K in an unsilvered dewar using a solid CO_2/ethanol mixture with illumination from the side with the above lamp. C. at room temperature the samples were placed in an unsilvered dewar and illuminated with a 650 W light source through an H_2O heat filter. D. some samples were also frozen to 77 K under continuous illumination from the 650 W lamp.

EPR spectra were recorded on a Dell microcomputer using data acquisition and manipulation software written by M.C.W.Evans and I.Davis in the ASYST language. The spectra presented are the average of at least 3 scans to improve the signal to noise ratio.

3.1 Photosystem Two Semiquinone EPR Signals

In purple bacteria the EPR lineshapes of the Q_A and Q_B semiquinones are dependent on a magnetic interaction with the non-haem iron. A semiquinone usually has a g=2 radical type EPR signal but in the reaction centre situation, Q^- is involved in an exchange interaction with the non-haem iron [Butler *et al.*, 1984] so that the main resonances are observed at g-values less than 2. For this reason the signals are often referred to as arising from the iron-semiquinone complex, Q^-Fe^{2+}. In the purple bacteria both $Q_A^-Fe^{2+}$ and $Q_B^-Fe^{2+}$ have similar EPR signals at g=1.8 [Butler *et al.*, 1984].

The primary and secondary plastoquinones of PS2 also have characteristic EPR signals that are influenced by the non-haem iron but the situation is somewhat different to that seen in purple bacteria. A signal from $Q_A^-Fe^{2+}$ in PS2 was first identified by Nugent *et al.* (1981) at g=1.8, in the green alga *Chlamydomonas reinhardii*. The signal was found to be similar to the semiquinone signals of the purple bacteria. Stable reduction of Q_A can be achieved either by chemical reduction, freezing under illumination (Q_B is doubly reduced) or by illumination at temperatures below 230 K where transfer of electrons to Q_B is thermodynamically unfavourable.

Further investigations by Rutherford and Zimmermann (1984) revealed a second form of the $Q_A^-Fe^{2+}$ EPR signal, the g=1.9 signal. They found that the yield of each signal was

pH dependent so that at pHs greater than 6 the g=1.9 form of the signal predominated. This was later shown to reflect the influence of bicarbonate over the $Q_A^-Fe^{2+}$ signal [Vermaas and Rutherford, 1984] and to be related to the effect this anion has over the electron transfer behaviour of the quinone binding region.

Formate is often used as an electron transport inhibitor in studies into the bicarbonate effect as this anion is thought to displace bicarbonate from its binding site(s) at or near the non-haem iron. Treatment of PS2 samples with formate dramatically increased the size of the g=1.8 iron-semiquinone signal [Vermaas and Rutherford, 1984].

A third PS2 EPR signal has been assigned to Q_A. McDermott et al. (1988) speculate that the g=1.65 signal, observed in the cyanobacterium Synechococcus sp. when illuminated at temperatures between 110 and 160 K, is a conformationally excited form of the $Q_A^-Fe^{2+}$ signal that cannot relax at lower temperatures. Studies by Corrie et al. (1991) using another cyanobacterium, Phormidium laminosum, have now shown that the g=1.65 signal actually arises from an interaction between the two iron-semiquinones of Q_A and Q_B. A signal due solely to $Q_B^-Fe^{2+}$ in PS2 has been reported by Rutherford et al. (1984) at g=1.9.

The work presented in this section is a short examination of the different types of semiquinone EPR signals observed in PS2 and their behaviour. In the case of the Q_A signals, comment is made as to the significance of

the influence exerted by bicarbonate over this cofactor and the electron acceptor region.

3.1.1 Lineshape, Temperature Dependence And Power Saturation Characteristics Of The Q_A Iron-Semiquinone EPR Signals

In the BBY type of PS2 preparation (the complex used by the majority of groups working on PS2) the g=1.9 $Q_A^-Fe^{2+}$ signal is the one normally observed before further treatments. With careful preparation this signal was seen in 100% of centres, unless the particles were subjected to pHs below 6. The lineshape of the g=1.9 signal is demonstrated in Figure 3.1, which includes the temperature variations of the signal seen at 14 K and 4.5 K. Below 15 K the lineshape was temperature dependent. As the temperature was lowered the relative size of the two peaks at g=1.9 changed so that the peak at higher field dominated at 4.5 K. Another peak at g=1.75 also appeared at lower temperatures.

This behaviour is in contrast to that of the g=1.8 signal. The g=1.8 signal has to be induced by non-physiological exposure to low pHs (although this tends to give a mixture of the g=1.9 and 1.8 signals) or by treatment with small inhibitory anions that are thought to displace bicarbonate. Alternatively, removal of the LHCII by the detergent OGP at pH 6.0 (pH 6.0 OGP PS2), shown here in section 3.3.2, results in bicarbonate depletion and allows a true bicarbonate free g=1.8 signal to be observed

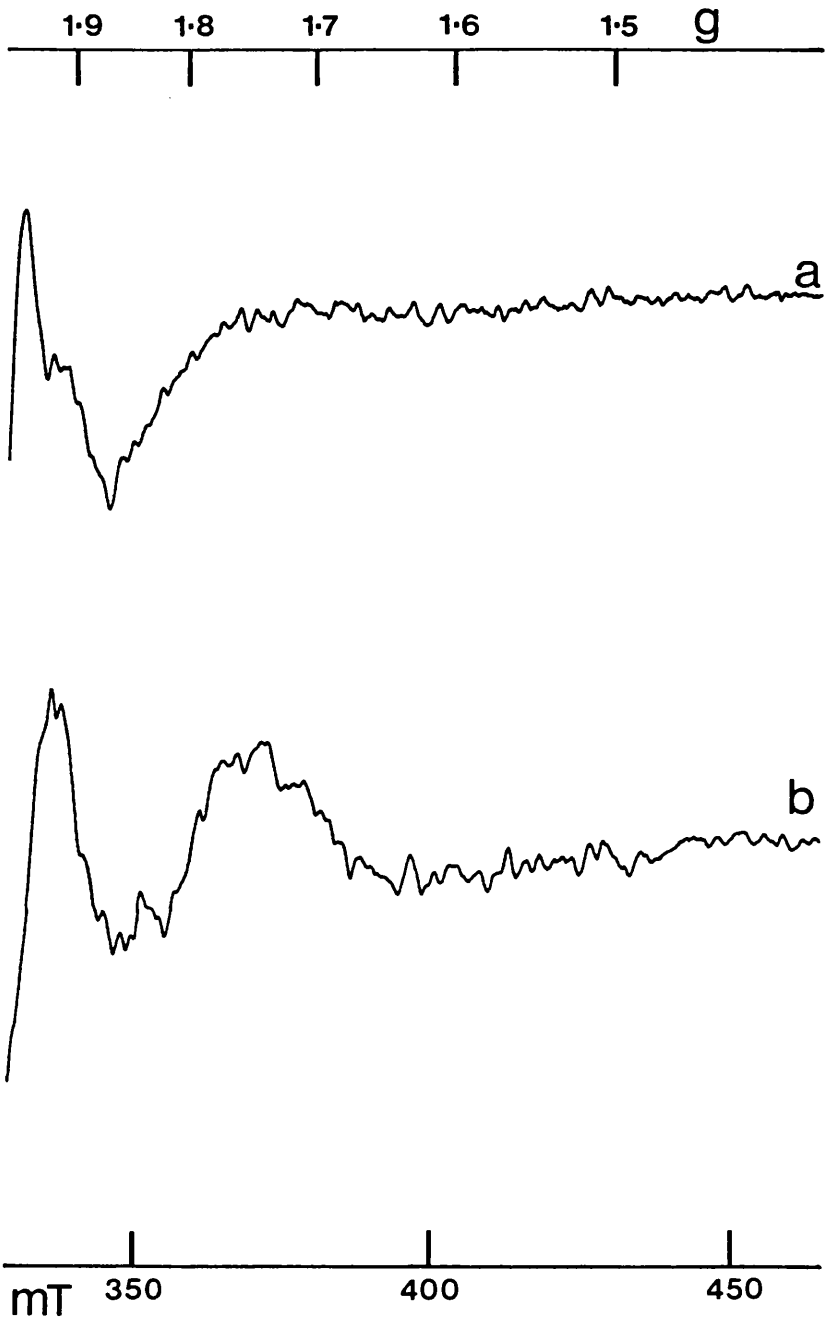

Figure 3.1 The native (bicarbonate dependent) g=1.9 Q_A iron-semiquinone EPR signal in BBY PS2 samples. Samples were dark adapted for one hour then illuminated at 77 K for 10 minutes, spectra recorded at (a) 14 K and (b) 4.5 K. EPR conditions: microwave power 10 mW, modulation width 1.25 mT, the instrument gain was the same for both spectra. Sample concentration 8 mg/ml Chl.

without the use of an inhibitor. The PS2 g=1.8 signals are similar to the Q_A and Q_B iron-semiquinone signals of purple bacteria.

The influence of bicarbonate over the g=1.9 $Q_A^-Fe^{2+}$ signal was demonstrated by the addition of HCO_3^- to a formate treated sample (Fig.3.2) and the subsequent conversion of the signal back to the g=1.9 resonance [Vermaas and Rutherford, 1984].

Figure 3.3 shows the effect that anion treatment has on the Q_A iron-semiquinone signal in BBYs. Several small monovalent anions are known to be potent inhibitors of PS2 electron transport [Stemler and Murphy, 1985] and most are known to affect the Q_A iron-semiquinone EPR signal. All the anions used here: nitrite, formate, acetate and propionate, induced a g=1.8 signal upon generation of the semiquinone. There were some slight variations in the lineshape of the various signals which must be due to the different chemical nature of each anion but interestingly nitrite also induced a shift in the g=1.8 peak to a slightly higher field position.

The different temperature dependent behaviour of the g=1.8 signal, compared to the g=1.9 signal, is shown in Figure 3.4. The amplitude of this signal, not the lineshape, was temperature dependent. The signal size was inversely proportional to the temperature so that as the temperature decreased the signal size increased. Therefore the g=1.8 signal is best observed at the lowest temperature possible.

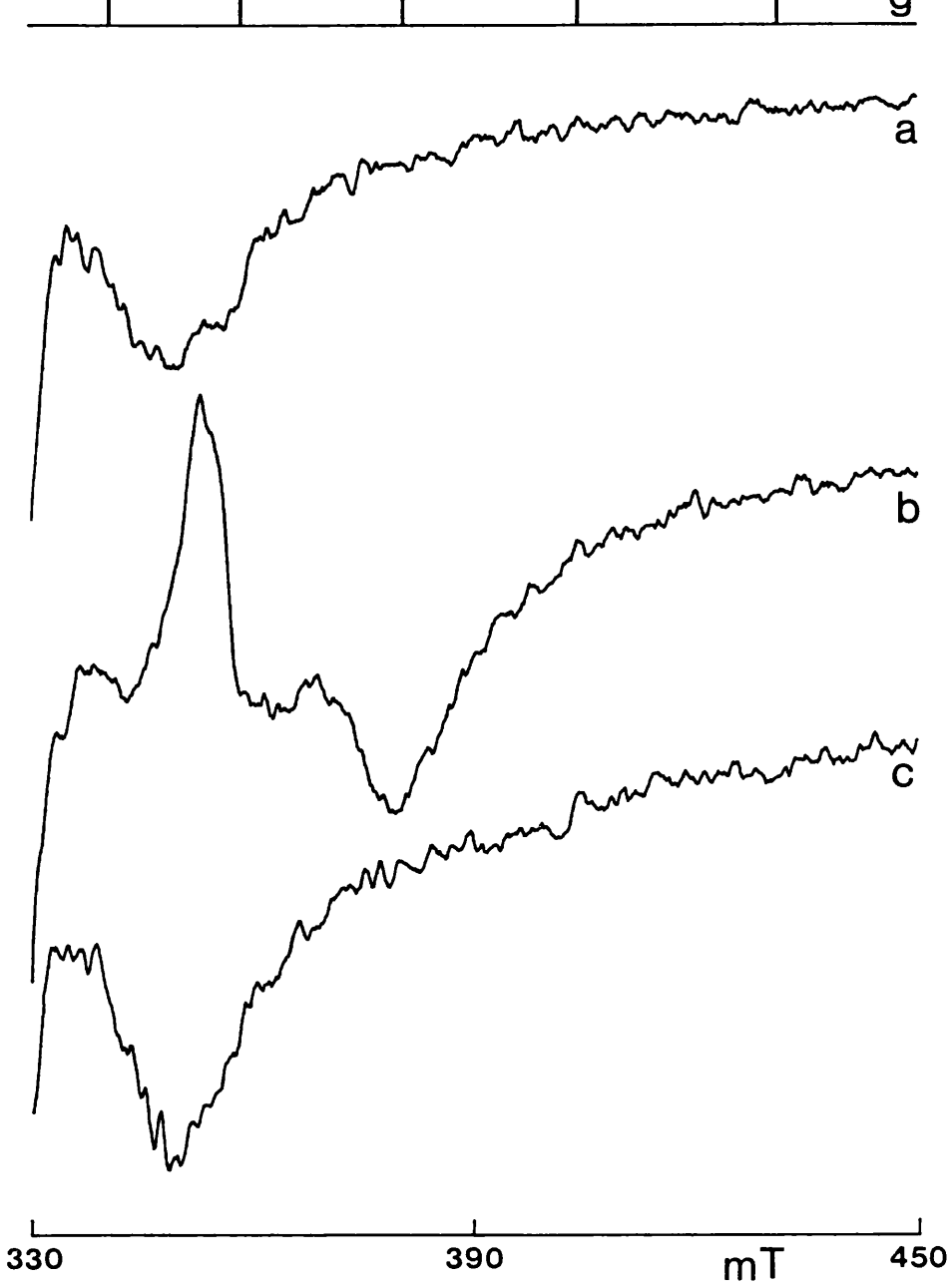

Figure 3.2 The reversibility of the formate induced g=1.8 $Q_A^-Fe^{2+}$ signal in BBY PS2. All spectra are from 77 K illuminated samples. (a) A sample incubated at 1 mg/ml Chl, on ice, in pH 6.3 resuspending medium (see BBY preparation section 2.1) for 30 min. The BBYs were then centrifuged and resuspended to 5 mg/ml Chl, for EPR analysis, in the same buffer plus 20% (v/v) glycerol and dark adapted for one hour before freezing to 77 K. The signal shown is the native g=1.9 Q_A iron-semiquinone. (b) A sample treated as (a) but incubated and resuspended in the same buffer + 50 mM formate. The signal is the g=1.8 HCO_2^- $Q_A^-Fe^{2+}$. (c) Sample treated as (b) but given a second 30 min incubation period in resuspending medium + 50 mM bicarbonate. The EPR sample was made using the bicarbonate containing buffer. EPR conditions: temperature 5 K, microwave power 10 mW, modulation width 1.25 mT.

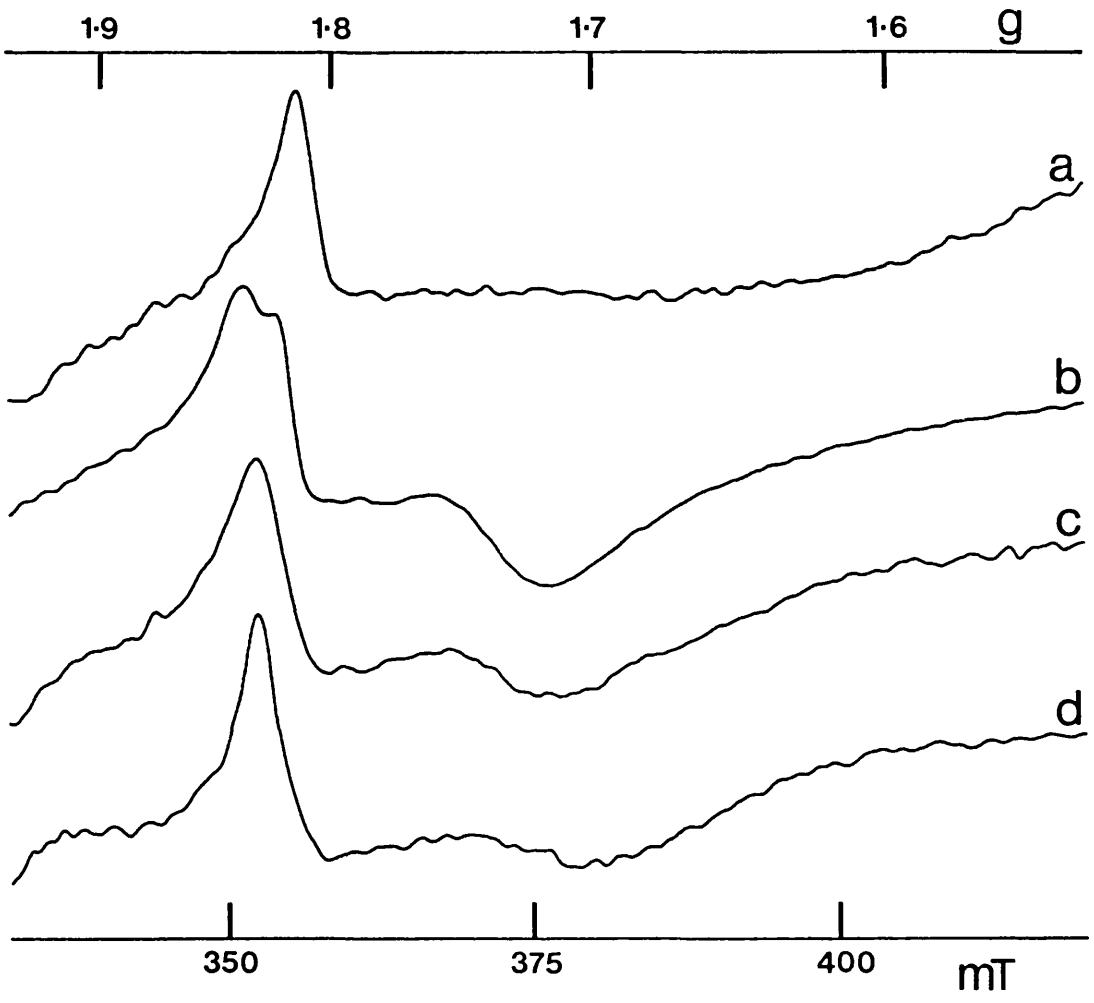

Figure 3.3 Different anion induced g=1.8 Q_A iron-semiquinone signals in BBY PS2 samples. 77 K illuminated spectra from samples treated with (a) 50 mM nitrite, (b) 50 mM formate, (c) 50 mM acetate, and (d) 50 mM propionate. Chl concentration 10 mg/ml. EPR conditions: temperature 5 K, microwave power 10 mW, modulation width 1.25 mT.

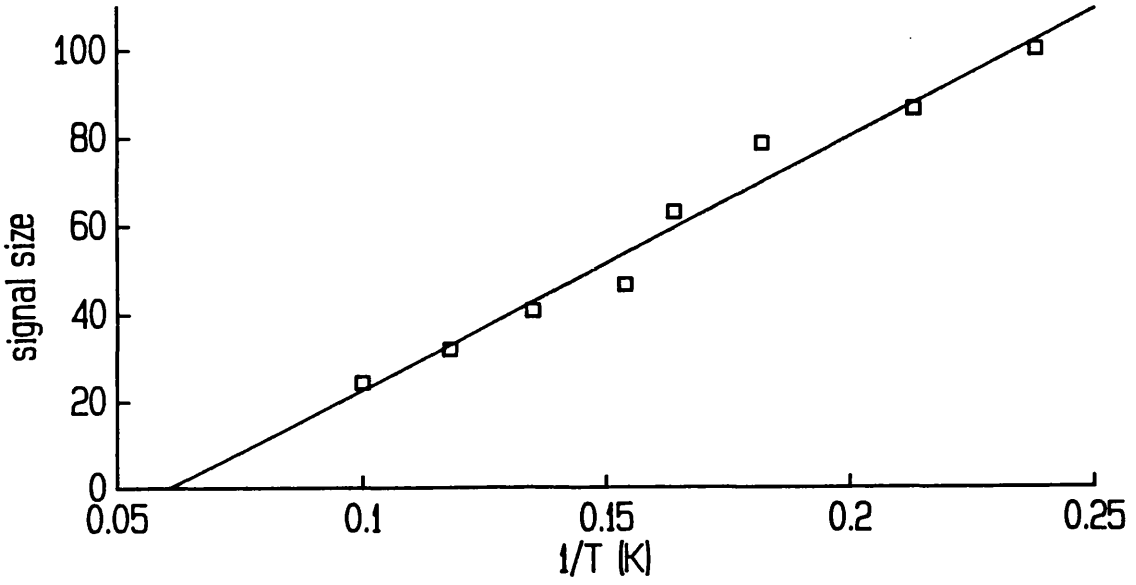

Figure 3.4 Temperature dependence of the g=1.8 $Q_A^-Fe^{2+}$ signal amplitude in BBY PS2 treated with 50 mM formate. Chl concentration 6 mg/ml. EPR conditions: microwave power 10 mW, modulation width 1.25 mT.

The two $Q_A^-Fe^{2+}$ signals not only differed in their temperature dependent behaviour but also in their microwave power saturation characteristics (Fig.3.5). The g=1.8 signal was more easily power saturated than the g=1.9 signal. Bicarbonate binding must change the quinone environment so that efficiency of spin relaxation is increased; $P_{\frac{1}{2}}$, the power at half saturation, is increased significantly to approximately 20 mW for the g=1.9 signal (Fig.3.5a) from less than 1 mW for the g=1.8 signal (Fig.3.5b). The temperature dependent and microwave power saturation characteristics of the g=1.8 signal in anion treated BBYs were very similar to those observed in pH 6.0 OGP PS2.

These differences in the basic behaviour of two signals from the same paramagnetic system were dependent on the presence or absence of bicarbonate and identify an important role for this anion in the electron acceptor side behaviour.

3.1.2 The Q_B EPR Signals

Native Q_B semiquinone EPR signals are best observed in Cyanobacteria because the secondary quinone is less labile in these PS2 preparations. In higher plant PS2 it is assumed that the purification treatment is relatively harsh and causes the loss of Q_B from the majority of reaction centres.

As already mentioned, the g=1.65 signal was first identified by McDermott et al. (1988) but incorrectly

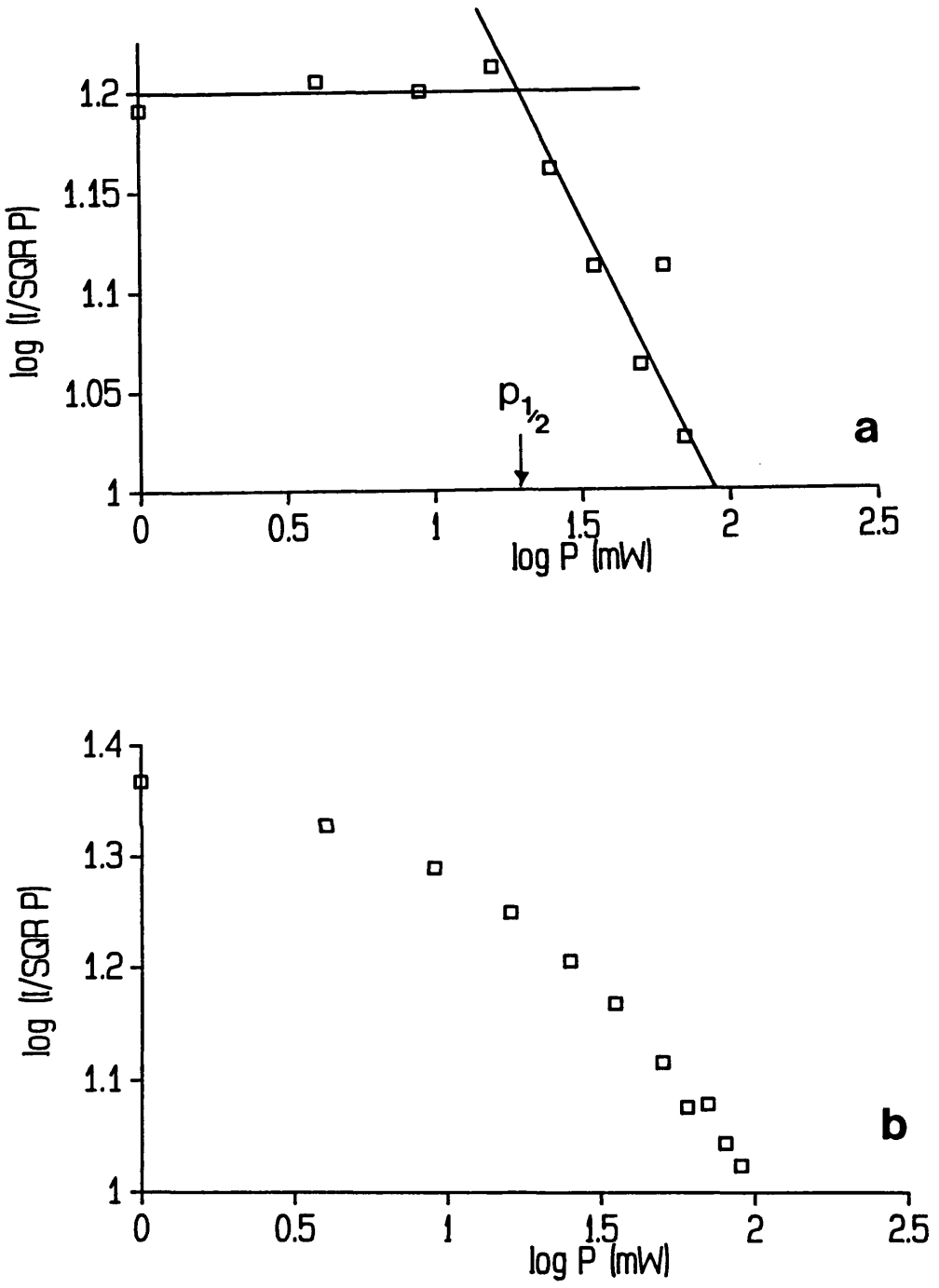

Figure 3.5 Microwave power saturation characteristics of the Q_A iron-semiquinone EPR signals. Signals induced in BBY PS2 samples by 77 K illumination for 10 min. (a) The g=1.9 native signal, $P_{\frac{1}{2}} \approx 20$ mW, and (b) the g=1.8 signal in a formate treated sample, $P_{\frac{1}{2}} < 1$ mW. Chl concentration 6 mg/ml. EPR conditions: temperature 5 K, microwave power 10 mW, modulation width 1.25 mT.

assigned to Q_A alone. Corrie et al. (1991) determined the origin of this signal as a situation where both the Q_A and Q_B semiquinones are generated in the same RC. The signal can be referred to as $Q_A^-Fe^{2+}Q_B^-$. A Q_B analogue, tribromotoluquinone (TBTQ) [Renger et al., 1987 and 1989], was found to mimic the behaviour of the native PQ [Corrie et al., 1991].

In higher plants attempts were made to observe a similar $Q_A^-Fe^{2+}Q_B^-$ signal. Figure 3.6 shows how the g=1.65 signal was generated in spinach BBYs with TBTQ. To obtain the maximum signal yield TBTQ treated samples were first illuminated for ≈30 secs at room temperature before a 45 minute period of dark adaptation followed by freezing to 77 K. In the dark (Fig.3.6a), when the artificial Q_B is bound to D1, TBTQ has a wide peak/trough signal over the g=1.8-1.5 range, presumably arising from the TBTQ iron-semiquinone [Hallahan et al., 1991]. When Q_A^- was generated in this sample, by 77 K illumination, the dark signal was lost and replaced by a signal peak at g=1.65 (Fig.3.6b). Only a small amount of g=1.9 $Q_A^-Fe^{2+}$ signal was observed.

To confirm that the dark and illuminated signals described in Figure 3.6 involved TBTQ binding Figure 3.7a plots the dependence of these signals on [TBTQ]. At lower concentrations the yield of the dark signal appeared to be less than the illuminated signal, but this difference is probably due to difficulties in measuring the small signal amplitudes observed at lower TBTQ concentrations. The signal amplitudes appeared to share the same reliance on

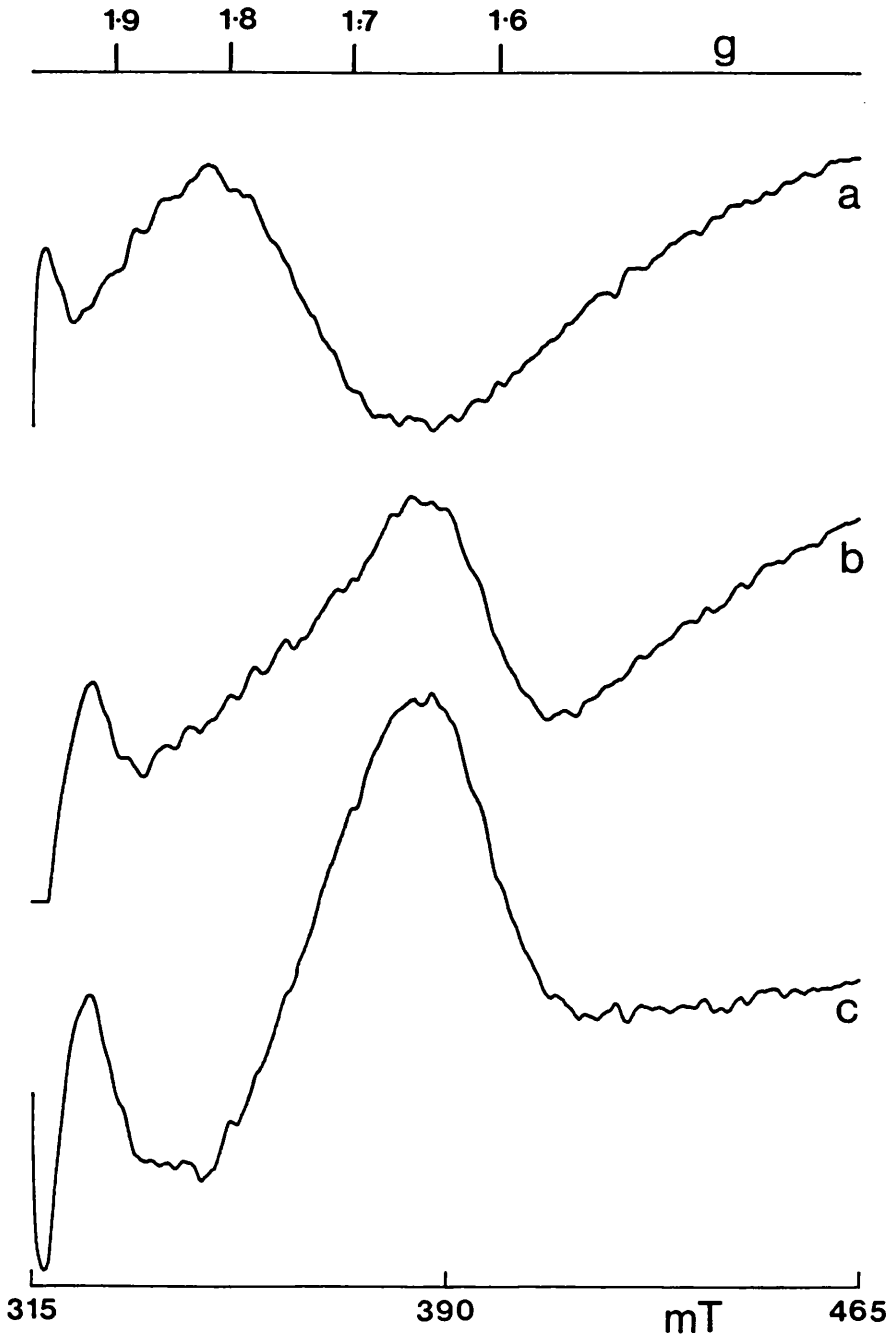

Figure 3.6 EPR signals of the Q_B analogue TBTQ. BBY PS2 samples treated with 500 μM TBTQ were illuminated for 30 secs at room temperature then dark adapted for 45 mins before freezing to 77 K. TBTQ was dissolved in DMSO but solvent concentration in the EPR sample was kept to below 2%. (a) Dark spectrum, (b) 77 K illuminated spectrum and (c) 77 K illuminated minus dark spectrum. Chl concentration 8 mg/ml. EPR conditions: temperature 5 K, microwave power 10 mW, modulation width 1.25 mT.

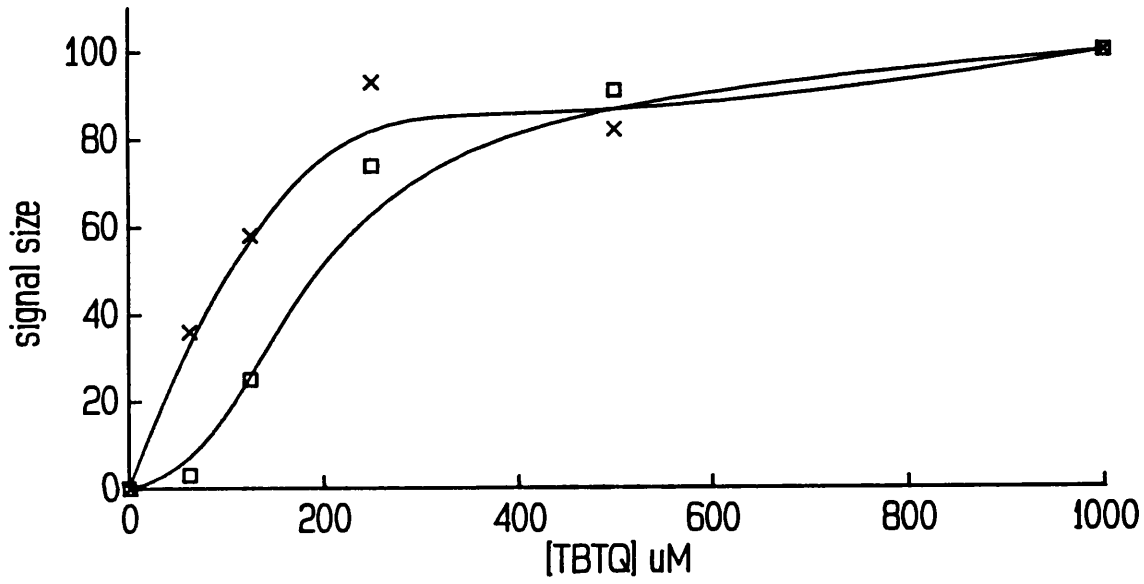

Figure 3.7 The size of the TBTQ related EPR signals, described in Fig.3.6, as a function of TBTQ concentration. Open squares: dark signal arising from $TBTQ^{-}Fe^{2+}$. Crosses: the 77 K illuminated signal peak at g=1.65 from Q_A^{-} $Fe^{2+}TBTQ^{-}$. Chl concentration 8 mg/ml. EPR conditions: temperature 5 K, microwave power 10 mW, modulation width 1.25 mT.

TBTQ concentration.

The $Q_A^-Fe^{2+}TBTQ^-$ signal in spinach BBYs (Fig.3.8c) is compared in Figure 3.8 with the Phormidium laminosum native signal (Fig.3.8a) and with the native signal in a preparation of pea BBYs (Fig.3.8b). It is interesting to note that a native g=1.65 signal was observed in higher plants although the signal yield was low because of Q_B loss. Previously low yield resonances at this g-value have been assigned to $Q_A^-Fe^{2+}$. Hallahan et al. (1991) found that treatment with FCCP, which stabilises the Q_B semiquinone, increased the yield of the $Q_A^-Fe^{2+}Q_B^-$ signal.

The g=1.65 signal cannot be produced in samples that would normally display the g=1.8 form of the Q_A iron-semiquinone signal [McDermott et al., 1988; Corrie et al., 1991]. Formate treated samples subjected to the protocol designed to maximise g=1.65 signal yield simply exhibited the g=1.8 $Q_A^-Fe^{2+}$ signal after 77 K illumination (see section 3.3.2). Therefore, bicarbonate is essential for observation of the g=1.65 signal.

The nature of the magnetic interaction between the iron-semiquinones that generates the g=1.65 signal is unknown but the situation is certainly different to that seen in purple bacteria where the comparable $Q_A^-Fe^{2+}Q_B^-$ interaction causes a reduction in the intensities of the g=1.8 signals [Wraight, 1978].

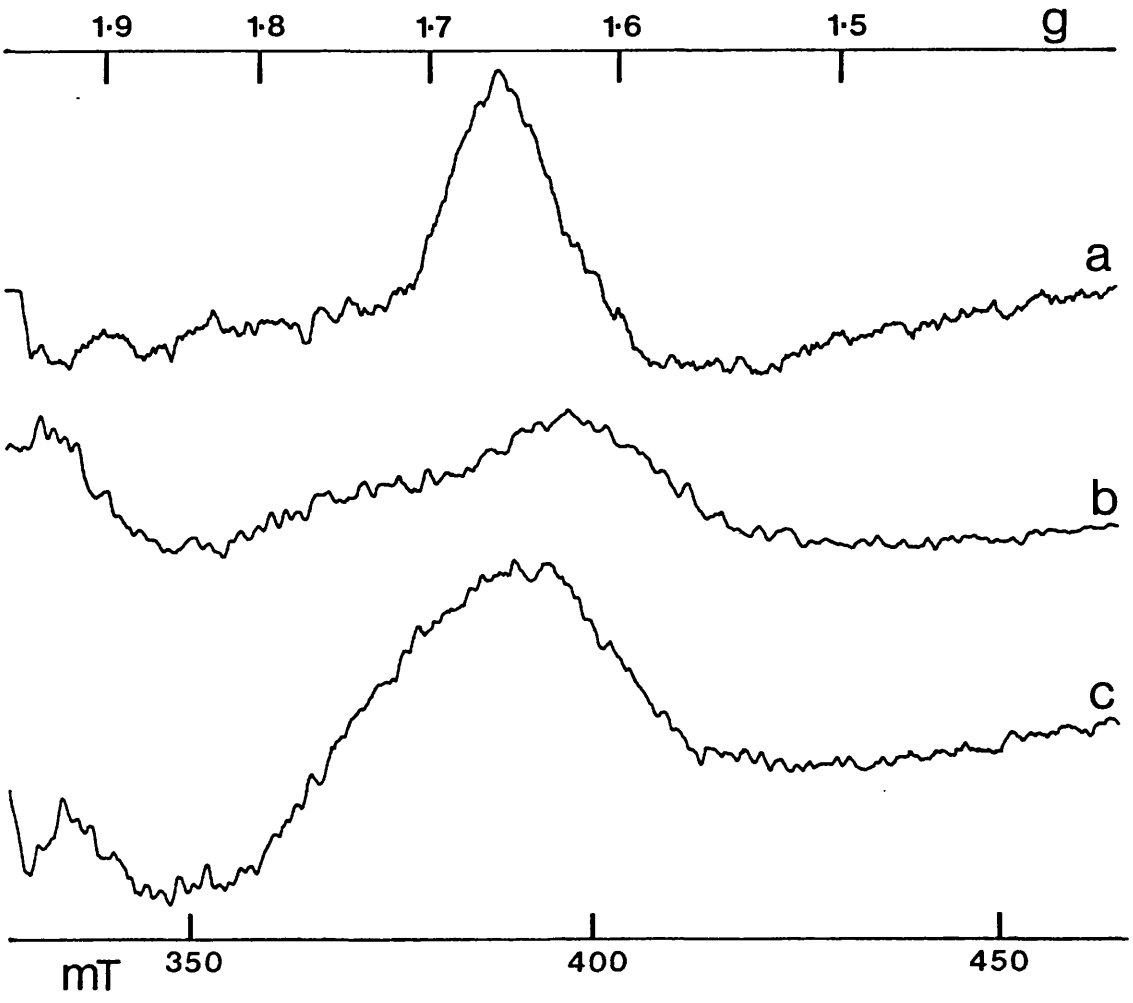

Figure 3.8 A comparison of native and artificial g=1.65 signals arising from the Q_A and Q_B iron-semiquinone interaction. 77 K illuminated minus dark difference spectra were obtained from samples illuminated at room temperature for 30 secs then dark adapted for 45 mins before freezing to 77 K. (a) The native $Q_A^-Fe^{2+}Q_B^-$ signal in the cyanobacterium Phormidium laminosum, (b) as (a) in pea BBYs and (c) the $Q_A^-Fe^{2+}TBTQ^-$ signal in spinach BBYs. Chl concentration in (a) 2 mg/ml, (b) and (c) 6 mg/ml. EPR conditions: temperature 5 K, microwave power 10 mW, modulation width 1.25 mT.

3.1.3 Discussion

A study of the PS2 quinone EPR signals confirms the important role played by bicarbonate in determining the behaviour of the electron acceptor side EPR signals. I can only assume that the changes observed when bicarbonate is removed are intimately related to the bicarbonate effect. Unfortunately the exact mode of bicarbonate action has yet to be determined.

In purple bacteria, the non-haem iron ligands are provided by four histidines and a glutamate residue, and there is no observed bicarbonate effect. In PS2, the homologous glutamate ligand is missing and it has been proposed that bicarbonate substitutes for the missing residue by providing one or two ligands to the non-haem iron [van Rensen et al., 1988; Michel and Deisenhofer, 1988; Blubaugh and Govindjee, 1988a; Diner and Petrouleas, 1990]. Both Mössbauer [Diner and Petrouleas, 1987b; Semin et al., 1990] and EPR [Aasa et al., 1989; Diner and Petrouleas, 1990] spectroscopy data has been interpreted to agree favourably with this possibility.

Nugent et al. (1991) concluded that the behaviourial differences observed between the g=1.9 and 1.8 EPR signals must result from structural changes in the first coordination sphere of the non-haem iron. However, they argue that this does not necessarily indicate that bicarbonate is a non-haem iron ligand; equally possible is that bicarbonate binds near the iron and that the effects of HCO_3^- depletion are transmitted indirectly through

effects on the histidine ligands.

The inter-conversion between the g=1.9 and 1.8 signals demonstrated in Figure 3.2 is comparable to experiments where bicarbonate is observed to alleviate the inhibitory effect of formate on electron flow. Experiments such as these, on the regulatory role of bicarbonate, assume that maximum electron flow is dependent on the presence of HCO_3^-. Stemler (1989) has questioned this assumption, he thought that if bicarbonate has a physiological role in electron transport then there should be a detectable release of CO_2 as reaction centres are treated with formate. However, he failed to detect such a release and concluded that under physiological conditions there is no bicarbonate bound to the RC and that the inhibitory effect of formate is in reality the result of HCO_2^- binding to empty sites. He suggested that the alleviation of inhibition occurred through the displacement of formate by bicarbonate. Govindjee et al. (1991) have now repeated the mass spectrometer experiments and refute Stemler's result, reaffirming the role of bicarbonate in regulating electron flow.

For Stemler (1989) to be correct about the inhibitory action of formate the lineshape of the g=1.9 $Q_A^-Fe^{2+}$ EPR signal would have to be independent of bicarbonate. However, the dependence of this signal on HCO_3^- is confirmed in section 3.3.2 where the signal conversion experiment outlined in Figure 3.2 is repeated without the use of formate or any other anion except bicarbonate.

The site of formate binding has also been of interest to Diner and Petrouleas (1990), who have suggested that formate does not bind at the non-haem iron. However, they concluded that bicarbonate is a non-haem iron ligand and so suggested that separate, but overlapping, binding sites exist for the two anions.

The exact binding site or sites of bicarbonate are still unknown but at least one molecule is bound either as a non-haem iron ligand or near to the iron ligands themselves. This is obvious from the EPR behaviour of the quinones and the non-haem iron shown in this section and in section 3.3. The bicarbonate bound at the second proposed binding site [Blubaugh and Govindjee, 1988a] may be involved in Q_B^{2-} protonation but the bicarbonate at or near the non-haem iron probably has a more structural role. This possibility is examined and discussed more closely in section 3.3 and 3.4 where the role of bicarbonate in the stability of Q_A binding and PS2 electron acceptor side conformation is investigated.

3.2 Trypsin As A Structural Modifier Of Photosystem Two

Trypsin is a protease that splits peptide bonds on the carboxyl side of lysine and arginine residues. It was first used to investigate the structure/function relationship of the PS2 electron acceptor region, exposed at the stromal side of the thylakoid membrane, by Regitz

and Ohad (1976) and Renger (1976). PS2 oxygen evolution was reported to become insensitive to DCMU inhibition after mild trypsin treatment when potassium ferricyanide was used as the artificial electron acceptor [Renger, 1976]. Renger suggested that a proteinaceous component, which normally shielded the acceptor side of PS2 from the aqueous environment, was being digested. As a result, accessibility of Q_A to ferricyanide was increased [Renger, 1977]. It was thought that the protein component incorporated the herbicide binding site, as digestion caused the loss of DCMU sensitivity. Renger also noticed that the ability of the Q_B analogue p-BQ to facilitate oxygen evolution was diminished after trypsin attack. Together these observations have been taken to indicate that trypsin specifically attacks the herbicide/Q_B binding site on D1.

Since the early protease experiments PS2 structural models have been refined, initially through identification of the homology shared by D1 and D2 with the purple bacterial reaction centre subunits, but more recently, through the availability of the Rps. viridis and Rb. sphaeroides crystal structures. This has enabled the development of quite detailed models of the quinone binding region [Trebst et al., 1990] and current predictions place the Q_A and Q_B binding sites in the loop regions between transmembrane helices IV and V. Protease studies can therefore be used to obtain more specific structural information about the PS2 electron acceptor side.

EPR is also a sensitive tool for structural studies as modifications in the environment around the paramagnet will alter the EPR signal characteristics. By monitoring both the PS2 acceptor side EPR signals and the changes in the oxygen evolution behaviour of the complex it should be possible to more accurately determine the effects of protease attack. I have used this approach to investigate further the effects of mild trypsin treatment on PS2 EPR signals and also the protective effect of calcium ions against protease damage.

3.2.1 The Effects Of Trypsin Treatment On Oxygen Evolution

Trypsin digestion of BBY PS2 samples at pH 6.3 was found to increase the rate of oxygen evolution when potassium ferricyanide was used as the artificial electron acceptor. The observed rate was dependent on the length of the digestion (Fig.3.9). This contrasts with previous experiments [Renger et al., 1986; Trebst et al., 1988] where oxygen evolution was shown to steadily decline over the same time-scale. Our result can be explained assuming that the electron transfer step from Q_A^- to ferricyanide is the rate limiting step in the evolution of oxygen. Trypsin digestion could then increase the accessibility of Q_A^- to ferricyanide so that the kinetics of the reaction are accelerated, thereby enhancing the rate of O_2 evolution.

Secondly, oxygen evolution was found to become increasingly DCMU insensitive (Fig.3.9). In an untreated sample (0 mins digestion) the concentration of DCMU used

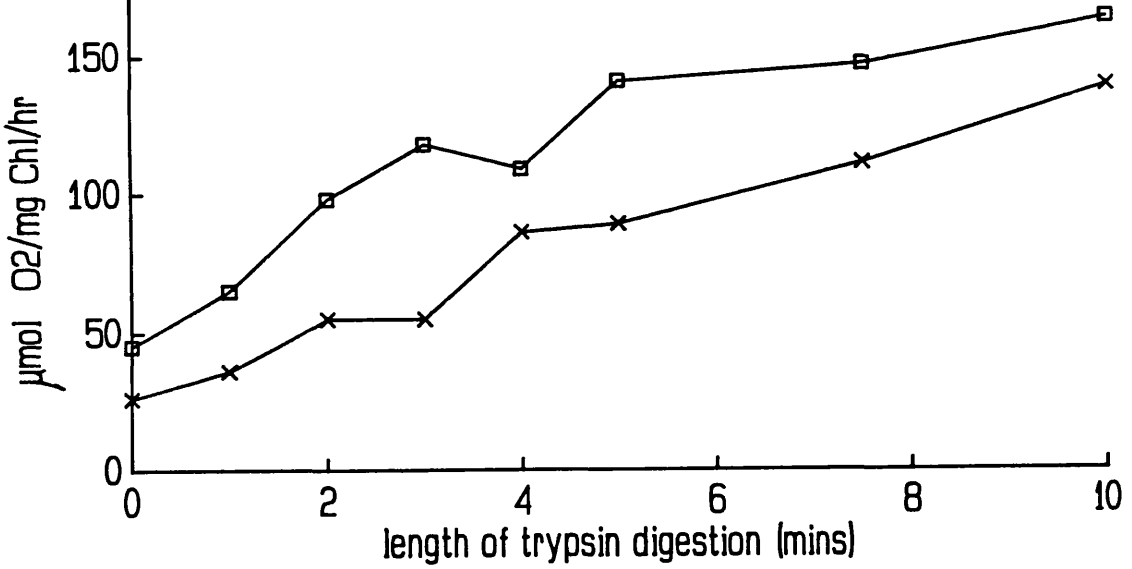

Figure 3.9 The rate of oxygen evolution (μmol O_2/mg Chl/hr) in BBY PS2 samples treated with trypsin when potassium ferricyanide is used as the artificial electron acceptor; without DCMU (open squares) and with 7 μM DCMU (crosses).

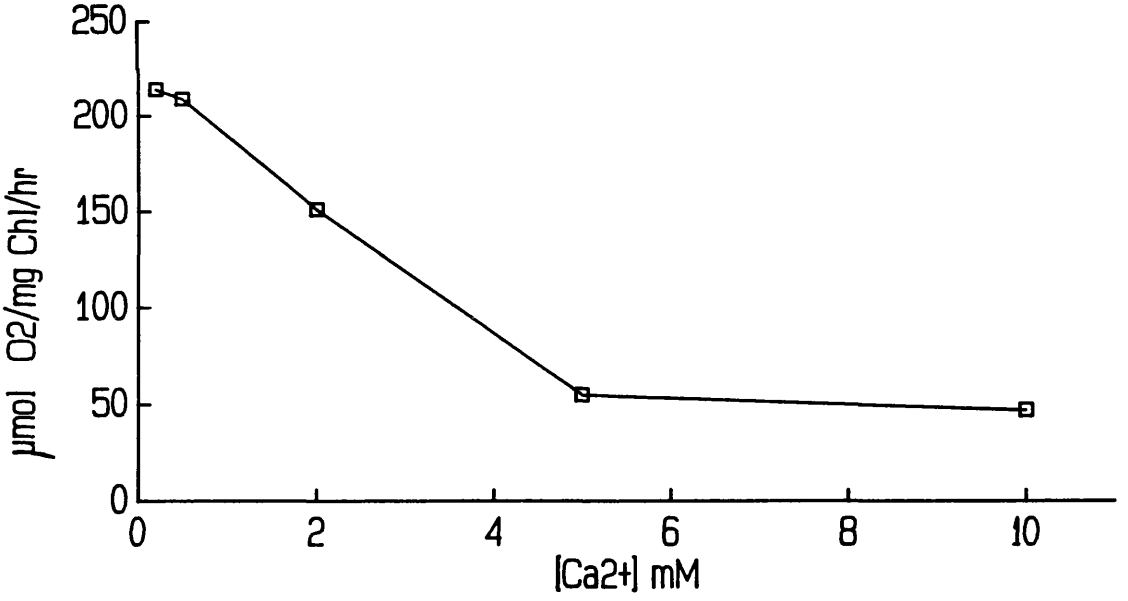

Figure 3.10 The concentration of calcium ions necessary to observe the protective effect of Ca^{2+} against trypsin digestion in BBYs. The rate of oxygen evolution (μmol O_2/mg Chl/hr) was measured in samples treated with $CaCl_2$ concentrations over the range 0.2-10 mM, in the absence of DCMU.

gave a 43% inhibition of O_2 evolution. The DCMU concentration of 7 μM approximates to around 50 DCMU molecules per RC and gives a marked, but not absolute, degree of inhibition. After 10 mins trypsin digestion this inhibition was reduced to only 15%. This demonstrated the susceptibility of the herbicide/Q_B binding site on D1 to trypsin attack, first observed by Renger (1976, 1977).

The action of trypsin at the Q_B binding site was also obvious when the Q_B analogue DMBQ was used as the artificial electron acceptor in the absence of DCMU. The rate of oxygen evolution with DMBQ decreased from 215 to 69 μmols O_2/mg Chl/hr after 10 mins trypsin treatment.

DCMU and DMBQ were also tested for any inherent ability to prevent damage of the D1 binding site when added prior to the digestion. DMBQ was found to be ineffective at blocking trypsin damage but DCMU addition inhibited the protease activity by approximately 50%. This may indicate different modes of binding between the herbicide and the Q_B analogue or a difference in their binding constants.

The effect of calcium ions on trypsin modification of the quinone binding region was also studied. Renger et al. (1986) first noted that an addition of calcium ions prior to the digestion had a protective effect against trypsin damage. Table 3.1 shows the effect of 10 mM $CaCl_2$ on O_2 evolution when the addition is made at different stages in the trypsin treatment.

Table 3.1 The Effects Of Calcium Ions On Trypsin Digestion Of PS2

	Rate of O_2 Evolution μmol O_2/mg Chl/hr
No added Ca^{2+}.	132
Ca^{2+} added before the digest.	75
Ca^{2+} added 5 mins into the digest.	260
Ca^{2+} added after the digest.	354

The rates of oxygen evolution shown are those obtained after a 10 minute trypsin digestion of BBY PS2 samples with potassium ferricyanide as the artificial electron acceptor.

The rate of oxygen evolution when calcium ions were added before the trypsin digestion was lower than the rate observed when Ca^{2+} was omitted. Therefore, calcium ions block trypsin cleavage of the reaction centre so that the enhancement effect of trypsin treatment on the rate of O_2 evolution is absent. This protective action against the protease activity was only observed if Ca^{2+} concentrations of 5 mM or above were used (Fig.3.10).

If the addition of Ca^{2+} was not made until after the trypsin inhibitor, ie. until the digestion was complete, then a different effect was observed; the rate of oxygen evolution increased to a level above that observed in the absence of Ca^{2+} (see Table 3.1). In this case there was no protective action of Ca^{2+} against trypsin, in fact, the opposite was observed as the effect of trypsin digestion on the rate of O_2 evolution was apparently enhanced.

The observed calcium phenomena were not due to effects of Ca^{2+} on the protease itself. Trypsin does have a calcium

binding site but bound Ca^{2+} protects the enzyme against autolysis and actually enhances the enzyme activity [Sipos and Merkel, 1970]. The calcium effects are also unrelated to the Ca^{2+} known to play a role in water oxidation in the OEC (see discussion section 3.2.3).

3.2.2 The Effects Of Trypsin Treatment On The Primary Quinone, Non-Haem Iron And Cytochrome b_{559} EPR Signals

Illumination of an untreated BBY PS2 sample, at 77 K, generated the g=1.9 Q_A iron-semiquinone signal (Fig.3.11a). However, no $Q_A^-Fe^{2+}$ signal was observed in the trypsin treated sample given the same illumination treatment (Fig.3.11b). The protective effect of 10 mM $CaCl_2$ added before the digestion is demonstrated in Fig.3.11c as the $Q_A^-Fe^{2+}$ signal was still generated. The calcium protected signal was also found to have a small g=1.8 signal (Fig.3.11c), indicating that some loss of bicarbonate binding had occurred. The behaviour of the formate induced g=1.8 iron-semiquinone signal (Fig.3.12) echoed that observed for the bicarbonate g=1.9 form of the signal.

The PS2 reaction centre non-haem iron can be oxidised by incubation with potassium ferricyanide in the dark. The resulting Fe^{3+} EPR signal has peaks at g=8 and 5.6 which disappear when illuminated at 77 K as Fe^{3+} is reduced by Q_A^- (Fig.3.13A). The dark spectrum of Fe^{3+} in trypsin treated PS2 (Fig.3.13B) was very different from the normal signal. The spectrum became more axial with the two peaks closer together at approximately g=6 and illumination for 10 mins

Figure 3.11 The effect of 10 minutes trypsin digestion on the native g=1.9 Q_A iron-semiquinone EPR signal in BBY PS2 samples. (a) 77 K illuminated spectrum from an untreated sample, (b) 77 K illuminated spectrum from a trypsin treated sample, and (c) 77 K illuminated spectrum from a calcium protected sample; 10 mM $CaCl_2$ added before the trypsin digestion. Chl concentration 5 mg/ml. EPR conditions: temperature 5 K, microwave power 10 mW, modulation width 1.25 mT.

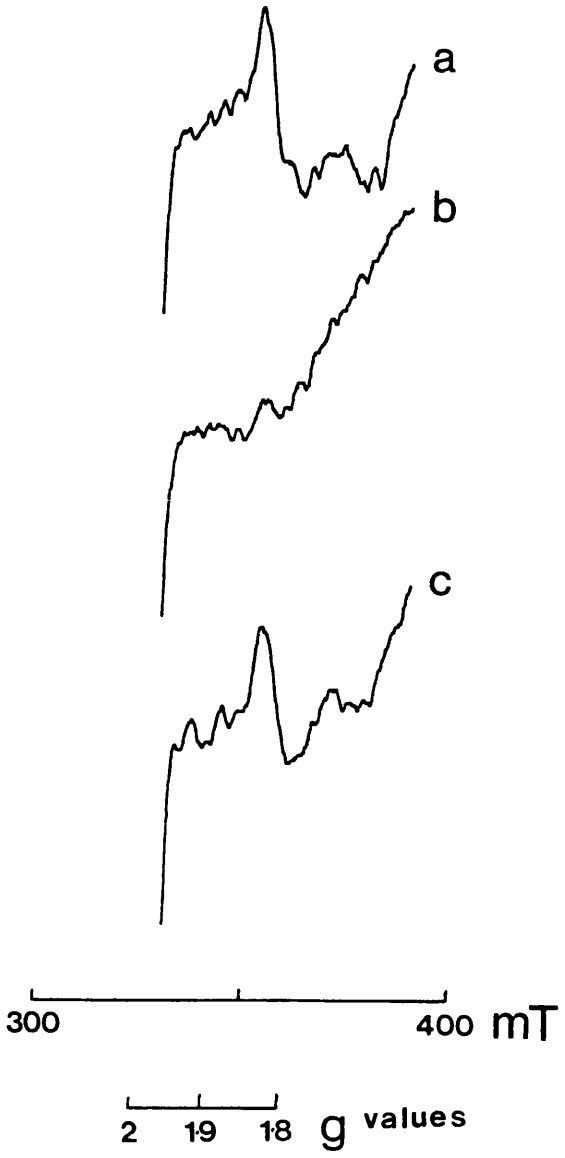

Figure 3.12 The effect of 10 mins trypsin digestion on the formate g=1.8 Q_A iron-semiquinone EPR signal in BBY PS2 samples. 77 K illuminated spectra from (a) an untreated sample, (b) from a trypsin treated sample, and (c) a calcium protected sample; 10 mM $CaCl_2$ added before the digestion. Chl concentration 5 mg/ml. EPR conditions: temperature 5 K, microwave power 10 mW, modulation width 1.25 mT.

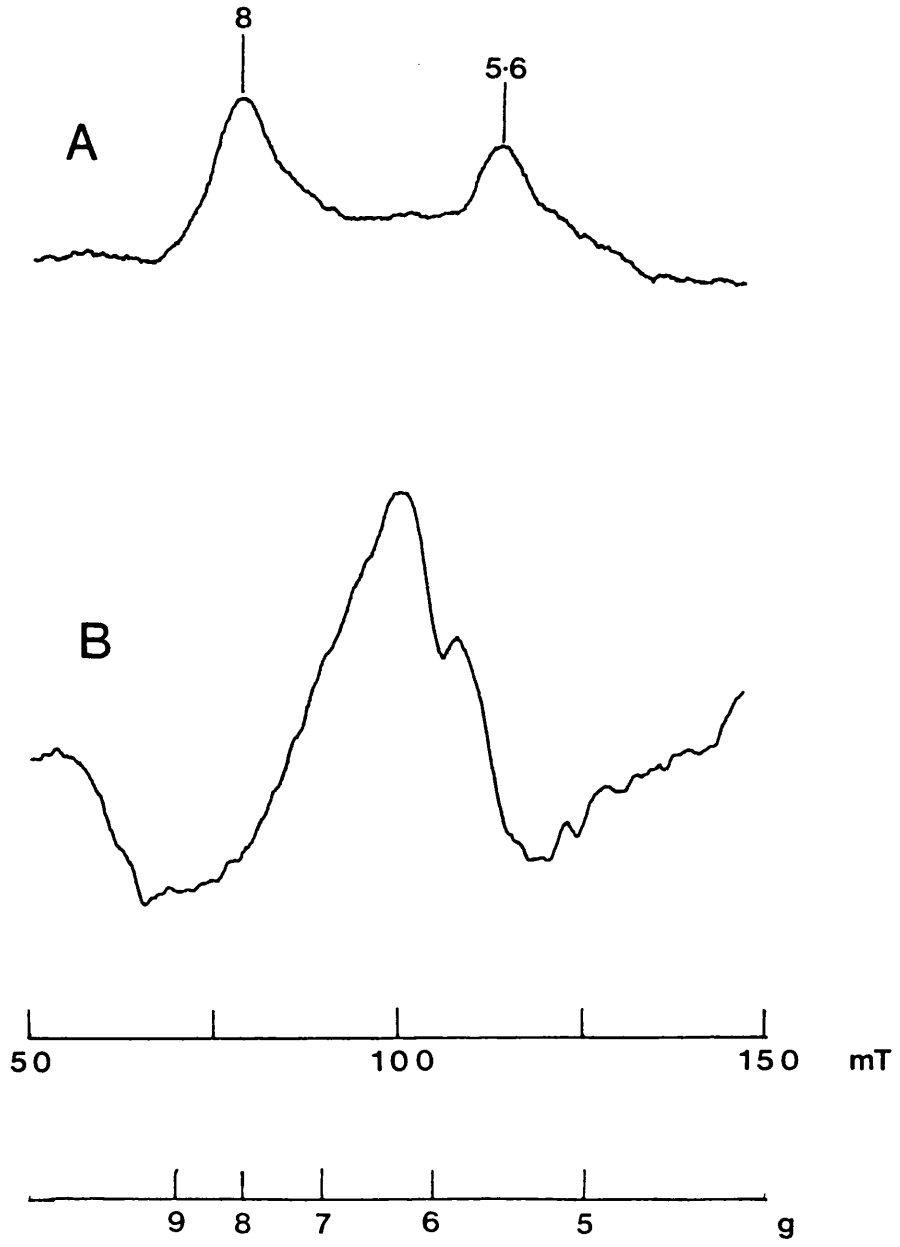

Figure 3.13 Changes in the BBY PS2 oxidised non-haem iron EPR spectrum in trypsin treated samples. Treated and untreated samples were resuspended in pH 7.5 buffer + 10 mM potassium ferricyanide and dark adapted for 45 mins before freezing to 77 K. (A) dark minus 77 K illuminated difference spectrum from an untreated BBY PS2 sample, and (B) dark spectrum from a sample subjected to 10 mins trypsin digestion. Chl concentration 10 mg/ml. EPR conditions: temperature 5 K, microwave power 10 mW, modulation width 1.25 mT.

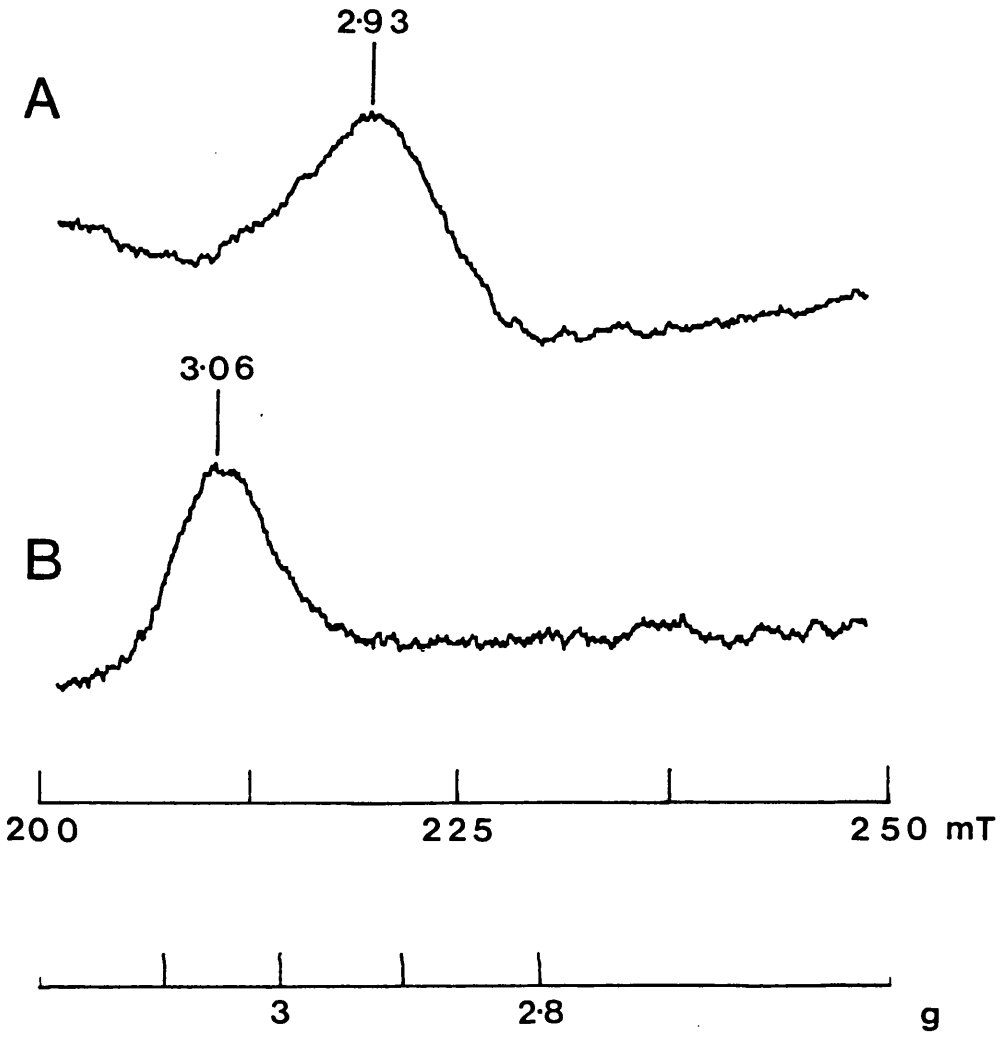

Figure 3.14 The EPR signals of cytochrome b_{559}. (A) Dark spectrum showing the low potential cytochrome signal at g=2.93, and (B) a 77 K illuminated minus dark difference spectrum showing the high potential cytochrome b_{559} signal at g=3.06. Chl concentration 5 mg/ml. EPR conditions: temperature 5 K, microwave power 5 mW, modulation width 1.25 mT.

at 77 K caused very little Fe^{3+} photoreduction. Such an alteration in behaviour indicates that a disruption of the non-haem iron ligand environment has occurred.

The third component studied was cytochrome b_{559}. The cytochrome is intimately associated with the D1/D2 heterodimer in the RC complex [Nanba and Satoh, 1987]. At 77 K the high potential form of b_{559} is the principal electron donor to $P680^+$ [de Paula et al., 1985] and so illumination of an untreated sample at this temperature generated the high potential b_{559}^+ signal at g=3.06 (Fig.3.14B). The low potential form of cytochrome b_{559} is normally oxidised at ambient redox potentials ($E_m \approx 0$ mV) so the signal is present in the dark at g=2.93 (Fig.3.14A). Mild trypsin treatment was found to increase the size of the low potential dark signal and no 77 K photooxidation of the high potential form was observed. This behaviour indicated that trypsin treatment induced a conversion of the high potential b_{559} to a low potential form.

3.2.3 Discussion

The EPR data obtained from trypsin treated PS2 samples showed that the environments around Q_A and the non-haem iron are susceptible to trypsin damage. This is in disagreement with Renger et al. (1985) where trypsin treatment was found not to affect the g=1.9 $Q_A^-Fe^{2+}$ signal. The oxygen electrode results show that trypsin treatment increases the exposure of Q_A^- to the stroma and that the Q_B/herbicide binding site is damaged. A disruption of both the Q_A and Q_B binding

regions is expected because Trebst et al. (1988) identified trypsin cut sites at Arg-238 in D1 and Arg-234 in D2. These residues are predicted to be located in the respective D1 and D2 loops between transmembrane helices IV and V (see Figure 1.6 taken from Trebst et al. (1990)).

Trypsin digestion of the PS2 electron acceptor region increased the rate of oxygen evolution with potassium ferricyanide, indicating more efficient oxidation of Q_A^-. Ferricyanide is known to be capable of oxidising the PS2 non-haem iron but only at pHs greater than 7. Therefore, at the pH of the assays, pH 6.3, O_2 evolution with ferricyanide is probably occurring through oxidation of Q_A^- only. This indicates that photoreduction of Q_A is still possible in trypsin treated samples despite the fact that the $Q_A^-Fe^{2+}$ EPR signal is lost. This is significant since it means that loss of the Q_A semiquinone EPR signal does not necessarily mean loss or inactivation of Q_A. The absence of the $Q_A^-Fe^{2+}$ EPR signal in trypsin treated samples probably reflects a disruption of the magnetic interaction between Q_A and the non-haem iron. The change in the oxidised non-haem iron EPR spectrum from trypsin treated samples and the lack of Fe^{3+} photoreduction at 77 K are further evidence that a disruption of the non-haem iron environment is occurring.

The observed effect of trypsin treatment on cytochrome b_{559} is in agreement with the results of Völker et al. (1986). It indicates that high potential cytochrome b_{559} haem is sensitive to protease damage, revealing its

exposure to the stroma. Tae et al. (1988) predict that the cytochrome haem is closest to the stromal side of the membrane which is consistent with the trypsin EPR data. However, treatments affecting the electron donor side of the PS2 complex, such as Tris-washing to remove the extrinsic subunits, are also known to change the EPR characteristics of the cytochrome.

Oxygen electrode experiments confirm the protective action of calcium ions against trypsin attack observed by Renger et al. (1986); they also illustrate the effect of Ca^{2+} on the rate of oxygen evolution when the addition is made after the trypsin digest is completed [Renger et al., 1988]. There is specific evidence that the trypsin related calcium effects involve a calcium binding site on the electron acceptor side of PS2. This is not related to the calcium binding site postulated to be on the electron donor side of PS2, thought to be involved in oxygen evolution. Firstly, generation of the $Q_A^-Fe^{2+}$ EPR signal at 77 K does not involve electron donation by the oxygen evolving complex so the protection by calcium ions of the iron-semiquinone EPR signal (Fig.3.11c) is independent of water oxidation. Secondly, Renger et al. (1988) measured the binding of [^{14}C]atrazine in +/- calcium protected samples and found that calcium increased the amount of bound herbicide by reducing trypsin degradation of the herbicide binding site. Barr et al. (1983) have also found evidence for an acceptor side calcium effect.

A simple explanation of the protective action of

calcium is that Ca^{2+} binding induces a conformational change in the RC quinone binding region reducing the accessibility of the trypsin cut sites to the protease. When calcium ions are added to samples already treated with trypsin then a conformational change must still occur but the exact nature of the structural transformation is altered so that Q_A^- is more easily oxidised by ferricyanide.

The physiological significance of this calcium binding site is unclear. The effects of Ca^{2+} ions demonstrated and discussed above were only obvious if a specific addition of calcium chloride was made to the sample. This would indicate that the site is "normally" unoccupied and that the phenomenon is non-physiological. However, Fromme and Renger (1990) suggest that the binding site is occupied under normal conditions in PS2 membrane preparations. They concluded that the site had a high affinity and calculated a binding constant of $\approx 10^{-7}$ M. Fig.3.10 indicates a much weaker binding with a constant of $\approx 10^{-3}$ M. Another important observation associated with this problem is that 10 mM $CaCl_2$ was found not to protect the Q_B binding site against trypsin damage in thylakoids [Renger et al., 1986]. This supports the view that calcium binding is non-physiological.

The binding site location remains to be determined. The protective effect of calcium encompasses both the trypsin cut sites so the site may be on either D1 or D2. Coleman and Govindjee (1987) made a study of possible PS2 calcium binding sites and proposed a site within residues

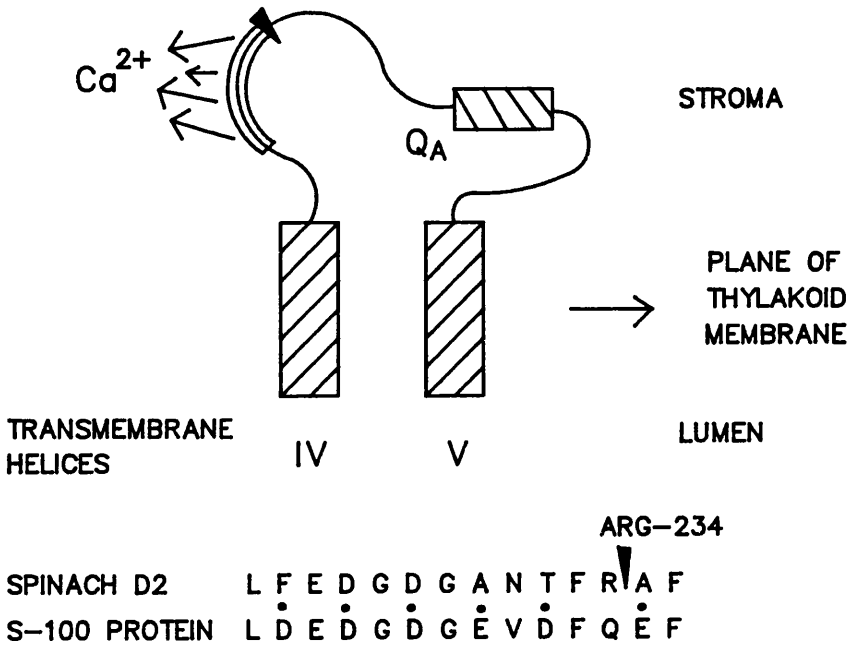

Figure 3.15 Diagram illustrating the location of a possible EF hand calcium binding site in the Q_A binding region of D2. The proposed secondary structure of this region fits well with known binding sites. The α-helices drawn are the transmembrane helices IV and V with the short helix thought to be orientated parallel to the membrane. The sequence proposed to bind calcium is compared to the calcium binding site identified in S-100 protein. Also marked is the trypsin cut site proposed by Trebst et al. (1988).

223-232 of D2. They found the sequence to have some homology with one of the calmodulin calcium binding sites. The suggested site is located in the region between transmembrane helices IV and V that is proposed to be on the outer surface of the membrane [Trebst and Draber, 1986]. Structural predictions include a short α-helix within this loop, orientated parallel to the membrane, so the region displays the helix-loop-helix motif of an EF hand calcium binding site [Kretsinger and Nockolds, 1973]. Homology of the site with known calcium binding sites is good, but not perfect, which would explain the observed low affinity. See Fig.3.15 for a diagram of the proposed binding site and an alignment of the sequence with the S-100 protein (bovine) alpha chain calcium binding site. S-100 is a member of the calmodulin super-family of calcium binding proteins.

3.3 Preparation And Characterisation Of Photosystem Two Core Particles With And Without Bound Bicarbonate.

The reaction centre of PS2 has now been identified as the D1/D2 heterodimer. Comparisons of PS2 subunits with purple bacteria reaction centres first led to this suggestion but Nanba and Satoh (1987) provided the necessary experimental evidence. They digested PS2 membranes with the detergent Triton X-100 and obtained a reaction centre complex containing D1, D2, cytochrome b_{559}

and the ≈ 4 kDa psbI gene product. This complex was found to photoaccumulate reduced pheophytin and EPR studies showed the presence of the spin polarised reaction centre triplet upon illumination at ≈ 4 K [Nanba and Satoh, 1987; Okamura et al., 1987; Nugent et al., 1989]. Unequivocal proof of the location of the PS2 primary reactants was obtained when the RC complex described above was digested further with OGP. This enabled the purification of a photochemically active RC heterodimer which was still capable of pheophytin reduction [Tang et al., 1990].

Other groups have devised alternative methods of isolating the RC complex using the detergent dodecylmaltoside (DM) [Dekker et al., 1989; Fotinou and Ghanotakis, 1990]. Analysis of the Dekker RC complex found 10-12 Chl a molecules per RC whereas Nanba and Satoh (1987) found five. This has created some debate over the exact pigment composition of the reaction centre but the argument appears to arise from whether or not the pigment analysis is based on two cytochrome b_{559} [Dekker et al., 1989] or two pheophytin a molecules [Kobayashi et al., 1990] per RC (see Gounaris et al. (1990) for a discussion).

All the current reaction centre preparations lack the primary plastoquinone. Akabori et al. (1988) claimed to have isolated an RC complex retaining one PQ per RC but they could not photoinduce charge separation between P680 and Q_A. The desire to study the electron transport behaviour in Q_A retaining reaction centres has led to work aimed at reintroducing either the native Q_A [Chapman et al.,

1991] or a Q_A analogue [Satoh et al., 1990].

The other major types of PS2 preparation are the "core" complexes which fall into two categories, the oxygen evolving and the non-oxygen evolving. The former group were first developed because of interest in the mechanism of water oxidation and a desire to determine the minimum subunit requirement for O_2 evolution. Ikeuchi et al. (1985) and Ghanotakis and Yocum (1986) used the detergent octylglucopyranoside (OGP) to remove the light harvesting complex (LHCII) and obtain a particle retaining manganese and the 33 kDa OEC extrinsic polypeptide. Tang and Satoh (1985) used digitonin to similar effect. The method of Enami et al. (1989) uses heptylthioglucoside to remove the LHCII but the treatment is less harsh as all three of the extrinsic polypeptides are retained.

An analysis of the EPR signals in OGP PS2 oxygen evolving particles [Bowlby et al., 1988] found that the $Q_A^-Fe^{2+}$ signal was of the g=1.8 type; the bicarbonate influence over this signal having been lost. Removal of a further subunit, CP29, reduced the yield of the iron-semiquinone signal while the yield of a second signal at g=6.1 was found to increase.

The non-oxygen evolving PS2 core particles are generally obtained by further detergent treatment of oxygen evolving core preparations (eg. by using DM [Dekker et al., 1989]). EPR studies by Petersen et al. (1990) on the Dekker non-O_2 evolving core particle, a D1, D2, cytochrome b_{559}, CP47 complex, found Q_A to be absent. However, they did

observe a split g=6 signal unlike any signal normally seen in BBYs. This split g=6 signal was suggested to arise from decoupling of the non-haem iron from the quinone and disruption of the non-haem iron ligands. Yamaguchi et al. (1988) obtained a similar CP43 deficient particle upon treatment of digitonin extracts from spinach thylakoids with the chaotrope potassium thiocyanate. They established that their complex retained Q_A in the majority of centres.

An analysis of the EPR data from the different preparations suggests that structural changes are taking place at the electron acceptor side of the reaction centre following detergent digestion of the PS2 complex. These changes seem to become more significant the smaller the complex gets until eventually the primary quinone is lost from the complex. The experiments demonstrated here were aimed at conserving the native state of the quinone binding region of PS2 in small core complexes. To achieve this the detergent methods of both Ghanotakis et al. (1987) and Dekker et al. (1989) have been used as a basis for the development of new preparations. These new preparations exhibit the native EPR signals from Q_A and the non-haem iron, indicating that the electron acceptor side of PS2 is relatively undamaged.

3.3.1 Characterisation Of The Different Detergent Preparations

The detergent concentration required for the preparation of O_2 evolving OGP PS2 core particles from BBYs

was selected as illustrated in Fig.3.16. The concentration chosen combined efficient LHCII removal with optimum PS2 core yield. At low detergent concentrations little digestion occurred and subsequently the Chl yield was low. At concentrations of 27.5-37.5 mM both the Chl a/b ratio of the complexes and the total Chl yield were found to increase. This reduction in the Chl b content indicated LHCII removal because the majority of Chl b is in the LHC II; the only subunit binding Chl b left in the core complex is CP29. The room temperature absorbance spectrum in 80% acetone of OGP PS2 (Fig.3.17b) showed a decrease in the Chl b absorbance peak at 460 nm compared to the BBY spectrum (Fig.3.17a). At the highest OGP concentrations the LHCII itself became solubilised and so the Chl yield continued to increase, but the Chl a/b ratio decreased. Therefore, 37.5 mM OGP was used in the preparation of OGP PS2 to secure both a high Chl a/b ratio (> 10) and a high RC yield.

Figure 3.17c shows the absorbance spectrum of the non-oxygen evolving PS2 core complexes prepared with dodecylmaltoside (DM PS2). The removal of the CP29 subunit by DM digestion further reduced the Chl b absorbance peak at 460 nm. There was also a change in the relative sizes of the Chl a peak at 434 nm and the pheophytin absorbance peak at 413 nm, due to an increase in reaction centre pheophytin concentration relative to the core Chl a. This effect was enhanced in the spectrum from reaction centre complexes with the removal of Chl a binding subunits CP43 and CP47 (Fig.3.17d).

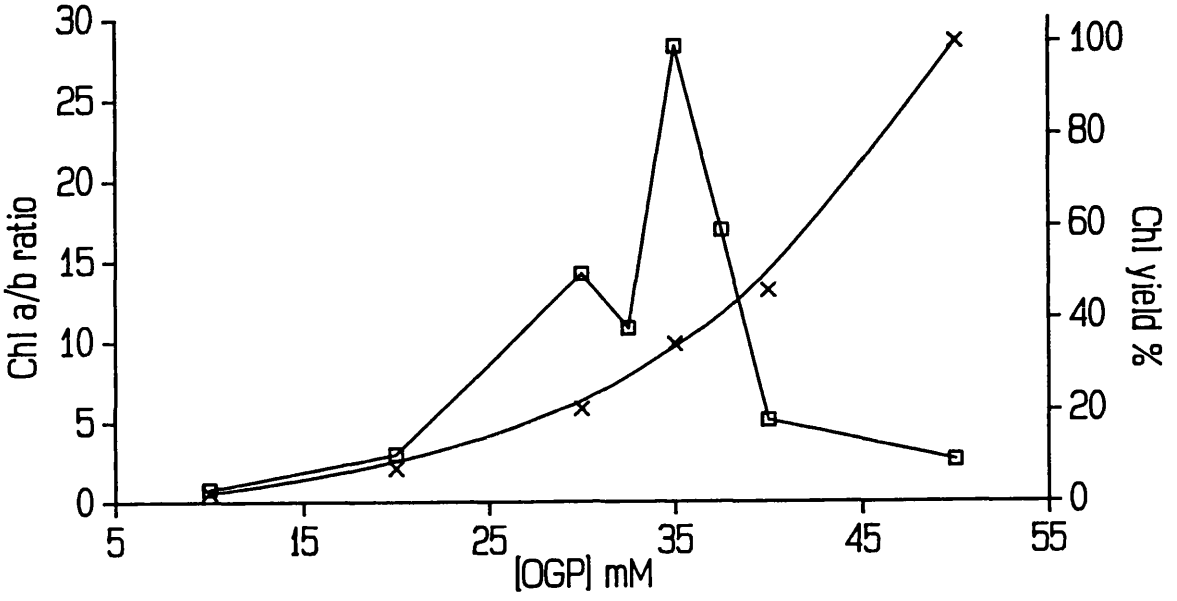

Figure 3.16 The preparation of OGP PS2 complexes from BBY PS2 particles; optimising chlorophyll yield (crosses) and desired Chl a/b ratio (open squares) with the detergent concentration used in a 12 min digestion.

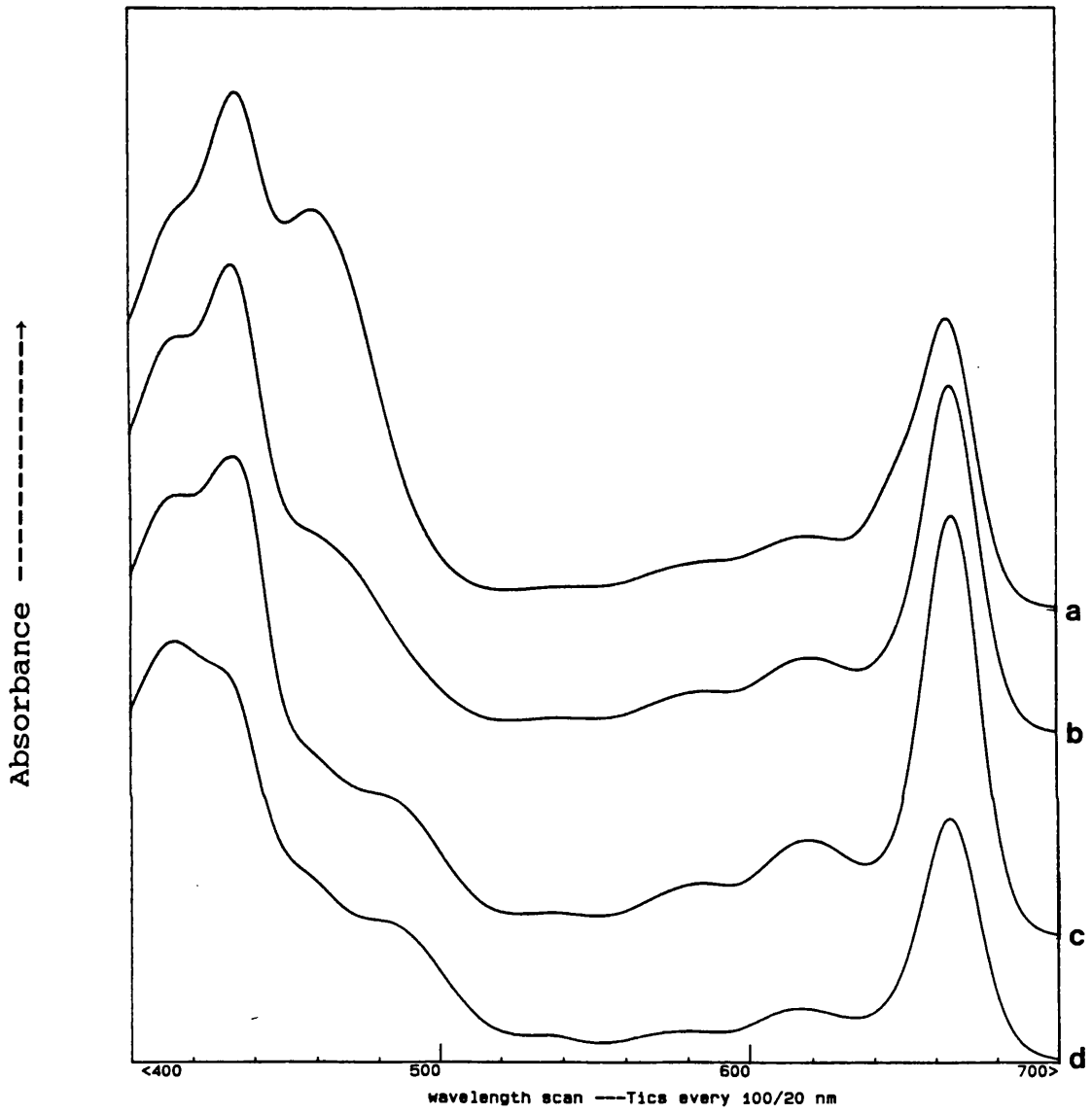

Figure 3.17 Absorbance spectra of different PS2 detergent preparations in 80% (v/v) acetone. (a) BBYs, (b) OGP PS2, (c) CP43, CP47, D1, D2, cytochrome b_{559} DM PS2 particles, and (d) reaction centre complexes.

Fig.3.18 shows the SDS-PAGE profiles of BBYs and the three extrinsic polypeptides removed by Tris-washing. Some subunits of the PS2 complex were obscured due to overloading of polypeptides in the 26-29 kDa range (Fig.3.18b), the subunits that constitute the LHCII. Fig.3.19 shows the SDS-PAGE profiles of the OGP and DM PS2 preparations. The polypeptides marked are the three chlorophyll proteins CP47, CP43 and CP29, the reaction centre subunits D1 and D2, the 33 kDa extrinsic, the 22 and the 10 kDa subunits and the 9 kDa cytochrome b_{559} component. The polypeptide composition of each preparation is summarised in Table 3.2 along with the g-values of the $Q_A^-Fe^{2+}$ and oxidised non-haem iron EPR signals observed in each case.

Digestion with OGP at either pH 6.0 or 7.5 removed the LHCII polypeptides but the raised pH caused the loss of further subunits. OGP PS2 prepared at pH 6.0 contained the 10 and the 22 kDa subunits (Fig.3.19a) [Ghanotakis et al., 1987], but these were lost when the method was carried out at pH 7.5 (Fig.3.19b).

3.3.2 Q_A And Q_B

Fig.3.20a shows the 77 K illuminated EPR spectrum of the quinone region in oxygen evolving PS2 core complexes prepared at pH 6.0 using the detergent OGP (OGP PS2). The EPR signal from $Q_A^-Fe^{2+}$ is of the g=1.8 type, associated with the removal of bicarbonate from PS2 [Vermaas and Rutherford, 1984]. If 50 mM formate was added to the pH

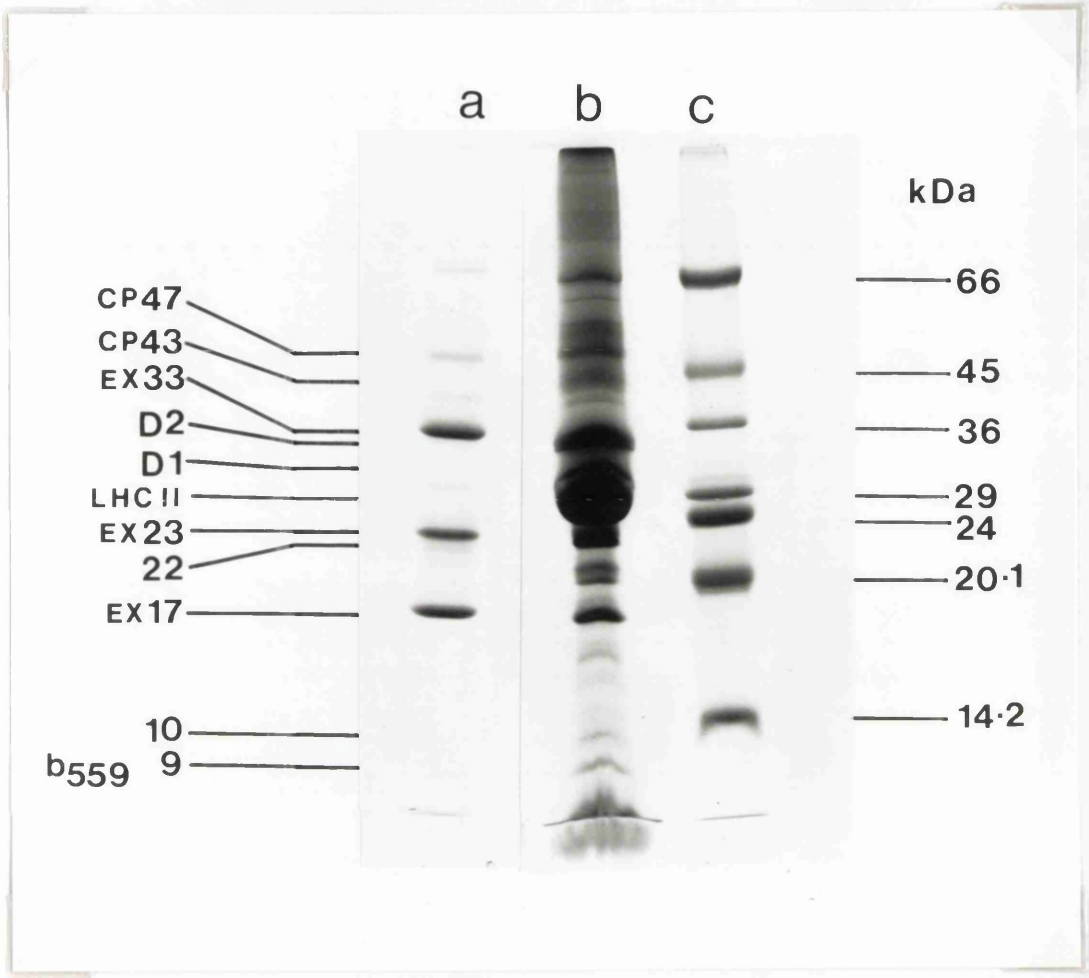

Figure 3.18 SDS-PAGE profiles of the OEC extrinsic polypeptides and BBYs run on a 15% acrylamide resolving gel with 6 M Urea. (a) the 33, 23 and 17 kDa extrinsic subunits of the OEC, removed by washing with 1 M Tris-HCl pH 8.8, (b) BBYs, and (c) Sigma Dalton Mark VII-L molecular weight markers.

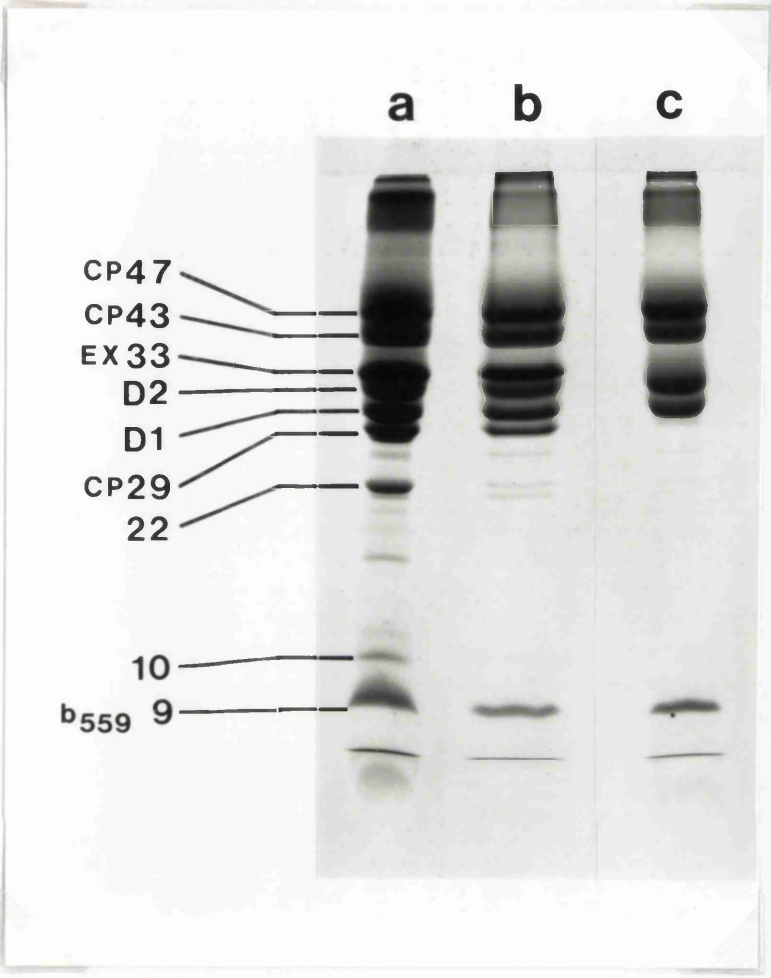

Figure 3.19 SDS-PAGE profiles of OGP and DM PS2 complexes run on a 15% acrylamide resolving gel with 6 M Urea. (a) pH 6.0 OGP PS2, (b) pH 7.5 OGP PS2 and (c) DM PS2. Molecular weights in kDa.

PS2 Preparation.	Polypeptides in addition to the D1,D2,CP47,CP43, cyt.b_{559} core.	Epr signal g-values $Q_A^-Fe^{2+}$	Fe^{3+}
BBY	CP29,22,10,LHCII, ex33,ex23,ex17	1.9	8.0 5.6
pH 6.0 OGP	CP29,22,10,ex33	1.8	6.2 5.75
pH 7.5 OGP	CP29,ex33	1.9	7.7 5.7
pH 7.5 DM	core only	1.9	7.6 5.7 split g=6

ex = extrinsic polypeptide
CP = chlorophyll protein
Polypeptide sizes in kDa

Table 3.2 A summary of the subunits composing the different PS2 detergent preparations described in section 3.3, see Figs.3.18 and 3.19 for SDS-PAGE analysis. The table also includes the g-values of the Q_A iron-semiquinone and oxidised non-haem iron EPR signals observed in each preparation.

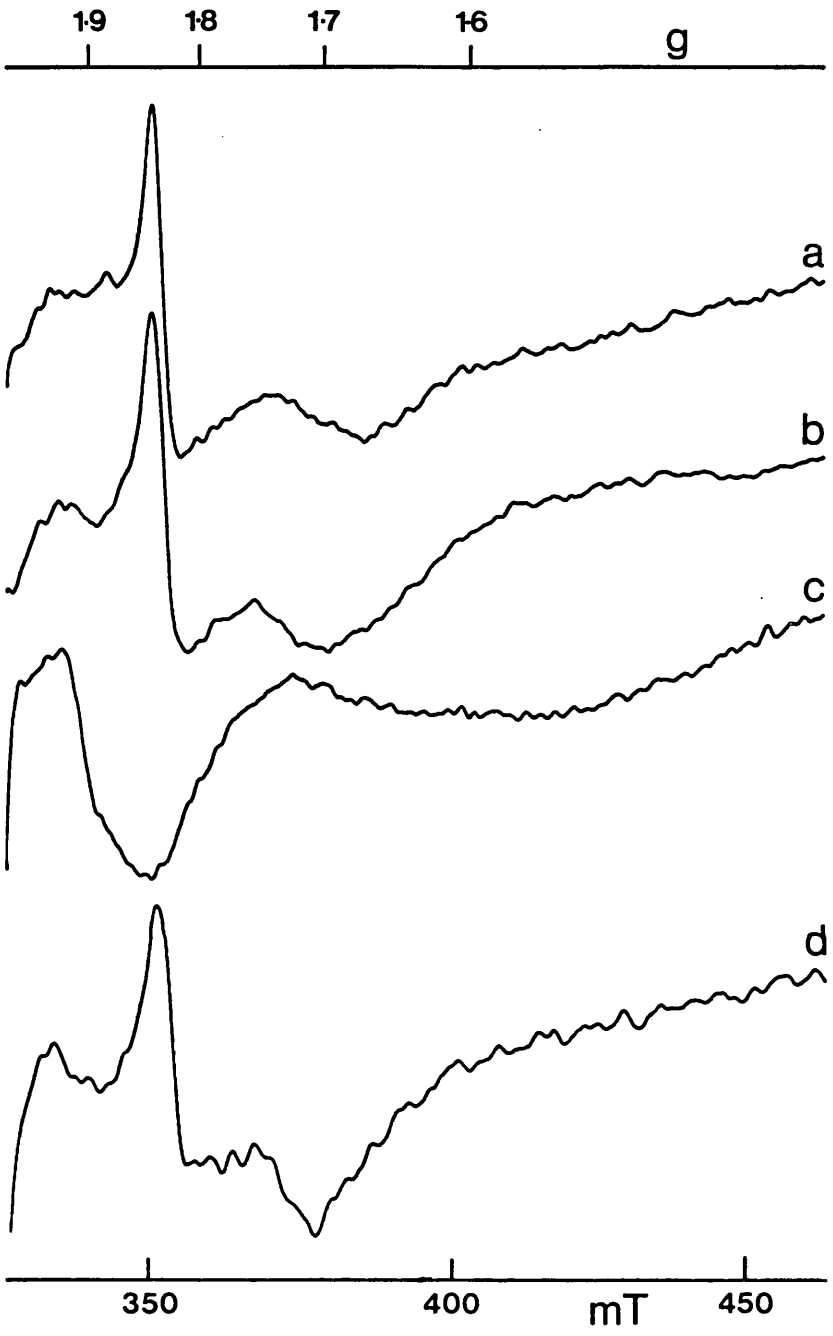

Figure 3.20 EPR spectra of the $Q_A^-Fe^{2+}$ signals in OGP PS2. (a) 77 K illuminated pH 6.0 OGP PS2, (b) as (a) + 50 mM formate, (c) 77 K illuminated pH 7.5 OGP PS2 + 50 mM bicarbonate and (d) as (c) but bicarbonate is replaced with 50 mM formate. Sample concentration, 2 mg/ml Chl. EPR conditions: temperature 5 K, microwave power 10 mW, modulation width 1.25 mT. Instrument gain for (d) was half that of (a), (b) and (c).

6.0 OGP PS2 sample (Fig.3.20b) the g=1.84 peak was broadened slightly and the trough near g=1.7 narrowed. However, formate addition did not increase the amplitude of the signal. The detergent treatment at pH 6.0 clearly altered PS2 so that bicarbonate was removed.

When OGP PS2 prepared at pH 6.0 was resuspended in a pH 7.5 buffer containing 50 mM bicarbonate, it was possible to restore the g=1.9 signal in some, but not all centres. To obtain complete restoration of the signal it was necessary to incubate the sample at higher pHs (8-9) + 50 mM HCO_3^- for at least one hour. However, if the preparation of OGP PS2 was carried out entirely at pH 7.5 with 50 mM bicarbonate present then the g=1.9 $Q_A^-Fe^{2+}$ native signal was retained (Fig.3.20c) and no g=1.8 signal observed. If bicarbonate was replaced with formate at pH 7.5 then the conversion to a g=1.8 $Q_A^-Fe^{2+}$ signal occurred (Fig.3.20d). The signal in Fig.3.20d has a broader g=1.84 peak and a larger amplitude than those in Fig.3.20a/b.

The pH sensitivity and reversibility of bicarbonate binding are demonstrated in Fig.3.21. If pH 7.5 OGP PS2 were placed in a pH 6.0 buffer with no bicarbonate present, then the EPR spectrum was altered from the g=1.9 signal (Fig.3.21a) to one containing both g=1.9 and 1.8 components (Fig.3.21b). This conversion was completely reversible for at least 30 min if the sample was then returned to the pH 7.5 buffer with bicarbonate present (Fig.3.21c).

Further evidence that the EPR behaviour exhibited by the pH 7.5 + bicarbonate OGP PS2 was indicative of a more

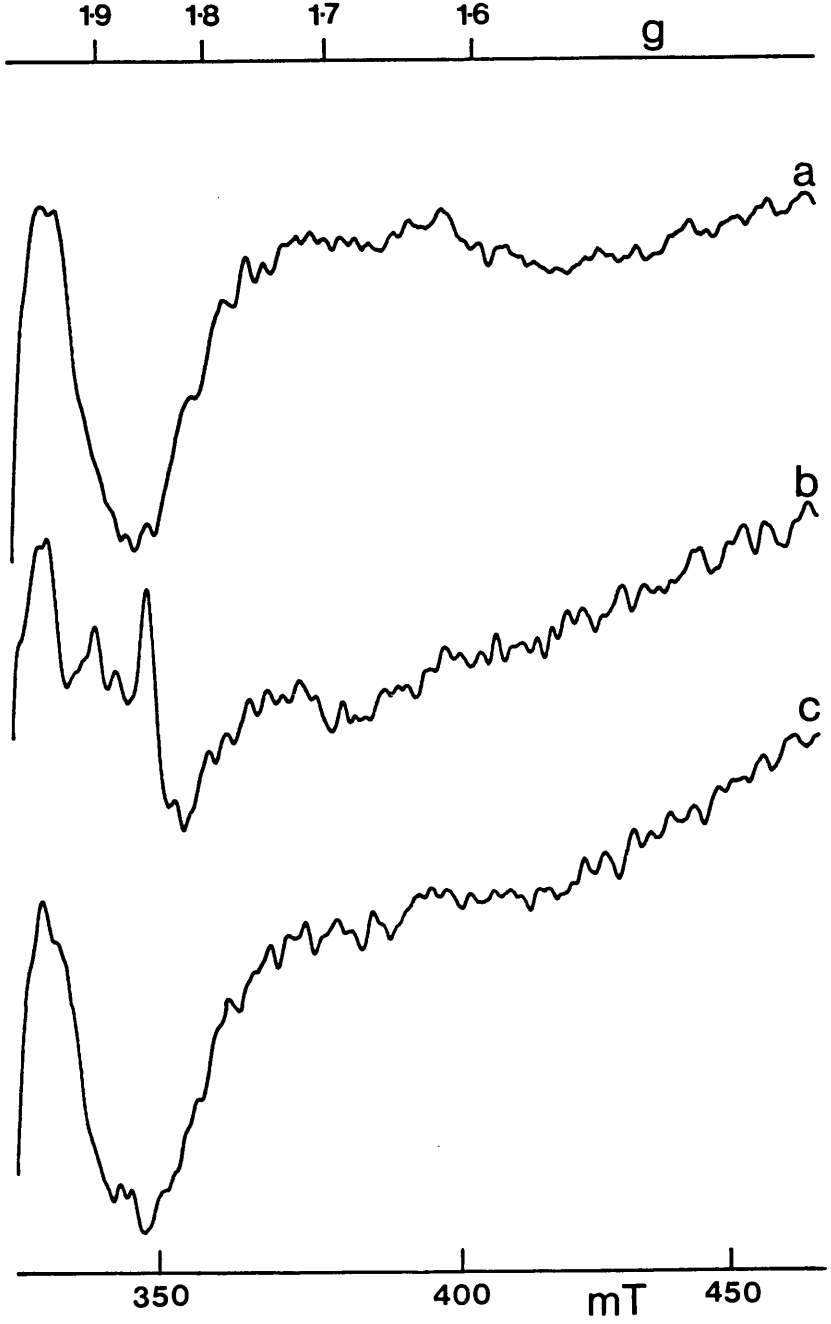

Figure 3.21 The pH reversibility of the $Q_A^-Fe^{2+}$ EPR signal from pH 7.5 prepared OGP PS2. 77 K illuminated spectra of (a) pH 7.5 OGP PS2 incubated for 30 mins in pH 7.5 + 50 mM bicarbonate buffer, then centrifuged and resuspended, dark adapted for one hour before freezing to 77 K, (b) as (a) but incubated and resuspended in pH 6.0 buffer, no bicarbonate, and (c) as (b) but given a second 30 min incubation period in pH 7.5 + 50 mM bicarbonate buffer. Amplitude of spectra were adjusted to a sample concentration of 2 mg/ml Chl for comparison. EPR conditions: temperature 5 K, microwave power 10 mW, modulation width 1.25 mT.

native electron acceptor region was obtained by using the Q_B analogue TBTQ. This compound is thought to bind to the Q_B binding site as a stable semiquinone (see section 3.1). All samples treated with TBTQ were first illuminated for 30 seconds at room temperature then dark adapted for 45 minutes before freezing to 77 K. This procedure was found to increase the yield of the TBTQ related EPR signals. Fig.3.22a shows the unilluminated spectrum of a pH 6.0 OGP PS2 sample with 500 μM TBTQ added. A broad signal with a peak near g=1.85 was observed. The 77 K illuminated (Fig.3.22b) spectrum shows a characteristic g=1.8 $Q_A^-Fe^{2+}$ signal. No significant change in the amplitude of the g=1.8 signal compared to the untreated pH 6.0 sample (Fig.3.20a) was seen but the size of the g=1.7 trough decreased. The g=1.65 signal attributable to an interaction between Q_A and Q_B semiquinones was absent. Previous studies on the g=1.65 signal have also described the inability to observe a signal in formate treated samples of cyanobacterial PS2 membranes [Nugent et al., 1988; McDermott et al., 1988]. Fig.3.22c is the unilluminated spectrum from TBTQ treated pH 7.5 OGP PS2. The Q_B analogue induced a broad signal around g=1.7 attributable to $TBTQ^-Fe^{2+}$ [Corrie et al., 1991; Hallahan et al., 1991]. When Q_A^- is formed by 77 K illumination, both Q_A^- and $TBTQ^-$ are present and a large signal was generated near g=1.65 (Fig.3.22d) from the interaction between the two iron-semiquinones. Therefore OGP pH 7.5 preparations retained the characteristics observed in BBYs whereas pH

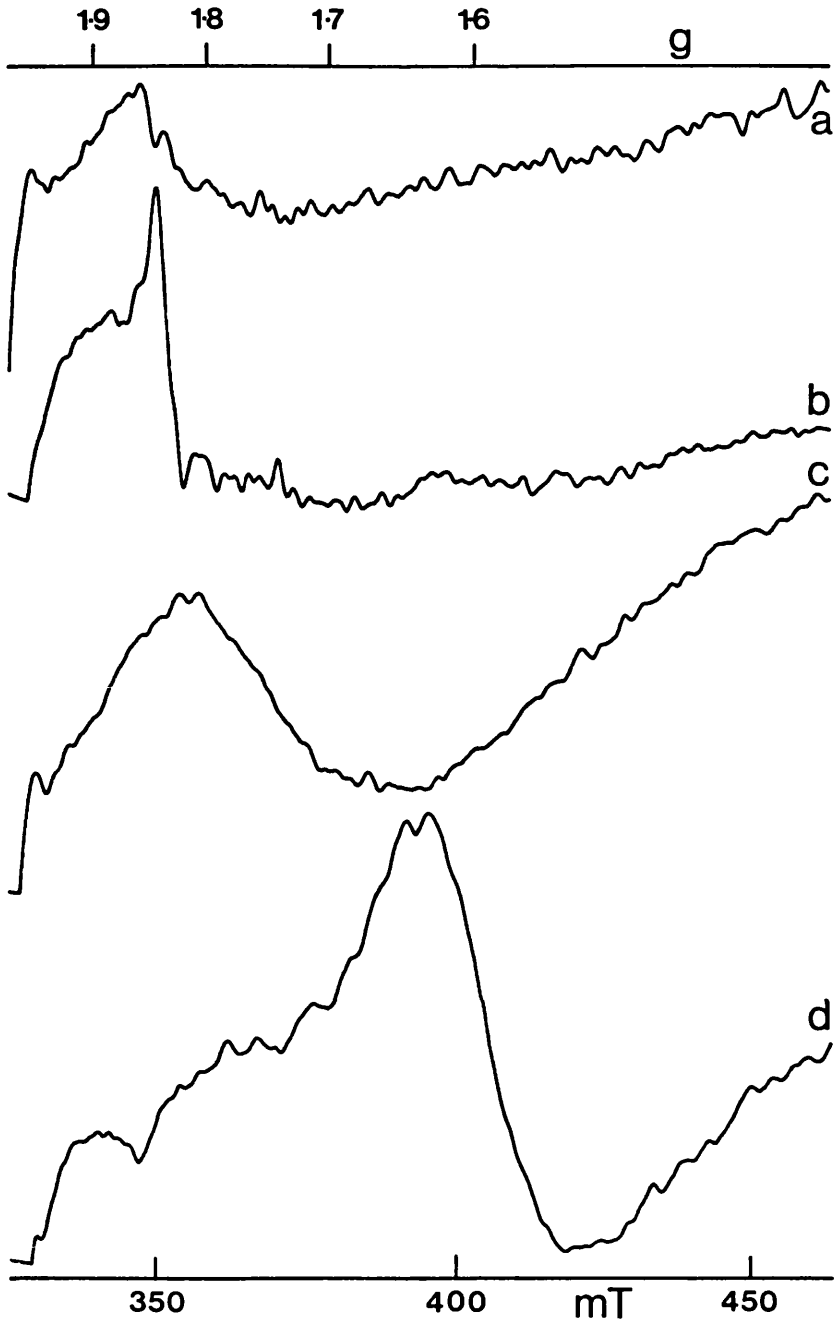

Figure 3.22 The effect of 500 μM TBTQ addition on the iron-semiquinone EPR signals from OGP PS2. Samples were illuminated for 30 seconds at room temperature then dark adapted for 45 minutes before freezing to 77 K. (a) Unilluminated spectrum of TBTQ treated pH 6.0 OGP PS2, (b) 77 K illuminated spectrum of TBTQ treated pH 6.0 OGP PS2, (c) and (d) are as (a) and (b) respectively but using pH 7.5 OGP PS2. Sample concentration, 2 mg/ml Chl. EPR conditions: temperature 5 K, microwave power 10 mW, modulation width 1.25 mT.

6.0 preparations did not.

The next step used by Ghanotakis et al. (1987) and Dekker et al. (1989) for the removal of polypeptides from OGP PS2 involves digestion by the detergent dodecylmaltoside. I have prepared DM PS2 core complexes using pH 7.5 buffer containing 50 mM bicarbonate at both 4 °C and room temperature. Under these conditions a complex containing CP47, CP43, D1, D2, cytochrome b_{559} was obtained (see Fig.3.19c and Table 3.2). Dekker et al. (1989) found that preparation at room temperature facilitated removal of the CP43 subunit but I failed to observe this. Other researchers looking at PS2 preparations and data from denaturation studies [Thompson et al., 1989b] have indicated that CP43 is more "loosely" associated with the reaction centre than CP47. Our inability to remove CP43 from the DM PS2 complex must be related to the raised pH at which preparation was carried out.

Analysis of the DM PS2 complex showed that it was possible to induce EPR signal II (D^+) if the samples were illuminated for several minutes at ≈ 17 K, although signal yield was low. Photooxidation of D was found not to require the addition of ferricyanide although ferricyanide was required to obtain D^+ in the CP47, D1, D2, cytochrome b_{559} complex of Petersen et al. (1990). A more significant difference between the DM PS2 and the Petersen et al. (1990) complex was that illumination at 200 K generated the g=1.9 $Q_A^-Fe^{2+}$ bicarbonate signal (Fig.3.23a). A very small amount of g=1.8 signal was present in DM PS2 but otherwise

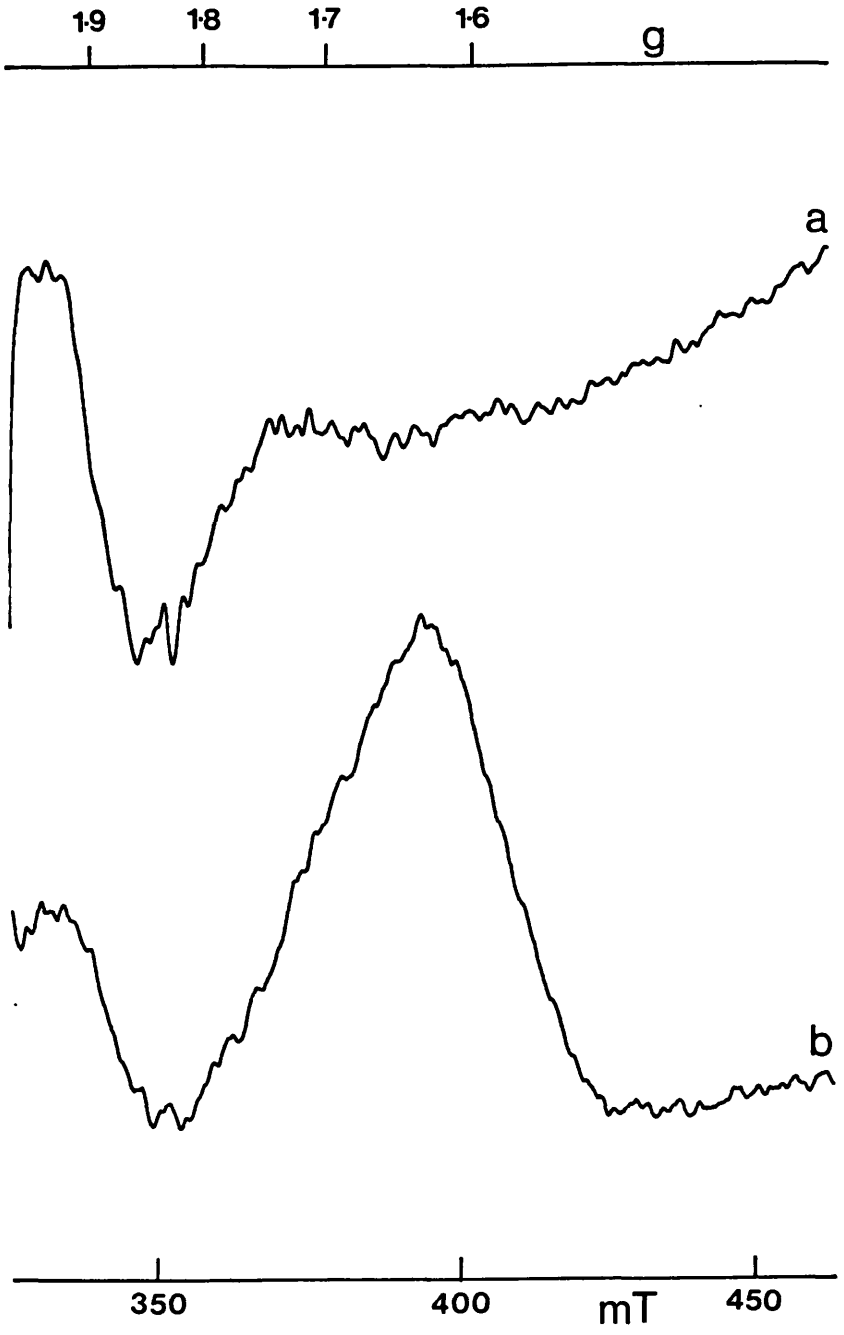

Figure 3.23 The iron-semiquinone EPR signals observed in DM PS2. (a) 200 K illuminated spectrum from untreated DM PS2 and (b) 200 K illuminated minus dark difference spectrum from 500 μM TBTQ treated DM PS2. Sample concentration, 1.25 mg/ml Chl. EPR conditions: temperature 5 K, microwave power 10 mW, modulation width 1.25 mT.

the indication was that native Q_A and bicarbonate binding were preserved. TBTQ was also added and Fig.3.23b is the 200 K illuminated minus dark difference spectrum showing the large g=1.65 signal of $Q_A^-Fe^{2+}TBTQ^-$ demonstrating that the Q_B site was also intact.

Initially the method used to obtain the DM PS2 complexes incorporated extended periods (normally overnight) with the particles bound to a relatively slow flowing Q-sepharose column. This ensured the complete removal of contaminants by prolonged washing with buffer. The DM PS2 particles obtained by this method did not display any $Q_A^-Fe^{2+}$ signal. The iron-semiquinone was not observed until purification was accelerated and carried out on fast flowing, short, wide-diameter columns and a PEG precipitation method employed for concentrating the particles. Combining these improvements meant that detergent digestion, purification and EPR analysis could be achieved within a few hours. The necessity for speed I have identified indicates that there is an inherent instability in the binding of Q_A in this core type of preparation.

Attempts were also made to obtain reaction centre complexes retaining Q_A. The two different methods employed for RC complex preparation were similar to the TX-100 and DM + $LiClO_4$ methods described by Dekker et al. (1989). Unfortunately, neither of these methods was successful and no Q_A related EPR signals were observed in the reaction centres.

3.3.3 The Non-Haem Iron.

Figure 3.24a is the Fe^{3+} dark minus 77 K illuminated difference spectrum recorded from BBYs oxidised with ferricyanide and shows the characteristic peaks at g=8.0 and 5.6. The dark minus 77 K illuminated difference spectrum from pH 6.0 OGP PS2 oxidised with ferricyanide (Fig.3.24b) had an altered spectrum with two peaks at g=6.2 and 5.75. The abnormal signal peaks obscured a smaller signal with a g=8 peak which was probably due to a minority of reaction centres still with bicarbonate bound. Fig.3.24c is the dark minus 77 K illuminated difference spectrum from ferricyanide oxidised pH 7.5 OGP PS2 and is almost identical to the normal spectrum from PS2 membranes seen in Fig.3.24a. A small g-value change in the positioning of the peaks to g=7.7 and 5.7 occurred.

Investigation of the oxidised non-haem iron in pH 7.5 + 50 mM bicarbonate DM PS2 complexes (Fig.3.25) revealed two different types of spectrum. In the absence of ferricyanide a prominent signal with two peaks at g=6.15 and 5.85 was present in the dark that was unchanged by 200 K illumination (see central peaks of Fig.3.25b). This is a similar signal to that observed by Petersen *et al*. (1990) in the CP47, D1, D2, cytochrome b_{559} complex. Following incubation of DM PS2 with ferricyanide, an additional signal at g=7.6 (Fig.3.25a) was observed that was completely removed by 200 K illumination (Fig.3.25b). The dark minus light difference spectrum (Fig.3.25c) has two peaks from oxidised non-haem iron but the g-values are

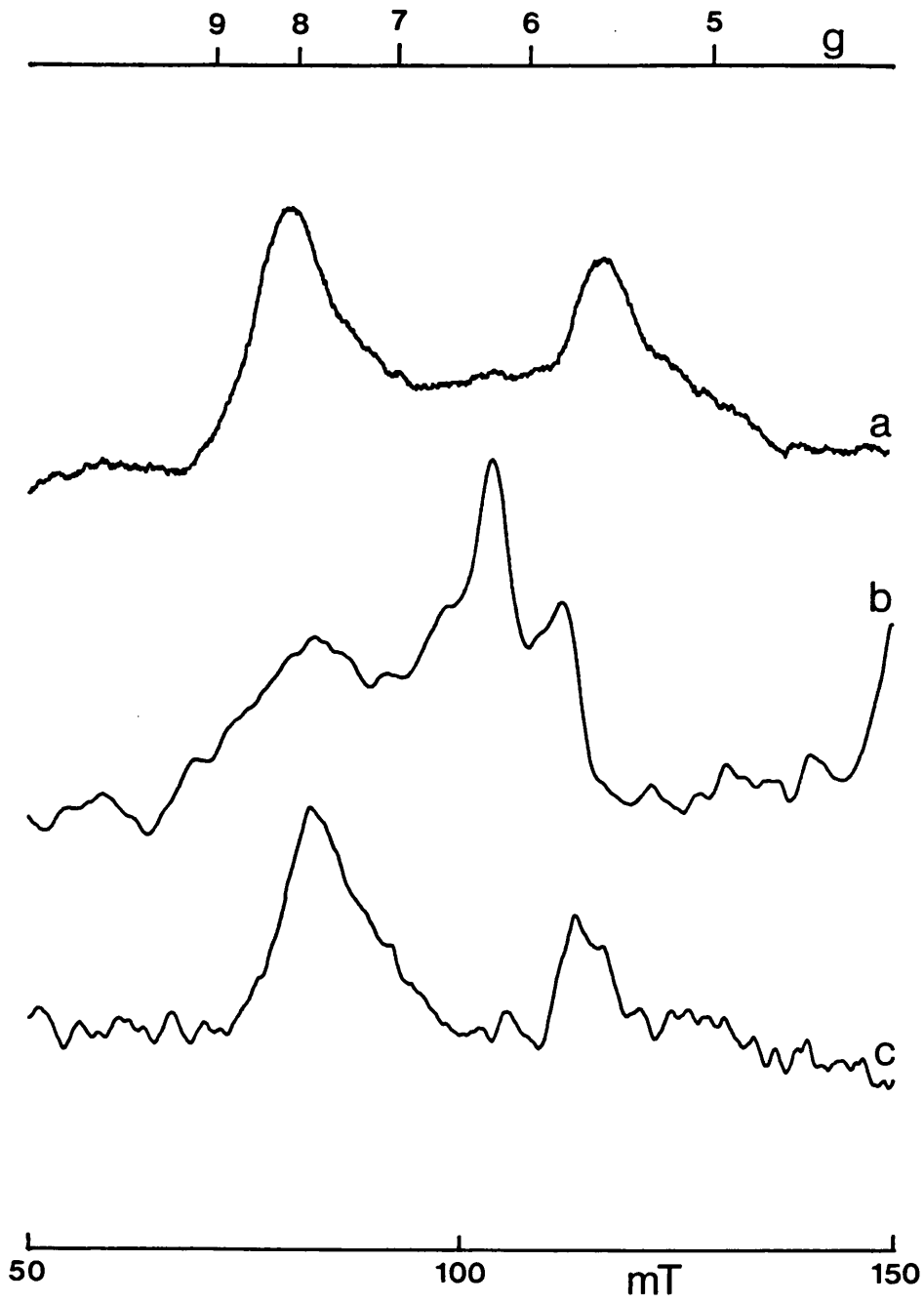

Figure 3.24 Ferricyanide oxidised non-haem iron EPR difference spectra in OGP PS2. (a) The dark minus 77 K illuminated difference spectrum from BBYs treated with 5 mM potassium ferricyanide, (b) as (a) but pH 6.0 OGP PS2 in a pH 7.5 buffer, and (c) as (a) but pH 7.5 OGP PS2. Sample concentration, 2 mg/ml Chl. EPR conditions: temperature 5 K, microwave power 10 mW, modulation width 1.25 mT.

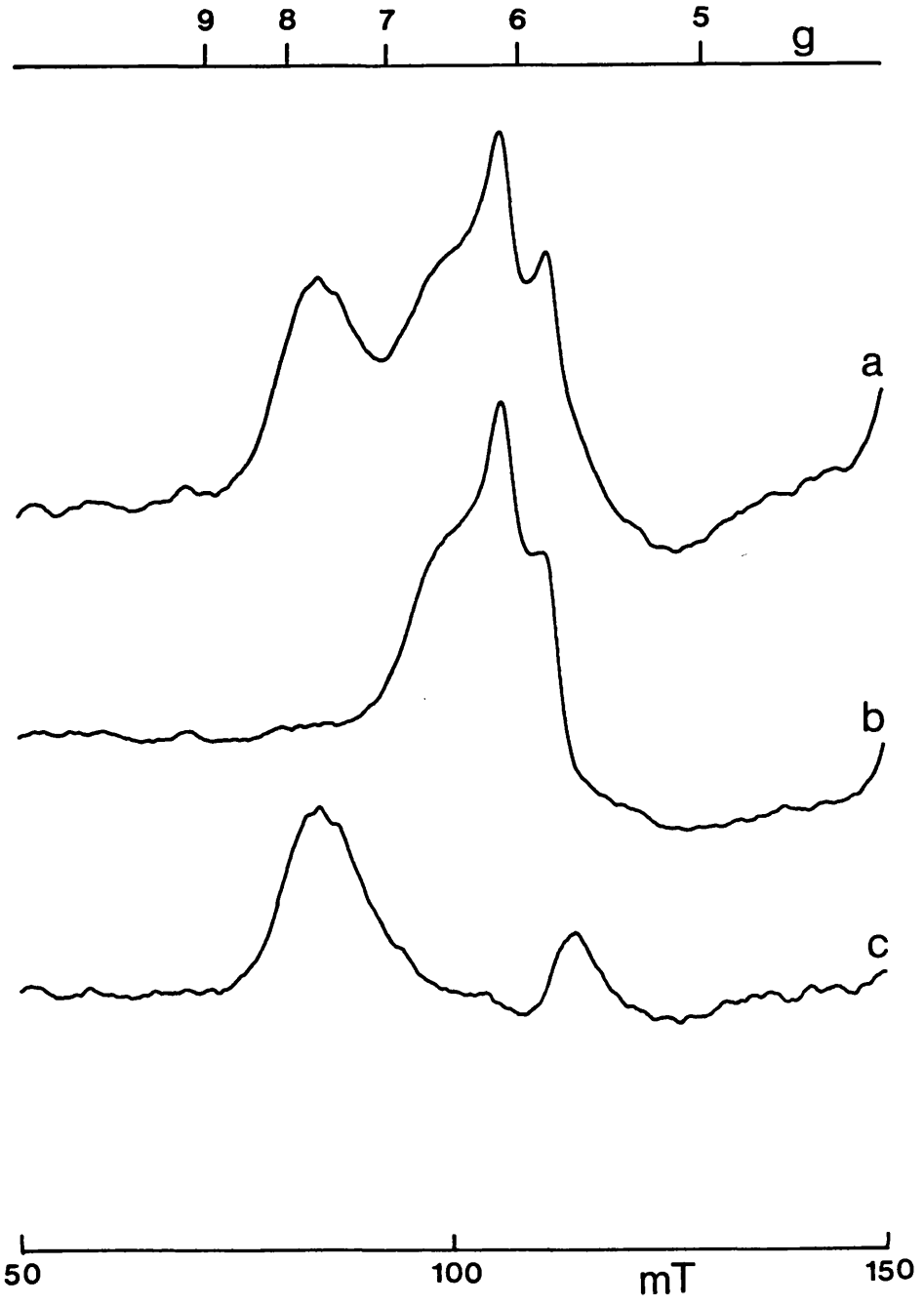

Figure 3.25 EPR signals observed in the g=5-8 region in DM PS2 treated with 5 mM potassium ferricyanide. (a) The dark spectrum, (b) 200 K illuminated spectrum, and (c) the dark minus 200 K illumination difference spectrum. Sample concentration, 1.25 mg/ml. EPR conditions: temperature 5 K, microwave power 10 mW, modulation width 1.25 mT.

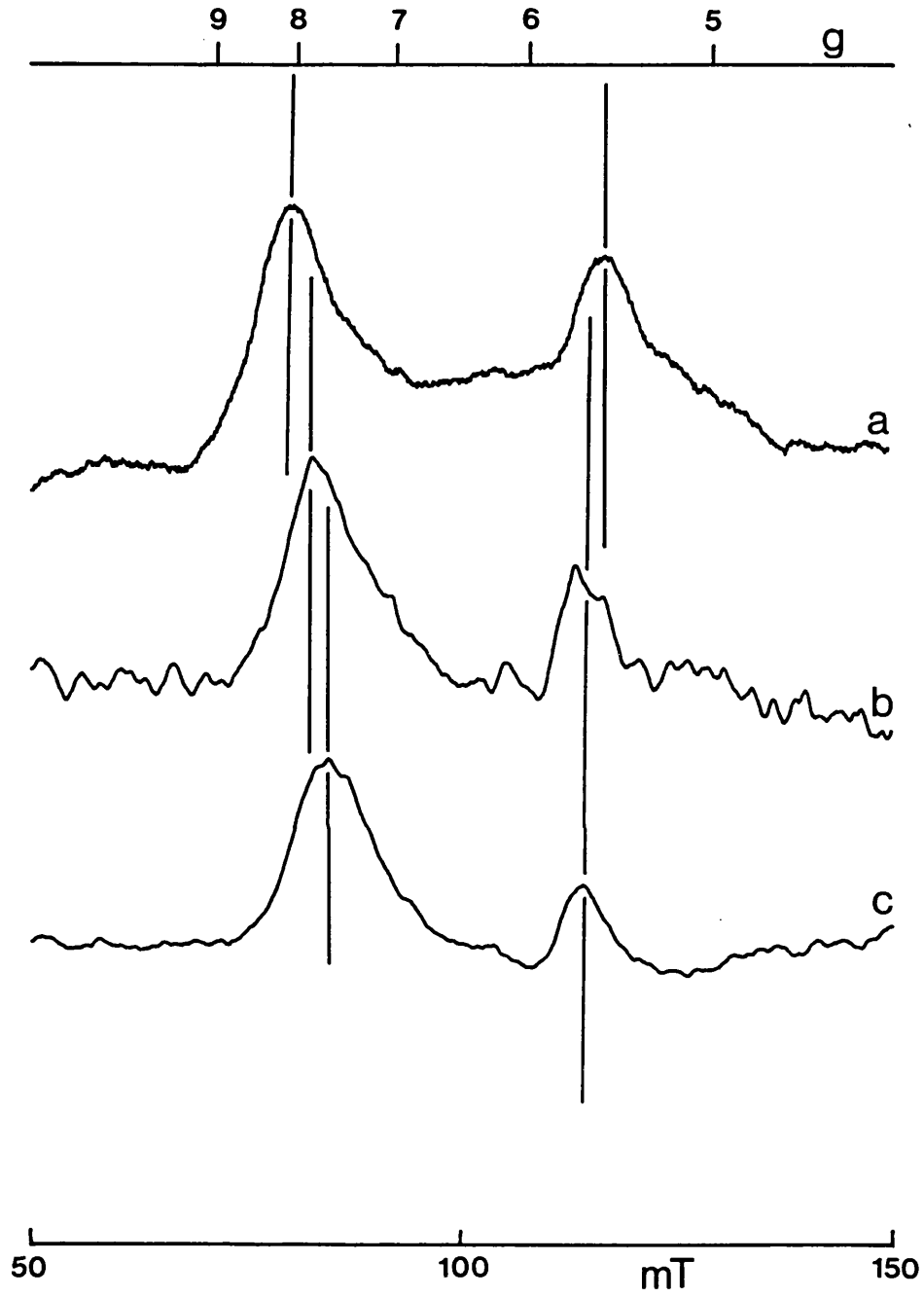

Figure 3.26 A comparison of the oxidised non-haem iron dark minus illuminated difference spectra in different PS2 detergent preparations. (a) BBYs, (b) pH 7.5 OGP PS2, and (c) DM PS2. EPR conditions: temperature 5 K, microwave power 10 mW, modulation width 1.25 mT.

altered so that the peaks are closer together at g=7.6 and 5.7.

Fig.3.26 is a comparison of the dark minus light Fe^{3+} difference spectra in BBY, pH 7.5 OGP and DM PS2 particles to demonstrate how the spectrum becomes narrower as the complex gets smaller. As more subunits are removed small changes in the ligand environment of the non-haem iron occur indicating a slight relaxation of the distorted ligand field.

3.3.4 Discussion

The results show that detergent removal of the light harvesting complex from PS2 membrane preparations at pH 6.0 also causes the loss of bicarbonate binding. Complete rebinding of bicarbonate, measured by conversion of the g=1.8 $Q_A^-Fe^{2+}$ EPR signal in the pH 6.0 OGP PS2 particles to the g=1.9 signal, is difficult though not impossible. To maintain the native situation in the electron acceptor region I have found it necessary to raise the pH and include bicarbonate at every stage in the preparation. The pH 7.5 particles display a g=1.9 $Q_A^-Fe^{2+}$ EPR signal that can be transformed easily and reversibly into the g=1.8 form of the signal using either a lower pH or formate replacement of bicarbonate [Vermaas and Rutherford, 1984]. Bicarbonate depleted pH 6.0 OGP PS2 samples show different characteristics to preparations where bicarbonate is displaced by formate. This is important since studies into the bicarbonate effect are normally carried out on formate

inhibited samples. The non-haem iron in pH 6.0 OGP PS2 can still be oxidised by potassium ferricyanide despite bicarbonate loss (Fig.3.24b). This contrasts with the observed behaviour if formate is added to PS2 membranes to displace bicarbonate where non-haem iron oxidation by ferricyanide [Nugent et al., 1988] or by artificial quinones [Zimmermann and Rutherford, 1986a] is inhibited due to a formate induced E_m increase of the Fe^{2+}/Fe^{3+} couple [Diner and Petrouleas, 1987a].

Differences in the electron acceptor side EPR behaviour of pH 6.0 OGP PS2 and BBYs probably reflect the changes in the oxygen evolution characteristics observed by other researchers. Ghanotakis et al. (1987) and Ikeuchi et al. (1985) found that the rate of oxygen evolution in pH 6.0 OGP PS2 with potassium ferricyanide remained comparable to the rates obtained with PS2 membranes but O_2 evolution using the Q_B analogue DCBQ was comparatively low. This could be related to the loss of bicarbonate that I have observed in the low pH OGP preparations because ferricyanide is known to directly oxidise Q_A^- but Q_B analogues act through the Q_B binding site, a process known to be slowed by HCO_3^- loss [Jursinic et al., 1976]. Sensitivity to DCMU was also found to be reduced [Ghanotakis et al., 1987; Ikeuchi et al., 1985] indicating that the Q_B binding site is susceptible to detergent damage. The difference in the $TBTQ^-Fe^{2+}$ dark spectra from the two OGP preparations (Fig.3.22a and c) demonstrates how the Q_B binding properties are altered by OGP digestion at low pH.

The signal yield is lower and the lineshape altered in pH 6.0 OGP PS2.

Preparation of OGP PS2 at a higher pH, in the presence of bicarbonate, maintains the native characteristics of the electron acceptor region normally observed in complete PS2 complexes. However, preparation at pH 7.5 does have a detrimental effect on the oxygen evolving capacity of the core complex. Preparation at pH 8.5 was found to remove the extrinsic 33 kDa OEC subunit and destroy O_2 evolution completely. Therefore, methods used by other researchers to obtain preparations for studies on water oxidation are optimised at pH 6.0 but modifications are required to obtain PS2 core complexes retaining native quinone and bicarbonate binding. The ability to obtain 100% bicarbonate retaining and bicarbonate free OGP PS2 particles makes our preparations an ideal system for further studies on the bicarbonate effect (see results section 3.4.1) as an anion is not required for HCO_3^- depletion.

The DM PS2 oxidised non-haem iron spectrum also contains the split g=6 component identified by Petersen et al. (1990) in the Dekker et al. (1989) CP47, D1, D2, cytochrome b_{559} complex. They assigned this signal to non-haem iron uncoupled from the quinone(s) and were unable to obtain any ferricyanide induced oxidation of the iron in their preparation. This split g=6 signal was also observed in our DM PS2 in the dark, without ferricyanide treatment, and could not be photoreduced by 200 K illumination.

Treatments altering the electron acceptor side of PS2 such as the preparation of OGP PS2 particles at pH 6.0 or trypsin treatment (see section 3.2), make the oxidised non-haem iron spectrum more axial, ie. the signal peaks move closer together towards g=6. Bowlby et al. (1988) noted a connection between the loss of the $Q_A^-Fe^{2+}$ EPR signal and subsequent increase in yield of a g=6.1 signal upon CP29 removal. This evidence indicates that the component giving rise to g≈6 signals in PS2 is the non-haem iron in damaged centres where the ligand environment has been disrupted. The only evidence against this assignment is that the abnormal split g=6 signal in DM PS2 is present in the dark without ferricyanide addition and for this signal to arise from the non-haem iron, the Fe^{2+}/Fe^{3+} mid-point potential would have to have decreased to below ≈ 100 mV. This could be conceivable if we assume the signal arises from centres where significant damage has occurred in the electron acceptor region, ie. a possible loss of both Q_A and bicarbonate.

Assigning the DM PS2 split g=6 signal to the non-haem iron and partly explaining its appearance by Q_A loss means I must conclude that our DM PS2 particles exhibit acceptor side heterogeneity. They display the g=1.9 $Q_A^-Fe^{2+}$ signal and a normal oxidised non-haem iron spectrum as well as the abnormal split g=6 signal. Therefore, some centres must retain the intact HCO_3^- Q_AFe^{2+} state while the rest have probably lost Q_A. Petersen et al. (1990) conclude that the loss of PQ from the reaction centre occurs in parallel with

the removal of the CP43 subunit. They proposed that the two events are related by the temperature dependence observed for both CP43 removal [Dekker et al., 1989] and quinone loss [Diner et al., 1988]. However, our initial attempts to obtain DM PS2 particles demonstrated that Q_A was lost from the reaction centre when the complex still retained CP43. I found this to occur at 4 °C, despite the fact that Diner et al. (1988) observed little Q_A extraction from the binding site at this temperature.

Recently Nagatsuka et al. (1991) investigated the polypeptide composition and plastoquinone content of three different types of non-O_2 evolving PS2 core particles, prepared with either DM, TX-100 or octylthioglucopyranoside (OTG). Q_A activity in all three complexes was reduced to a greater or lesser extent although actual Q_A content remained relatively high. They found that some of the lost activity in the OTG particle could be restored by reconstitution of the complex with some low molecular weight PS2 polypeptides. The function of these small subunits has so far remained unexplained but Nagatsuka et al. (1991) propose that at least some of them are essential for maintaining normal Q_A activity. Restoration of activity in the OTG particle is also interesting as this complex appears to have partially lost the CP43 subunit.

Rögner et al. (1991) have used site-directed mutagenesis to create Synechocystis mutants lacking the psbC gene product, CP43. The mutants were found to assemble CP43-less PS2 complexes although they accumulated

at a reduced level: 10% of the wild-type concentration. The isolated core complexes exhibited photoreduction of Q_A with a quantum yield comparable to the wild-type, which is further evidence for the lack of involvement of the CP43 subunit in Q_A binding.

There is clearly a problem with Q_A stability in detergent prepared core PS2 particles. The instability of the primary quinone is probably due to a combination of factors. Firstly the quinone is able to leave the Q_A binding site in intact reaction centres, a process enhanced by the use of detergents [Diner et al., 1988]. I have shown that this loss can be minimised by maintaining a low temperature (< 4 °C) and, more importantly, by using fast isolation procedures at a high pH in the presence of bicarbonate. Alternatively non-detergent methods of subunit removal can be used. Yamaguchi et al. (1988) used the chaotrope potassium thiocyanate to remove CP43 from digitonin PS2 particles. Although Q_A activity was retained in the majority of centres they still found some inactivation of the primary quinone. Secondly, it may simply be that the binding affinity of the Q_A binding site decreases as more subunits are removed from the PS2 complex. The stability of the binding site may depend on the support of a complete PS2 complex; although only D2 may actually be involved in Q_A binding. The observations of Nagatsuka et al. (1991) are interesting but their suggestions of specific roles for some small polypeptides may be wrong. The reactivation of Q_A activity which they

observe may not be that specific; it could be that reconstitution with any subunit(s) would increase the recovery of primary quinone activity.

From the EPR behaviour exhibited by the different OGP PS2 preparations it is obvious that a disruption of the environment surrounding the non-haem iron and Q_A occurs as early as pH 6.0 OGP removal of the LHCII from BBYs. The reaction centre is modified by bicarbonate loss even before DM is used in further purification steps, making the reaction centres susceptible to Q_A loss. In Cyanobacteria the reduced complexity of the PS2 complex compared to higher plants, mainly due to the absence of an integral membrane LHCII, probably makes the reaction centre structure more stable. Rögner et al. (1991) have shown that a fully functional CP43-less core complex can be isolated from a Synechocystis mutant even though a detergent solubilisation of the thylakoid is necessary [Rögner et al., 1990]. This means that isolation of a PS2 reaction centre complex retaining the native Q_A may be achieved first with a cyanobacterium.

3.4 Investigations Of The PS2 Split Pheophytin Signal And The Redox Titration Phenomenon Of This Signal

The split (bacterio)pheophytin signal was first observed in Chromatium (C.) vinosum chromatophores frozen under illumination in the presence of dithionite [Evans et al., 1974]. Analysis of this and other purple bacterial systems [Tiede et al., 1976; Prince et al., 1977; Okamura et al., 1979] determined that the split signal was generated by photoreduction of I, the intermediate electron acceptor, in centres with chemically reduced Q_A.

Similar EPR signals, observed in enzyme systems requiring coenzyme B_{12}, were interpreted as arising from a weak electrostatic exchange interaction between an organic radical at g=2 and a lower field component of low-spin cobalt (II) [Schepler et al., 1975]. Comparing the bacterial system with the coenzyme B_{12} system suggests that the high field g=1.82 signal from $Q_A^-Fe^{2+}$ could be paired with the lower field g=2 BPh^- signal in a similar interaction. The split signal was consequently assigned to a splitting of the BPh^- g=2 signal through an exchange interaction with the iron-semiquinone [Tiede et al., 1976].

In Rps. viridis the split signal was found to exhibit some hyperfine structure that indicated a possible magnetic dipole-dipole interaction between the two paramagnets [Prince et al., 1977]. Further evidence for this was the absence of the iron-semiquinone EPR signal in samples exhibiting the split signal. Subsequent oxidation of BPh^-

in these samples, by warming to room temperature to allow recombination of BPh^- with cytochrome c_{553}^+, restored the $Q_A^-Fe^{2+}$ g=1.82 signal. The temporary "disappearance" of this signal was suggested to be a consequence of the dipolar-coupling component of the interaction with BPh^- that caused a splitting and broadening of the g=1.82 signal itself.

Generation of the split signal in both C. vinosum and Rps. viridis was found to be associated with the appearance of a g=2 radical. In Rb. sphaeroides the initial attempts of Okamura et al. (1979) to observe the split signal were unsuccessful and only the g=2 radical was obtained. However, they found that replacement of the native ubiquinone Q_A with menaquinone, as in C. vinosum, enabled generation of the split signal. Okamura et al. (1979) identified the g=2 radical as BPh^- observed in centres where the primary quinone had undergone double reduction. The activation energy for the reduction of the Q_A semiquinone was found to be smaller with ubiquinone than menaquinone.

The ability to generate a split pheophytin signal has also been demonstrated in PS2 [Klimov et al., 1980a; Klimov et al., 1980b]. It was concluded that an exchange interaction similar to that in bacteria occurs between Ph^- and a paramagnet with a g-value near g=1.8, probably $Q_A^-Fe^{2+}$. The iron-semiquinone in higher plant PS2 has since been shown to exhibit two different EPR signals, the g=1.9 and g=1.8 signals [Nugent et al., 1981; Rutherford and Zimmermann, 1984], and the width of the split signal has been demonstrated to depend on which of these signals is

observed. The splitting was found to be largest when the iron-semiquinone signal was of the g=1.9 type [Rutherford and Zimmermann, 1984].

In bacteria the ability to form the split signal occurs in parallel with the reduction of Q_A. Therefore, a redox titration of the split signal provides a single n=1 Nernst curve with a mid-point potential equal to that of the Q_A/Q_A^- couple [Tiede et al., 1976; Rutherford et al., 1979]. In PS2 however, experiments of this type have found that the split signal titrates in two steps with E_m values of approximately 0 mV and -250 mV [Rutherford and Mathis, 1983; Evans et al., 1985; Evans and Ford, 1986]. Two steps with comparable mid-point potentials are also observed in fluorescence titrations of PS2 [Horton and Croze, 1979; Diner and Delosme, 1983] where the respective fluorescence quenchers are known as Q_H and Q_L (high and low potential). Together these observations have made it difficult to ascribe a single mid-point potential to the primary quinone electron acceptor Q_A and were thought to indicate the existence of PS2 sub-populations differing either in their Q_A/Q_A^- mid-point potential or in the possession of an extra electron acceptor operating in series with, or parallel to, Q_A.

Multiple steps have been observed in redox titrations of the Q_A iron-semiquinone EPR signal in PS2 [Evans et al., 1985] that were taken to confirm the existence of an electron acceptor between Ph and Q_A, a suggestion that will be discussed in more detail later (section 3.4.4). Evans

et al. (1985) also found that reduction of a further component "U" (E_m -430 mV) was necessary before the P680 triplet could be formed. This phenomenon has since been suggested to represent the double reduction of Q_A [van Mieghem et al., 1989], an event not so readily achieved as in bacteria. In PS2 the presence of $Q_A^-Fe^{2+}$ greatly reduces triplet production, possibly through an electrostatic interaction reducing the yield of the $P680^+Ph^-$ radical pair [van Mieghem et al., 1989].

The principal functional differences between the purple bacterial reaction centre and PS2 generally relate to the ability of the latter to oxidise water. Events on the other side of the membrane, the electron acceptor side, are known to be very similar. The split pheophytin signal titration data is complicated and has so far been unsatisfactorily explained. Therefore an analysis of the data based on comparisons with the purple bacterial system and existing knowledge would be more appropriate, to provide an explanation that does not invoke the existence of heterogeneous RC populations or new components between Ph and Q_A. The experiments undertaken here are an effort to provide an alternative explanation for the two step phenomenon and to investigate further the nature of the split signal in PS2. The OGP PS2 preparations described earlier (section 3.3) are an improved system in which to carry out studies of this type as they can be used at greater reaction centre concentrations to yield larger EPR signals. As a result the signals have a greater

signal/noise ratio and therefore allow more accurate measurements of signal amplitude in redox titration experiments.

3.4.1 The Split Pheophytin Signal In OGP PS2

The split signals obtained from the two types of OGP preparation are very different. Fig.3.27 shows the 200 K illuminated minus dark difference spectra from OGP PS2 reduced with 25 mM sodium dithionite. The spectrum from pH 6.0 OGP PS2 (Fig.3.27a) displayed the characteristic narrow splitting. This preparation exhibited a g=1.8 $Q_A^-Fe^{2+}$ signal in 100% of centres without the need for anion displacement of the native HCO_3^- [Bowden et al., 1991; see section 3.3]. Previously a narrow signal has only been observed in formate treated samples or low pH samples containing a mixture of the g=1.8 and 1.9 iron-semiquinone signals. The signal generated in pH 7.5 + 50 mM HCO_3^- OGP PS2 (Fig.3.27b) was the wide split signal normally observed when the native situation is maintained with bicarbonate present in 100% of reaction centres.

The effect of bicarbonate on the splitting is even more obvious when the 1st derivative EPR spectra of Fig.3.27 are integrated to give the microwave absorbance spectra (Fig.3.28). The integral of the wide, HCO_3^- influenced, split signal had two very distinct absorbance peaks (Fig.3.28b). The signal splitting is measured as the difference in the magnetic field position of these peaks, in this case 4.4 mT (see the insert in Fig.3.28 to see how

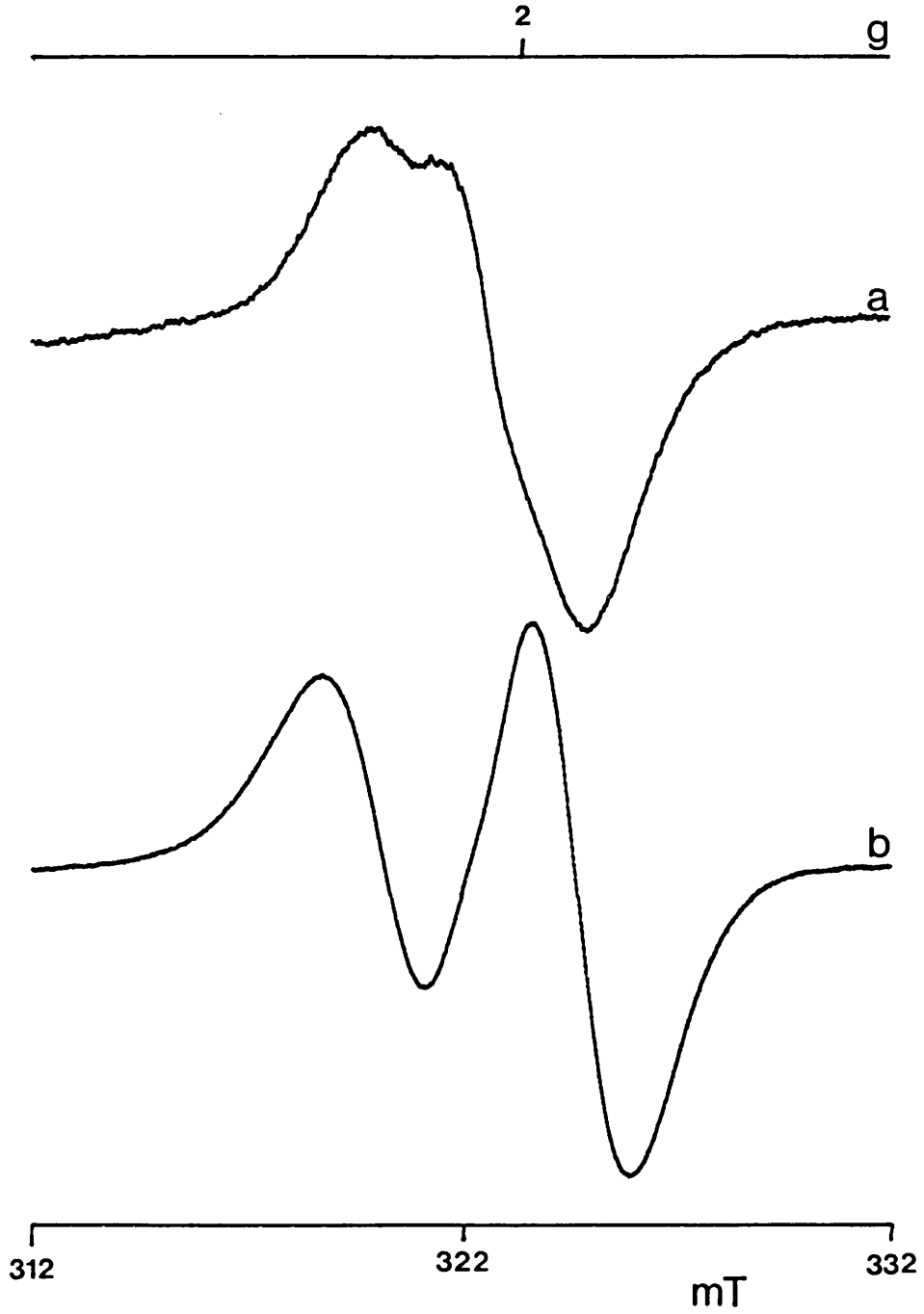

Figure 3.27 The split pheophytin EPR signals in OGP PS2. (a) 200 K illuminated minus dark difference spectrum from pH 6.0 OGP PS2 reduced with 25 mM sodium dithionite, and (b) as (a) but pH 7.5 + 50 mM bicarbonate OGP PS2. Chl concentration 2.5 mg/ml. EPR conditions: temperature 5 K, microwave power 25 mW, modulation amplitude 0.4 mT.

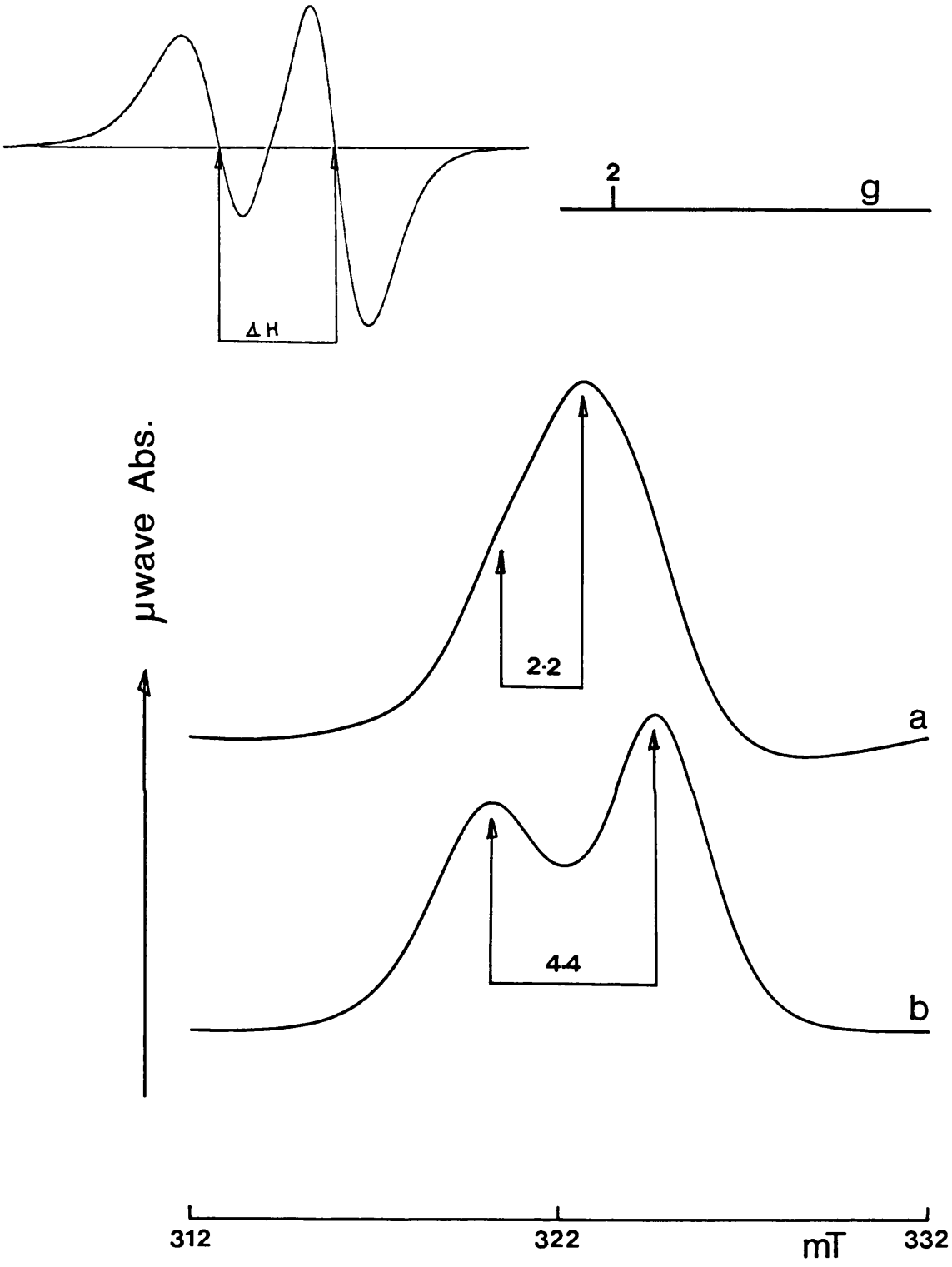

Figure 3.28 Integrated split pheophytin spectra from OGP PS2 to show the microwave absorbance peaks. The first derivative spectra used were those shown in Fig.3.27. (a) pH 6.0 OGP PS2 and (b) pH 7.5 + 50 mM bicarbonate OGP PS2. The values indicated are the measured signal splittings in mT and the insert shows how these relate to the original spectra.

this relates to the 1st derivative spectrum). The integral of the narrow signal (Fig.3.28a) had only a single peak with a slight shoulder at lower field, hence the splitting was less well defined at approximately 2.2 mT. Using the magnetic dipole interaction [Mathur et al., 1987] the splitting can be used to calculate the distance between the two interacting paramagnetic species. The distance between Q_A^- and Ph^- in pH 7.5 + 50 mM HCO_3^- OGP PS2 was calculated to be ≈ 10.8 Å. However, in pH 6.0 OGP PS2 the reduced splitting corresponds to an increase in the separation of the interacting species to ≈ 13.7 Å. Both these values are inaccurate because the exact nature of the interaction is unknown but the second one more so because of difficulties determining the exact signal splitting. However, it is apparent from the calculations and the signals themselves that bicarbonate removal may cause an increase in the distance between the primary quinone and the primary electron acceptor, pheophytin.

The dependence of the split signal size on the length of illumination at 200 K was plotted in Fig.3.29. The curves drawn are for samples exhibiting the two different types of split signal described in Fig.3.27. Both signals increased in size in a similar manner, showing that even after 30 mins illumination at 200 K some pheophytin remained unreduced. The pH 7.5 + 50 mM HCO_3^- OGP PS2 was found to display unexpected behaviour in the first three minutes of illumination. During this time the width of the splitting increased from approximately 3.5 mT, after 1 min,

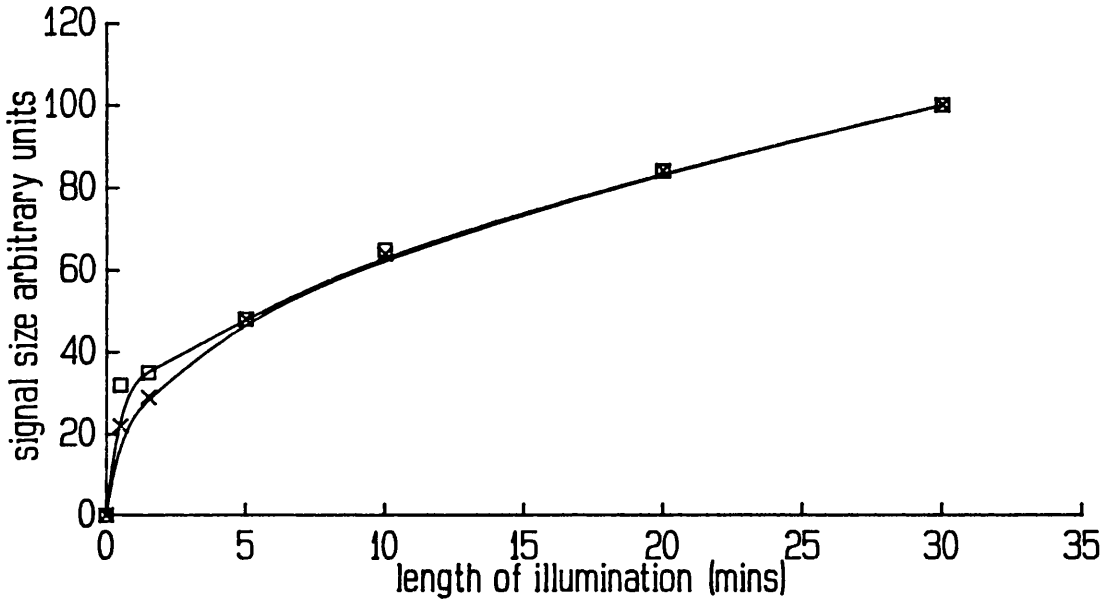

Figure 3.29 OGP PS2 split pheophytin signal size as a function of length of illumination at 200 K; 200 K illuminated minus dark difference spectra of pH 6.0 OGP PS2 (open squares) and pH 7.5 + 50 mM bicarbonate OGP PS2 (crosses).

to 4.4 mT, after 3 mins. Additional illumination did not induce any further changes in the signal splitting and no underlying signals were discovered that could account for this behaviour. As yet there is no explanation for this phenomenon.

In Rps. viridis the width of the splitting has been shown to be sensitive to pH [Prince et al., 1977]. Fig.3.30 shows the behaviour of the light minus dark difference spectra of pH 7.5 OGP PS2 + 50 mM HCO_3^- obtained at pH 6.0, 7.5 and 10. The signal splitting appeared to be almost pH independent over the pH 6-10 range but at low pH there was a change in the relative sizes of the high and low field peaks. This may represent a change in the type of interaction occurring between the two paramagnets.

The temperature dependency of the split signal is shown in Fig.3.31. The signal was largest at temperatures below 10 K. Above 30 K the splitting was lost completely and the Ph^- radical could be resolved. The Ph^- radical can also be viewed at lower temperatures by using a microwave power of 1 μW. Under these conditions the signal was centred at g=2.005 and 1.2 mT wide. Klimov et al. (1980a) described a similar signal for reduced pheophytin at g=2.0033 ± 0.0003 that was 1.26 ± 0.03 mT wide.

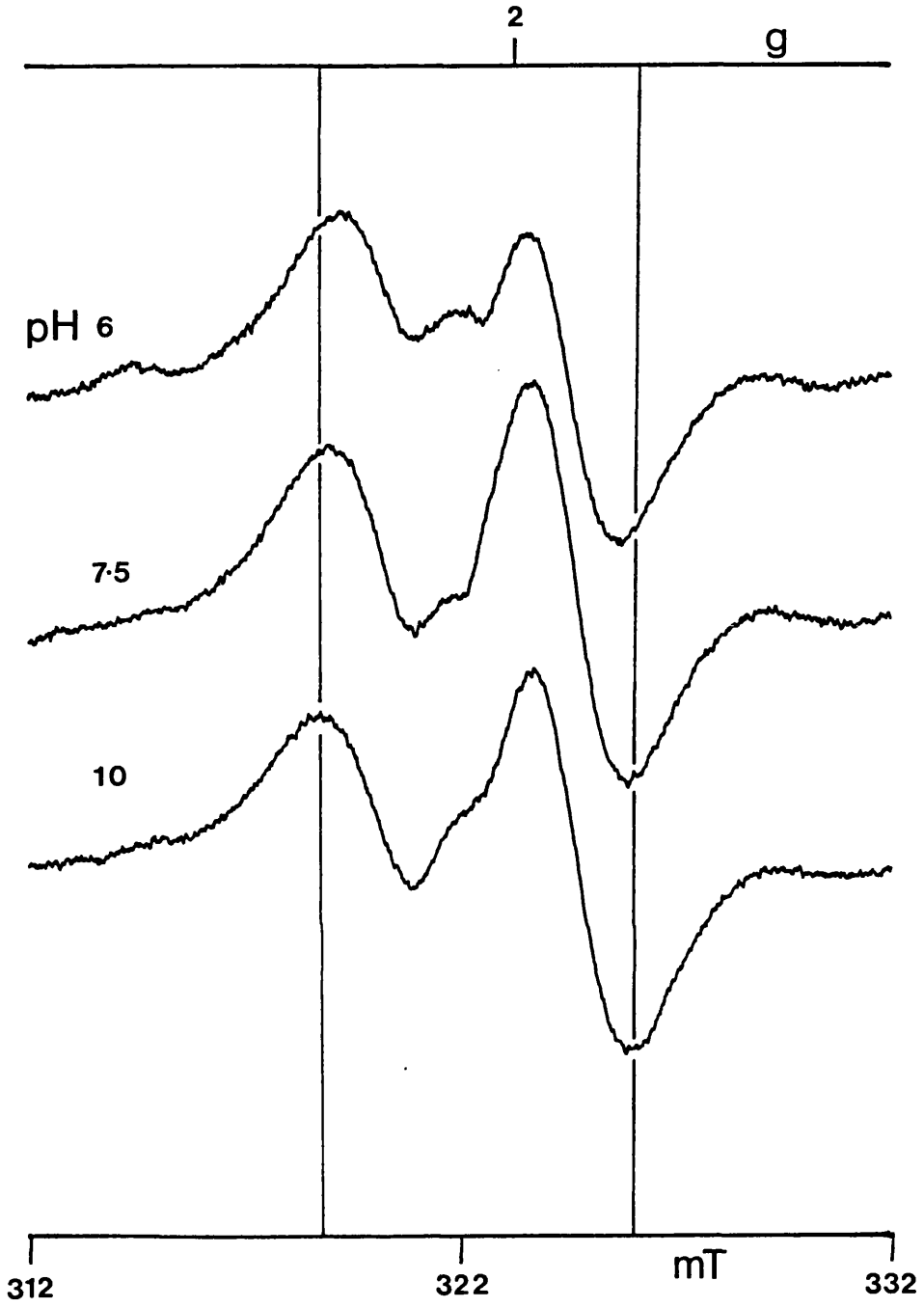

Figure 3.30 pH dependence of the split signal width in pH 7.5 OGP PS2. 200 K illuminated minus dark difference spectra were recorded from in samples in pH 6.0, pH 7.5, and pH 10 buffer. Chl concentration 2 mg/ml. EPR conditions: temperature 5 K, microwave power 25 mW, modulation amplitude 0.4 mT.

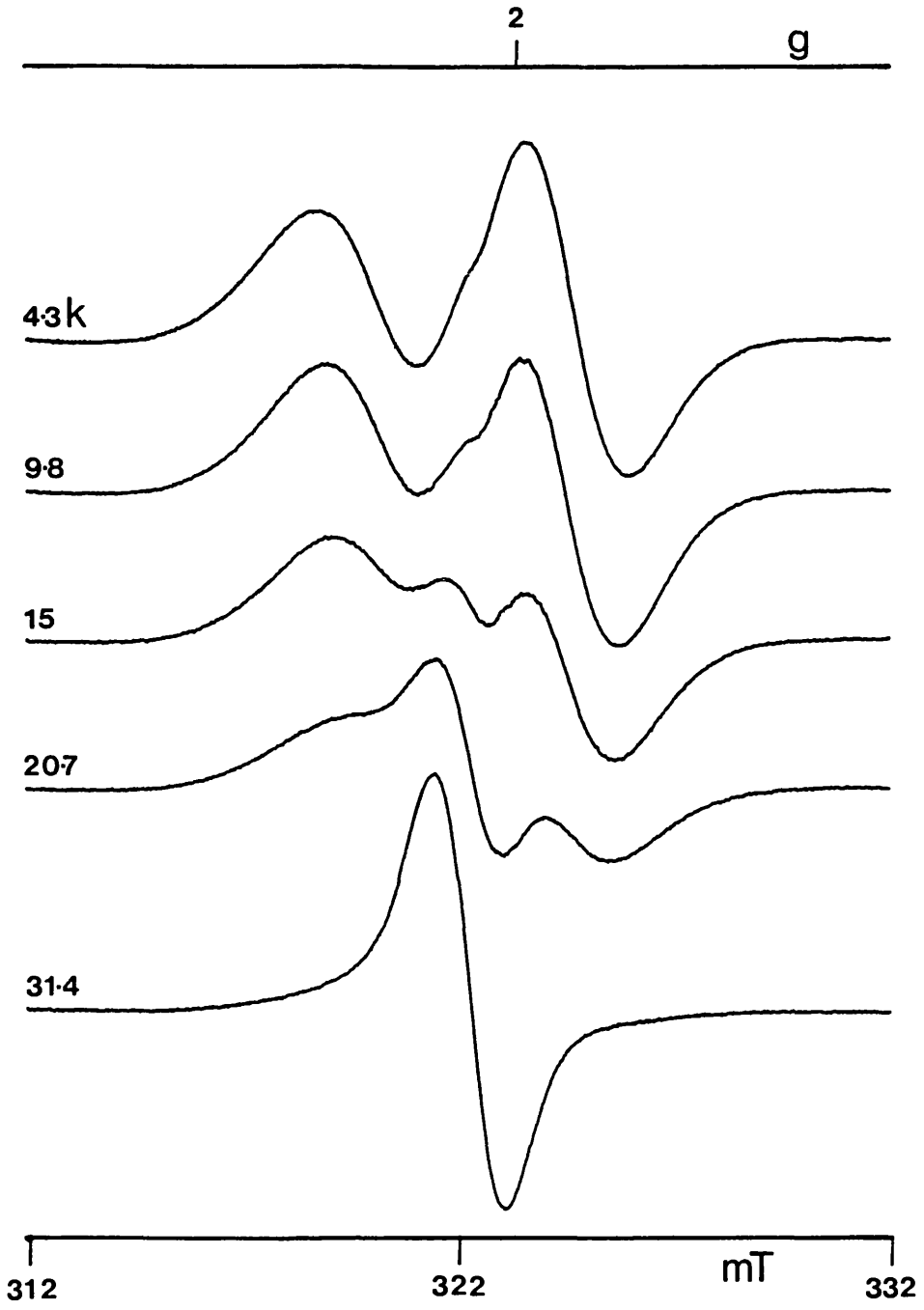

Figure 3.31 Temperature dependence of the pH 7.5 OGP PS2 split pheophytin EPR signal. Above 30 K the splitting is lost and only the pheophytin radical is observed. Chl concentration 2.5 mg/ml. EPR conditions: temperature 5 K, microwave power 25 mW, modulation amplitude 0.4 mT.

3.4.2 Redox Titrations Of The Q_A Semiquinone EPR Signals

To determine the exact role of the primary quinone in the split pheophytin signal titration phenomenon it was necessary to investigate the Q_A/Q_A^- mid-point potential and also the behaviour of the E_m in +/- bicarbonate systems. All the titrations were carried out at pH 7.0; other pHs mentioned refer to the pH at which the different PS2 complexes were prepared.

A redox titration of the g=1.9 $Q_A^-Fe^{2+}$ EPR signal observed in pH 7.5 OGP PS2 + 50 mM HCO_3^- showed that the signal titrates in a single step (Fig.3.32). An n=1 Nernst fit gave a curve with an E_{m7} of -32 mV. In the several titrations performed on the bicarbonate dependent signal the mid-point potential was found to vary between +5 and -32 mV. This variability probably originated from errors inherent in the titration method, possibly due to insufficient equilibration after dithionite additions.

A titration of the g=1.8 $Q_A^-Fe^{2+}$ EPR signal in pH 6.0 OGP PS2 (Fig.3.33) gave an E_{m7} of -102 mV. This was lower than that for the Q_A/Q_A^- couple obtained by titrating the g=1.9 signal. However, the significance of this result is questionable because the $Q_A^-Fe^{2+}$ EPR signal obtained in this titration was a mixture of both the g=1.8 and 1.9 forms. The partial conversion back to the native bicarbonate situation may have occurred because of CO_2 contamination in the N_2 used to keep the titration anaerobic or during the prolonged incubation in 1 M Tris-HCl pH 8.8 required for inactivation of the OEC. It proved difficult to maintain

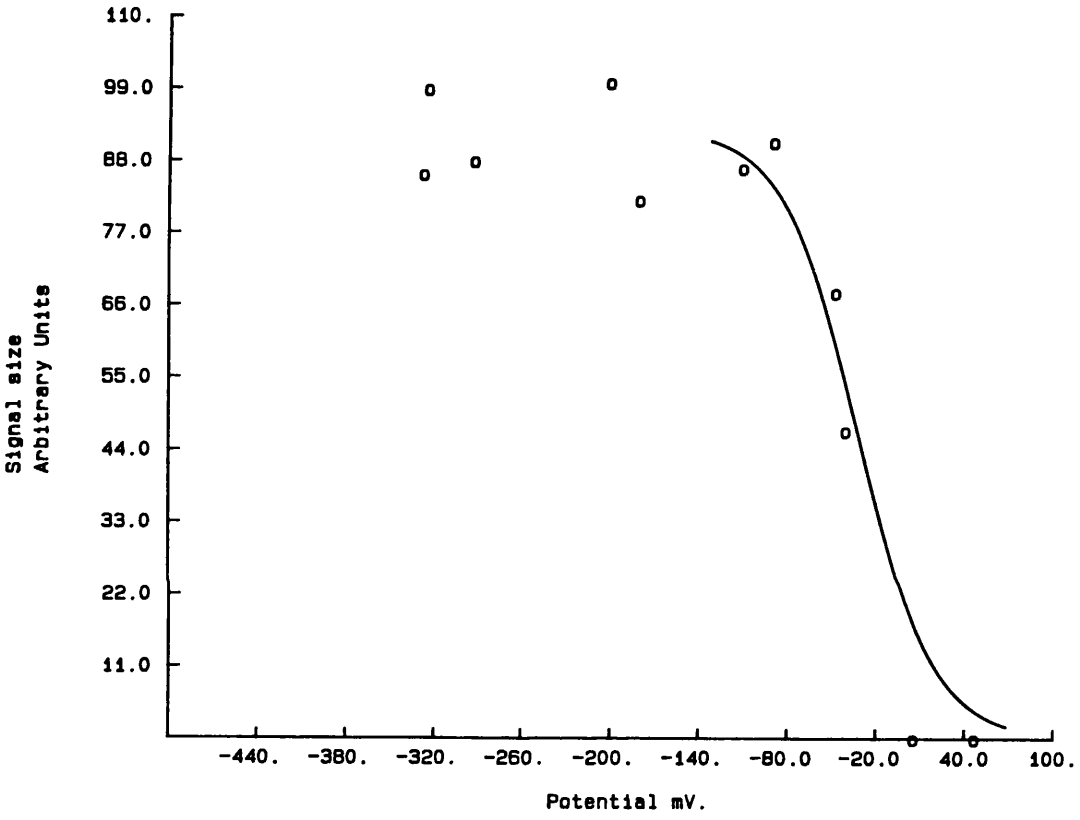

Figure 3.32 Determination of the mid-point potential of Q_A/Q_A^- in pH 7.5 + 50 mM bicarbonate OGP PS2. A theoretical one electron Nernst curve is plotted for the rise of the g=1.9 native Q_A iron-semiquinone EPR signal as the potential is lowered. The E_{m7} was calculated to be -32 mV but this was found to vary between +5 and -32 mV in the several titrations performed.

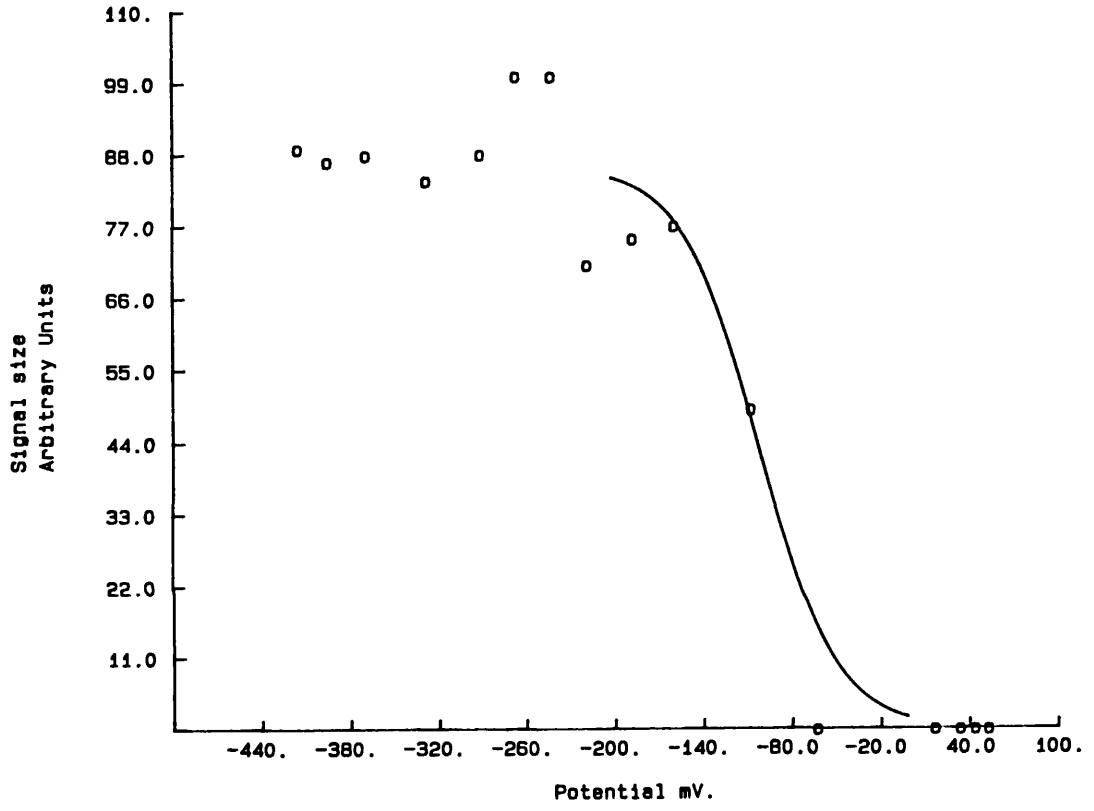

Figure 3.33 Redox titration of the g=1.8 Q_A iron-semiquinone EPR signal in pH 6.0 OGP PS2 to determine the mid-point potential of the primary quinone. The theoretical one electron Nernst curve fitted to the data gives a value of -102 mV for the Q_A/Q_A^- couple in this bicarbonate depleted system.

the g=1.8 signal in 100% of reaction centres at pH 7.0, in the pH 6.0 OGP PS2, without the addition of formate. The g=1.8 $Q_A^-Fe^{2+}$ signal in pH 6.0 OGP PS2 + 50 mM HCO_2^- was found to titrate in a single step but with a higher E_m of -5 mV (Fig.3.34).

The narrow splitting of the pheophytin signal observed in the g=1.8 $Q_A^-Fe^{2+}$ type of samples presented a further problem (the split signal in formate treated samples had a similar lineshape and width as that observed in Fig.3.27a). Contaminating signals were found in the g=2 region in all the titrations which obscured the true size of the narrow split signal and prevented any accurate measurements. No conclusions about the effects of bicarbonate depletion on the split pheophytin signal titrations could be drawn. The wider bicarbonate dependent split signal was unaffected by this problem. The contaminating radicals displayed various widths and sizes, depending on the potential, so were thought to arise from the redox mediators. Mediators are normally chosen because they are thought to undergo a single step two electron reduction but it is possible that the semi-reduced states can become stabilised, perhaps by association with proteins.

In an effort to ensure adequate redox mediation in the -100 to -250 mV range anthraquinone-1,5-disulphonate (E_{m7} -170) was initially included in the titrations. Some of the spectra obtained are shown in Fig.3.35. Fig.3.35a is the g=1.9 $Q_A^-Fe^{2+}$ signal in a pH 7.5 OGP PS2 + 50 mM HCO_3^- dark sample poised at -106 mV. Fig.3.35b is an identical sample

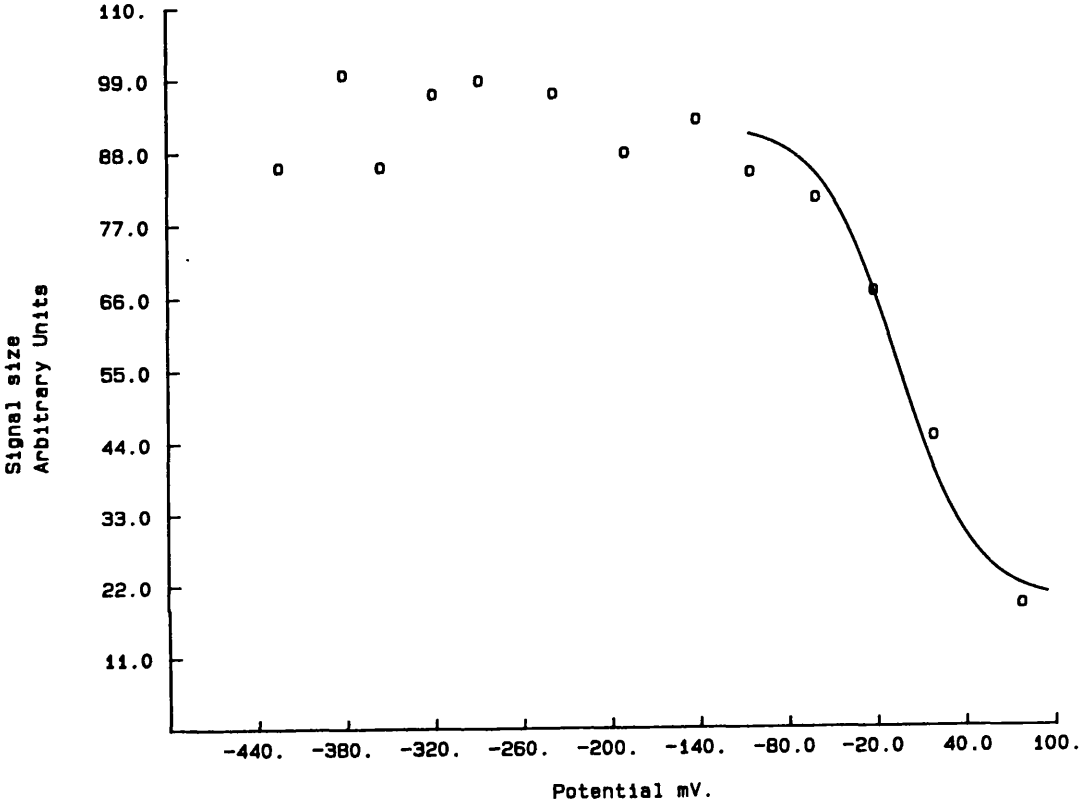

Figure 3.34 Redox titration of the g=1.8 Q_A iron-semiquinone EPR signal in pH 6.0 OGP PS2 + 50 mM formate to determine the mid-point potential of the primary quinone. The theoretical one electron Nernst curve fitted to the data gives a value of -5 mV for the Q_A/Q_A^- couple.

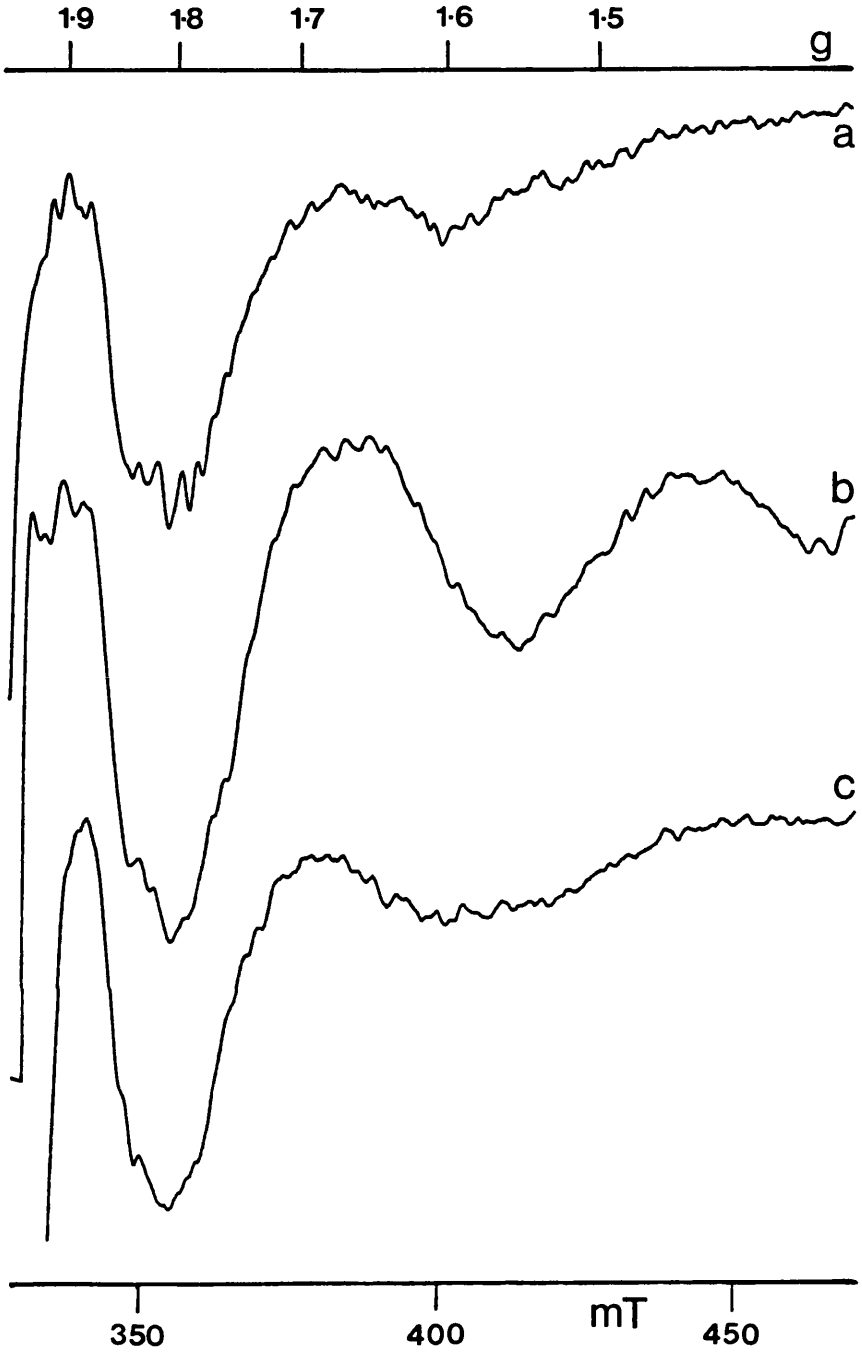

Figure 3.35 Q_A iron-semiquinone EPR signals obtained from a redox titration of this signal in pH 7.5 + 50 mM HCO_3^- OGP PS2 where the mediator anthraquinone-1,5-disulphonate was included. (a) dark spectrum from a sample poised at -106 mV, (b) as (a) but poised at -337 mV, and (c) is a 200 K illuminated spectrum from a non-reduced dark adapted control sample lacking the mediator. Chl concentration 2.5 mg/ml. EPR conditions: temperature 5 K, microwave power 25 mW, modulation amplitude 1.25 mT.

at -337 mV but in addition to the g=1.9 signal the spectrum also includes a large signal peak at g=1.65 and a trough at g=1.55. This signal was only observed in samples in the potential range -250 to -350 mV but was absent if the mediator was excluded.

Anthraquinones are known inhibitors of PS2 electron transport [Ottmeier et al., 1988] and probably act at the Q_B binding site. EPR signals at g=1.65 have previously [Corrie et al., 1991] and here (section 3.1) been shown to be associated with an interaction between the Q_A and Q_B iron-semiquinones. Therefore the new signal probably represents an interaction between the Q_A iron-semiquinone and the semi-reduced anthraquinone bound either in the Q_B binding site on D1 or nearby. The deviation of the mediator from the quoted mid-point potential to a lower potential could be an effect of the binding environment. It is concluded that quinone mediators of this sort should be avoided in EPR titrations of the PS2 quinones. Stable potentials were obtained with the range of mediators described in section 2.6.

Fig.3.35c is a non-(dithionite)reduced 200 K illuminated control, a g=1.9 $Q_A^-Fe^{2+}$ signal in pH 7.5 OGP PS2 + 50 mM HCO_3^-. The g=1.9 $Q_A^-Fe^{2+}$ signal arising from chemical reduction at 283 K (Fig.3.35a) was different to that obtained by photoreduction at 200 K (Fig.3.35c). The low field peak was significantly broader in the chemically reduced samples. This may be due to reaction centres assuming a preferred conformation upon Q_A reduction at 283

K. At cryogenic temperatures this reorganization could be blocked.

The titrations of the Q_A^- EPR signals in OGP PS2 reported in this section show that reduction occurs in a single step. There was no heterogeneity in the mid-point potential of the Q_A/Q_A^- redox couple that could account for the split signal titration phenomenon.

3.4.3 Redox Titrations Of The Split Pheophytin Signal

Redox titrations of the split pheophytin signal in pH 7.5 OGP PS2 + 50 mM HCO_3^- showed two steps (Fig.3.36). The curves fitted to the data describe two n=1 Nernst transitions with E_{m7} values of -31 and -272 mV. The size of the split signal obtained after the first step was approximately half that of the signal obtained in samples poised after the second step, ie. at potentials below -300 mV. The split signal was generated in the titration samples by 10 minutes illumination at 200 k.

Several titrations of the above type were carried out and the data from five titrations were averaged in 25 mV steps to give a single point in each range. This analysis ignored the slight variation observed for the E_m of the high potential step corresponding to the variation in the Q_A/Q_A^- mid-point potential mentioned in section 3.4.2. The mid-point potentials were determined to be -15 and -290 mV (Fig.3.37). The best fit was obtained by associating the high potential step with the appearance of 0 to 35% of the split signal but the low potential step with 45-100%, so

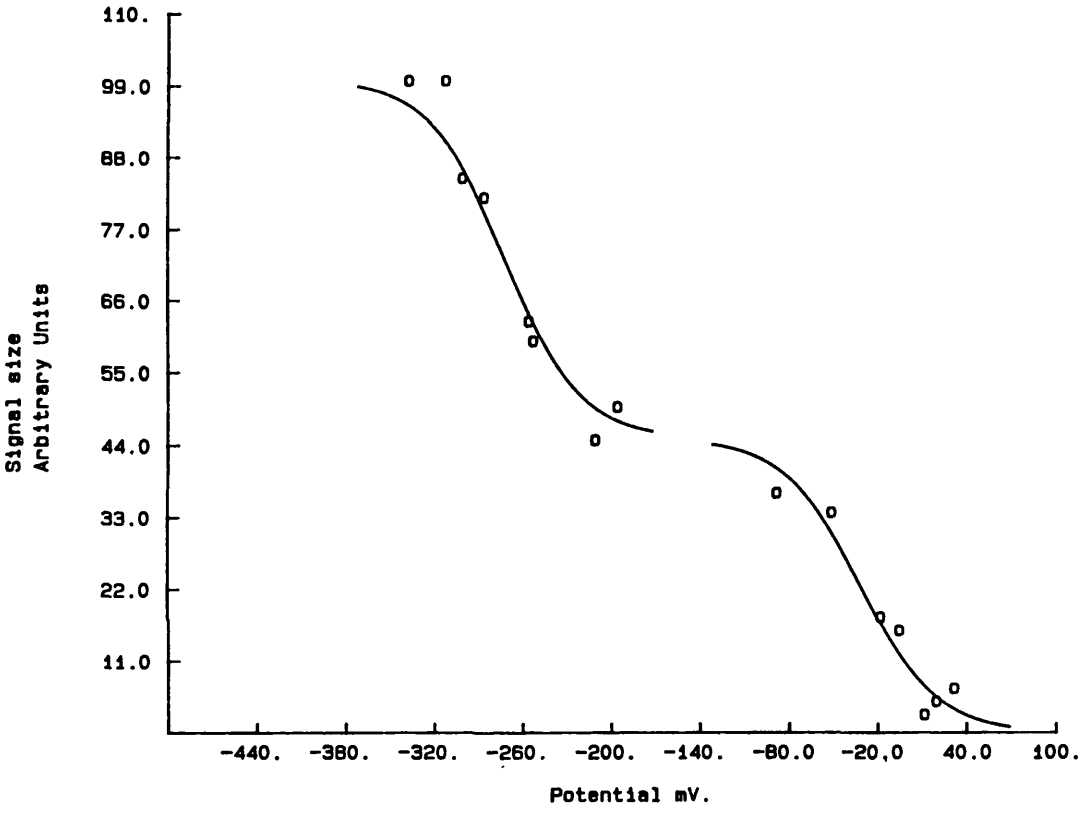

Figure 3.36 Redox titration of the split pheophytin EPR signal in pH 7.5 + 50 mM bicarbonate OGP PS2. Two theoretical one electron Nernst curves are fitted to the data with mid-point potentials of -31 and -272 mV.

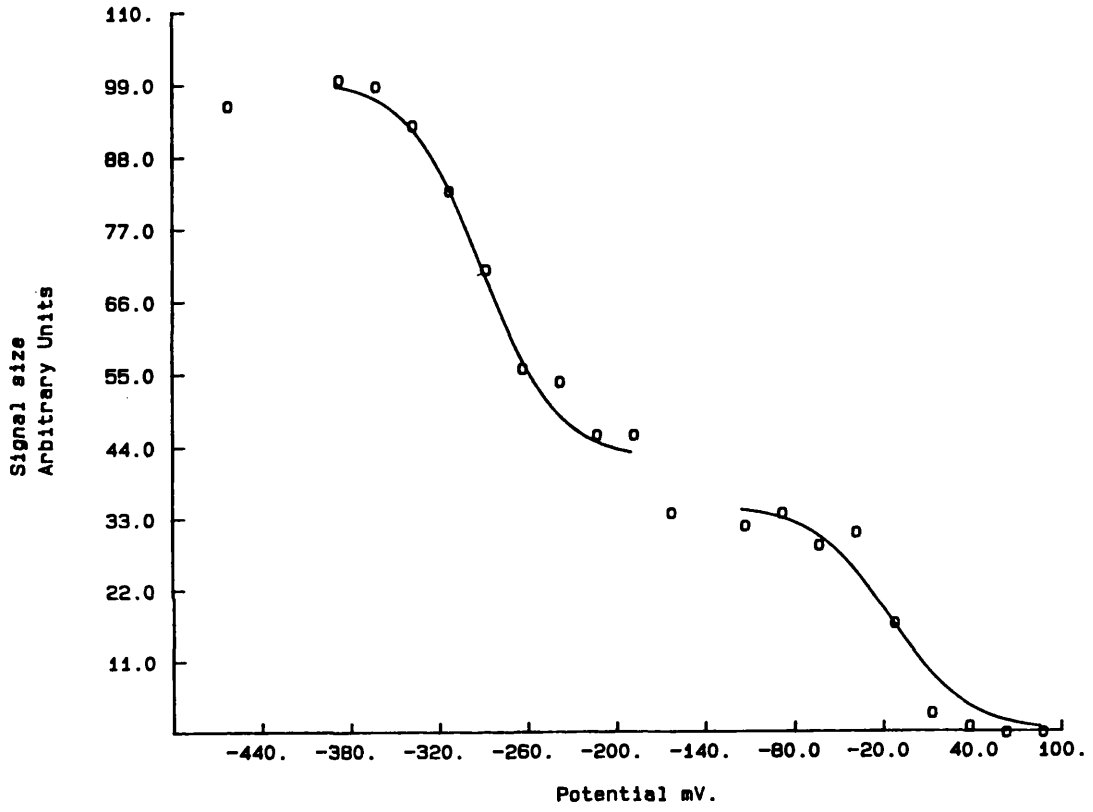

Figure 3.37 Data from five redox titrations of the sort described in Fig.3.36 were pooled and the average signal size in each 25 mV step plotted. The theoretical n=1 Nernst curves for the two steps in the split signal titration are fitted to mid-point potentials of -15 and -290 mV.

the "plateau" region between the two steps is not as clearly defined in the averaged data. This is due to a slight variability seen in the proportion of the split signal acquired in the first step, between 35 and 50%.

Mediators have often been suspected as a possible source of artifactual data. The two step phenomenon of the split signal titration may be explained by the appearance of an efficient electron donor at low potentials as a mediator becomes reduced. However, when titration control samples, without mediators, were reduced with 25 mM sodium dithionite and illuminated for 10 mins at 200 K they were found to generate split signals equivalent in size to the titration samples poised below -300 mV. Mediators were therefore not thought to produce any artifactual results in the titration.

Attempts were made to identify the low temperature donor(s) responsible for stable pheophytin reduction. At 200 K the OEC is the preferred electron donor to $P680^+$ but samples used here were Tris-washed to avoid manganese contamination and to inactivate the OEC. Below $\approx$ 0 mV the other known low temperature e^- donors, cytochrome b_{559} and Chl, were found to be reduced before and after 200 K illumination. No EPR signals, from possible electron donors, were found to be associated with 200 K illumination and no signals were identified that could be connected with the component responsible for the low potential step in the split signal titration. It is probable, as suggested by Rutherford and Zimmermann (1984), that dithionite is the

ultimate source of electrons for pheophytin reduction.

Several tests were carried out to try to identify differences in samples representing the state before and after reduction of the low potential component in the titration. The first of these examined the relationship between split signal size and length of illumination in samples poised at -252 and -336 mV (Fig.3.38a). Illumination for 10 mins at 200 K did not completely reduce the pheophytin in either sample, in fact the signal was still increasing in size even after 40 mins. Prolonged illumination was not found to significantly alter the relative proportions of split signal obtained in each sample. The ratio of signal size in the -252 mV sample to the -336 mV sample decreased slightly from 0.61 after 10 mins to 0.58 after 40 mins. The g=1.9 $Q_A^-Fe^{2+}$ signal in each sample was also checked after each period of illumination. The signal amplitude was found to be exactly the same in both samples. The size of the Ph^- radical EPR signal was also examined by raising the temperature to ≈ 30 K (these samples were chosen because of the small degree of g=2 mediator signal contamination). The proportion of Ph^- radical signal obtained in the low and high potential samples matched that obtained for the split signals. Therefore it is the ability to photoreduce pheophytin that is redox dependent and so the degree of pheophytin reduction determines the split signal size obtained at different potentials. This confirms that the split signal

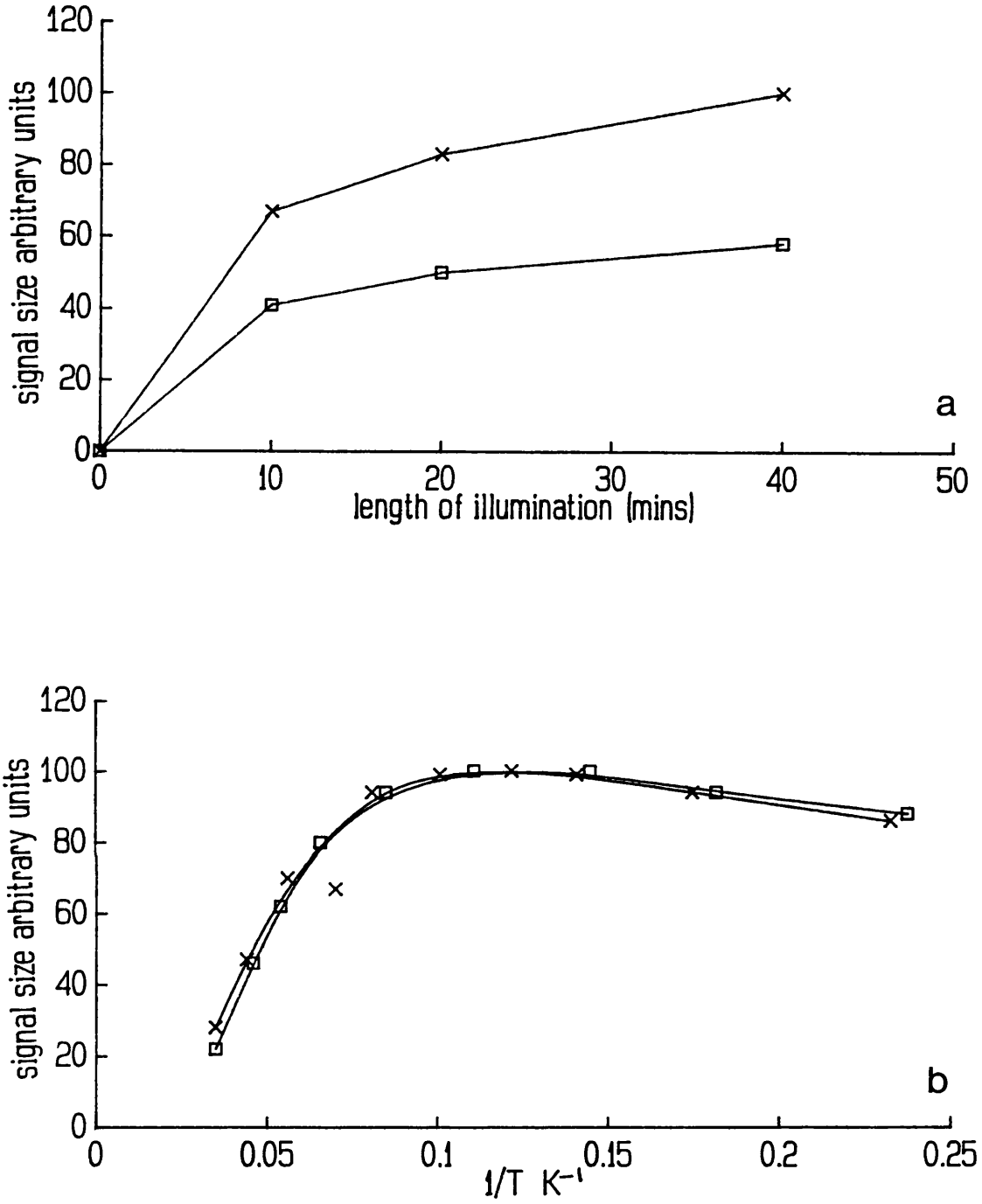

Figure 3.38 Characteristics of samples poised at potentials either side of the split pheophytin signal low potential titration step. (a) The dependence of pH 7.5 + HCO_3^- OGP PS2 split signal size on the length of 200 K illumination in samples poised at -252 (open squares) and -336 mV (crosses). (b) The same samples as (a) but the temperature dependence of the split signal size is shown; signal sizes are normalised to a percentage of the largest signal seen in each sample. EPR conditions: microwave power 25 mW, modulation amplitude 0.4 mT.

phenomenon is not related to the mid-point potential of Q_A.

In addition, temperature and power saturation studies were carried out. The temperature dependence of the split signal in the previously mentioned samples is shown in Fig.3.38b. The signal sizes are normalised to a % of the largest signal in each case. The two curves proved to be exactly the same, with a temperature of 8 or 9 K giving optimum signal amplitude. This unusual behaviour is probably a result of signal saturation at the power used to obtain the spectra, 25 mW.

The power saturation behaviour of both the split signal (Fig.3.39a) and the Ph^- radical (Fig.3.39b) were examined. The high and low potential samples appear to exhibit the same power saturation characteristics as each other for both signal types. $P_{\frac{1}{2}}$ (the power at half saturation) for the split signal is approximately 5 mW while the Ph^- signal is saturated even at 0.1 mW.

Therefore it would appear that the signals in the samples poised at -252 and -336 mV share the same linewidth, temperature and power saturation characteristics, indicating that the environment giving rise to the split signal is identical before and after reduction of the low potential component. By studying the yield of the pheophytin radical in these samples it appears that the split signal titration phenomenon is dependent on the redox potential dependence of the ability to photoreduce Ph.

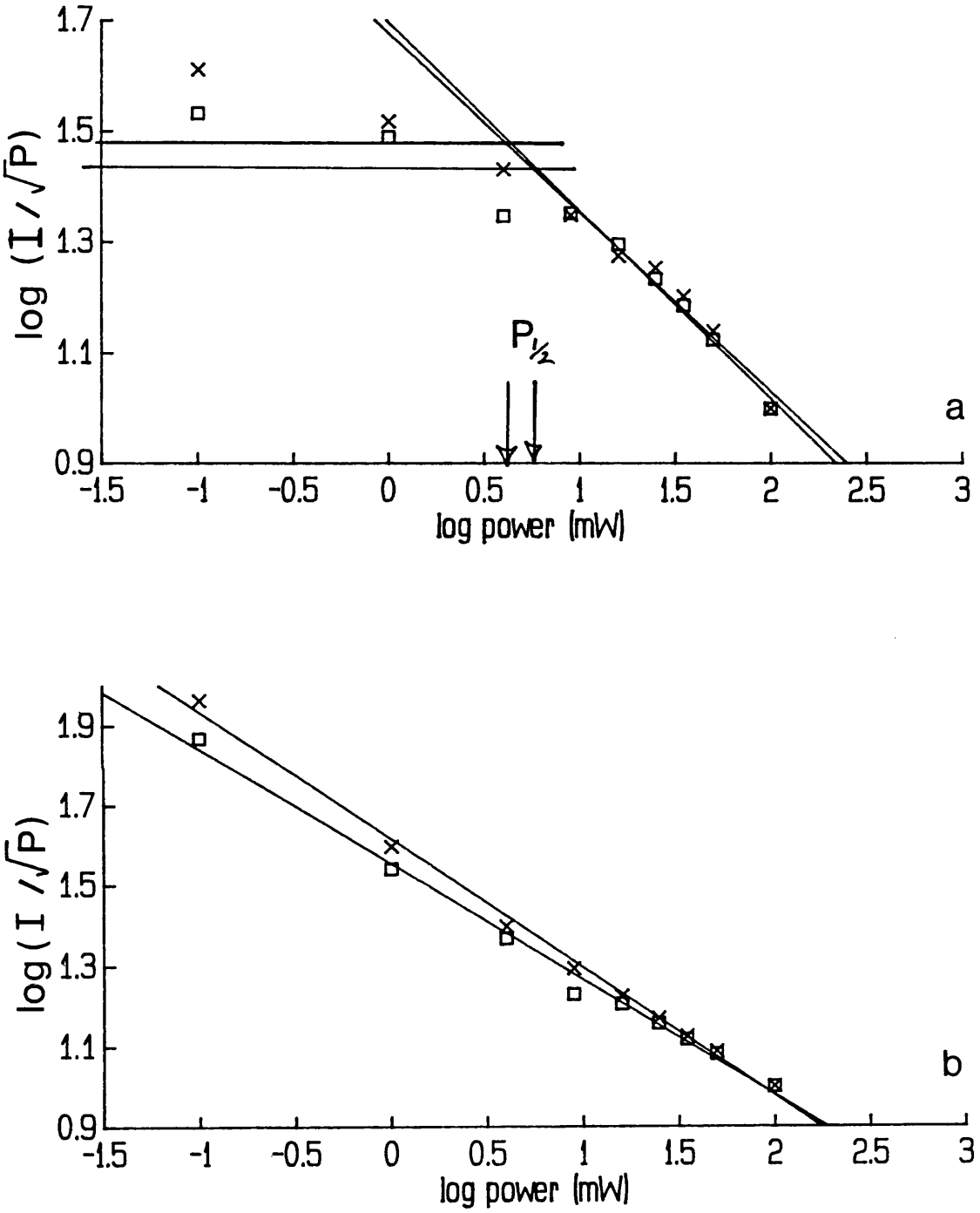

Figure 3.39 Microwave power saturation characteristics of the split pheophytin signal and Ph^- radical in pH 7.5 + 50 mM bicarbonate OGP PS2, (a) the split signal recorded at 5 K in samples poised at -252 (open squares) and -336 mV (crosses), $P_{½} \approx 5$ mW, (b) same samples as (a) but at 30 K, revealing the Ph^- radical, $P_{½} < 0.1$ mW.

3.4.4 Discussion

In PS2 the environment that gives rise to the split pheophytin signal, ie. that which determines the nature of the Ph^- $Q_A^-Fe^{2+}$ interaction, appears to be different to the bacterial system. The PS2 split signal is much narrower than the signals observed in bacteria and the iron-semiquinone signal at g=1.9/1.8 is unaffected by split signal generation. In Rps. viridis and C. vinosum the signal splittings at pH 7 are ≈ 17 and ≈ 7.5 mT respectively [Prince et al., 1977] whereas in PS2, values of 4.0 and 3.1 mT have been reported for bicarbonate retaining and formate treated samples [Vermaas and Rutherford, 1984]. Klimov et al. (1980a) first demonstrated the signal in PS2 and measured the splitting as 5.2-5.5 mT. The results in section 3.4.2 give widths of 4.4 mT in $+HCO_3^-$ samples and 2.2 mT in bicarbonate free and formate treated samples. The variation between these reports may stem from the different types of preparation used or it may be that different methods for measuring the splitting have been employed. In the case of the $+HCO_2^-$ split signal previous measurements of the splitting have possibly been distorted by radicals at g=2 or made on samples incompletely depleted of bicarbonate.

In bacteria the wider signal splittings may indicate shorter distances between (B)Ph and Q_A than in PS2. Alternatively it is possible that other factors may be important in determining the splitting such as the chemical nature of Q_A. This uncertainty obviously makes the

calculation used in section 3.4.2, to calculate the distance between Q_A and Ph, inaccurate, because it assumes a pure dipole-dipole interaction and does not accommodate any other variables. For instance, the calculated distance of 10.8 Å described here for bicarbonate retaining OGP PS2 compares well with the distance of 9.6 Å (between the two closest points) measured from the Rps. viridis crystal structure. However, calculating the distance from the Rps. viridis split signal gives a value of only 8.2 Å. Therefore, the calculated distances from different organisms perhaps should not be compared but in PS2 we are investigating splitting differences in a single system. It is likely that the values calculated for the two different OGP split signals are comparable, even if they are inaccurate. If we assume this is the case then depletion of bicarbonate in the low pH OGP PS2 samples would appear to be increasing the distance between Ph^- and $Q_A^-Fe^{2+}$.

In PS2 bicarbonate may provide one or two ligands to the non-haem iron and one of the suggested roles for the non-haem iron is to maintain the reaction centre conformation on the electron acceptor side. If HCO_3^- is a ligand then removal will indirectly destabilise the RC structure. Even if HCO_3^- is not a non-haem iron ligand it is known to have a significant influence over the electron acceptor region through the bicarbonate effect. The site of bicarbonate action has been shown to be between Q_A and Q_B as bicarbonate depletion slows the oxidation of Q_A^-

[Jursinic et al., 1976]. However, a recent paper by El-Shintinawy and Govindjee (1990) proposed a second site of action for bicarbonate, between Z and Q_A, possibly between pheophytin and Q_A. Their in vivo experiments in spinach leaf discs found that formate inhibition at this second site quenched the variable Chl a fluorescence while inhibition after Q_A is known to increase this fluorescence. This behaviour is consistent with our hypothesis of an effect of bicarbonate on the distance between Ph and Q_A as changes in the separation will affect electron flow between the two components.

The redox titrations of the $Q_A^-Fe^{2+}$ EPR signals all exhibit single step reductions of the primary quinone. There is no heterogeneity in the mid-point potential of the primary quinone, Q_A. This is in contrast to the experiments of Evans and Ford (1986) which showed two steps in the titration of Q_A/Q_A^- in formate treated pea BBYs. However, other groups have shown single step n=1 Nernst reductions in EPR redox titrations of Q_A [van Mieghem et al., 1989; Corrie et al., 1991] and in fluorescence titrations [Diner and Delosme, 1983] where Q_A is known as the quencher Q_H. The data presented here give a value for the E_{m7} of Q_A/Q_A^- between +5 and -32 mV in reaction centres binding bicarbonate (Fig.3.32) and an E_{m7} of -5 for formate treated OGP PS2 (Fig.3.34). The E_{m7} determined for the g=1.8 pH 6.0 OGP PS2 $Q_A^-Fe^{2+}$ EPR signal of -102 mV may be inaccurate (Fig.3.33) because of the difficulty involved in maintaining a completely bicarbonate free sample. However,

this measurement of the rise of the g=1.8 peak does show that bicarbonate presence/absence is unrelated to the low potential step in the split signal phenomenon (E_{m7} ≈ -280 mV). Also, the use of formate to displace bicarbonate does not significantly alter the mid-point potential of the primary quinone. This agrees with the results of Corrie (1991) obtained in the cyanobacterium Phormidium (P.) laminosum although the mid-point potentials in P. laminosum were higher: $E_{m7.8}$ of +27 mV ($+HCO_3^-$) and +20 mV ($+HCO_2^-$). Van Mieghem et al. (1989) present contrasting data by proposing an E_{m7} of -16 mV for formate treated PS2 but a much lower value of -100 mV for bicarbonate (non-treated) samples. Compared with the above results and the available fluorescence data [Horton and Croze, 1979; Diner and Delosme, 1983] this E_{m7} of -100 mV is at least 50 mV below previously quoted values. Their titration is also interesting because a decrease in signal size occurs between -200 and -300 mV, which could be due to semi-reduced anthraquinone mediators interacting with $Q_A^-Fe^{2+}$ as described in section 3.4.2. The g=1.65 signal is only generated in samples displaying a g=1.9 $Q_A^-Fe^{2+}$ EPR signal (the + HCO_2^- titration of van Mieghem et al., (1989) does not show this reduction in signal size) and the amplitude of the iron-semiquinone signal is reduced by the interaction [Bowden et al., 1991].

The Q_A titration results prove that the two step phenomenon seen in redox titrations of the split pheophytin signal is not related to heterogeneity of the Q_A mid-point

potential. By studying the EPR signals observed in samples poised at potentials either side of the low potential step it has been established that it is the degree of pheophytin reduction that determines the size of the split signal, all the primary quinone being reduced at a higher potential. This means previous explanations can now be discounted. Rutherford and Mathis (1983) suggested that a PS2 sub-population with a Q_A/Q_A^- E_m of $\approx$ -275 mV could exist. Evans and Ford (1986) suggested that two iron-quinones of different mid-point potential were active in each reaction centre between pheophytin and the secondary quinone Q_B. Both these suggestions have now been shown to be incorrect.

The split signal titrations in OGP PS2 illustrate that the split pheophytin signal appears in two well defined steps that can be fitted with n=1 Nernst curves of mid-point potential $\approx$ -30 and $\approx$ -280 mV (Figs.3.36 and 3.37). The first step is associated with the appearance of 35-50% of the split signal observed at lower potentials and occurs in concert with the reduction of Q_A. The low potential step is associated with the reduction of an unknown component. PS2 has another unidentified component known to titrate with an E_m near this value, the fluorescence quencher Q_L, $E_{m7.8}$ -247 mV [Horton and Croze, 1979] and $E_{m7.5}$ -240 mV [Diner and Delosme, 1983]. It is highly probable that the unknown low potential component reduced in the split signal titration is Q_L and consequently the available fluorescence titration data must be taken into account when explaining the EPR titration results. Corrie (1991) obtained two

steps in a titration of the split signal in P. laminosum with E_ms of +35 and -150 to -250 mV. The proportion of split signal associated with each step was different to spinach PS2 with 75-80% of the signal appearing with the first Q_A^- dependent step. The small amount of split signal associated with the "Q_L" low potential step is probably related to the suggestion of Bowes et al. (1981) that P. laminosum does not possess the fluorescence quencher Q_L.

In higher plants no EPR signals have been identified, either in this work or elsewhere, that could be associated with the Q_L potential range. The only other component identified with a redox potential relatively close to Q_L is "U", E_m -430 mV [Evans et al., 1985], now identified as the irreversible second reduction of Q_A occurring at potentials below -350 mV [van Mieghem et al., 1989].

Reduction of Q_H is associated with an increase in the membrane potential as an electron is transferred across the membrane whereas Q_L reduction is not [Diner and Delosme, 1983]. This is similar to the behaviour of the PS2 fluorescence quenchers Q_1 and Q_2 identified by Joliot and Joliot (1979) [Diner and Delosme, 1983]. The primary quinone can probably be identified as the quenchers Q_H and Q_1 while the low potential component in the split signal titration is probably both Q_L and Q_2. Joliot and Joliot (1981) concluded that Q_2 was not a plastoquinone.

The PS2 split signal titration could be explained if Ph^- donates electrons to Q_L when Q_A is reduced and if Q_L is present in only 50-65% of reaction centres. This

explanation implies that PS2 sub-populations exist within the grana but there is, at the moment, no explanation as to what purpose this heterogeneity would serve. It would be more correct to assume a homogeneous system and suppose that Q_L is present in every reaction centre. There is no evidence to suggest that Q_L is active between Ph and Q_A.

There are two main differences between PS2 and the purple bacteria in which the split signal has been studied. Firstly there is no analogous Q_L component and secondly reduction of BPh is achieved through the irreversible oxidation of a low temperature electron donor, a cytochrome either bound to the reaction centre (C. vinosum, Rps. viridis) or added exogenously (Rb. sphaeroides). The cytochrome electron donation is relatively slow and has to compete against the faster backreaction occurring between the oxidised special pair and BPh^-. In PS2 no low temperature electron donor has been identified below 0 mV except possibly dithionite.

It is obvious from the data that reduction of Q_L somehow facilitates an increase in the stable reduction of pheophytin. This could represent the appearance of a fast donor to $P680^+$ or the blocking of an acceptor pathway from Ph^-. The model presented here to explain the split signal phenomenon is based on a combination of these possibilities and the known characteristics of Q_L. It is extremely difficult to explain a two step reduction assuming a homogeneous population but this model attempts to and suggests that the problem lies with the presence of an

acceptor capable of oxidising Ph^- in the presence of Q_A^-.

It is possible that three competing pathways of electron transfer are active in PS2 samples poised between ≈ -30 mV (the E_{m7} of Q_A/Q_A^-) and ≈ -280 mV (the E_{m7} of Q_L/Q_L^-). The fastest, and therefore the most probable reaction following primary charge separation, is the Ph^-P680^+ backreaction (Fig.3.40 scheme 1). This does not give rise to the P680 triplet and actual radical pair formation may be reduced in the presence of $Q_A^-Fe^{2+}$ [van Mieghem et al., 1989]. Schatz et al. (1988) suggest that the rate constant of charge separation is reduced by a factor of ≈ 6 in closed centres (Q_A reduced). The second possible pathway would be a cyclic flow, initiated by the reduction of $P680^+$ by a donor. This would be a slower reaction than the radical pair recombination so would occur less frequently. Formation of $D^+P680Ph^-$ (where D is an unspecified donor that is not necessarily tyrosine residue D) would be followed by Q_L reduction by Ph^-. The cyclic flow would explain the absence of an oxidised donor as Q_L^- reduces D^+ (Fig.3.40 scheme 2), via cytochrome b_{559}(?). To explain the stable reduction of pheophytin that does occur at these potentials it is proposed that dithionite competes with Q_L^- for reduction of the oxidised donor (Fig.3.40 scheme 3). When dithionite reduces D^+ the next donation to $P680^+$ by D will generate a state where both Ph and Q_L are reduced. This is the stable reduction of pheophytin that allows the split signal to be observed. Therefore, in this model the split signal yield depends on dithionite winning the competition

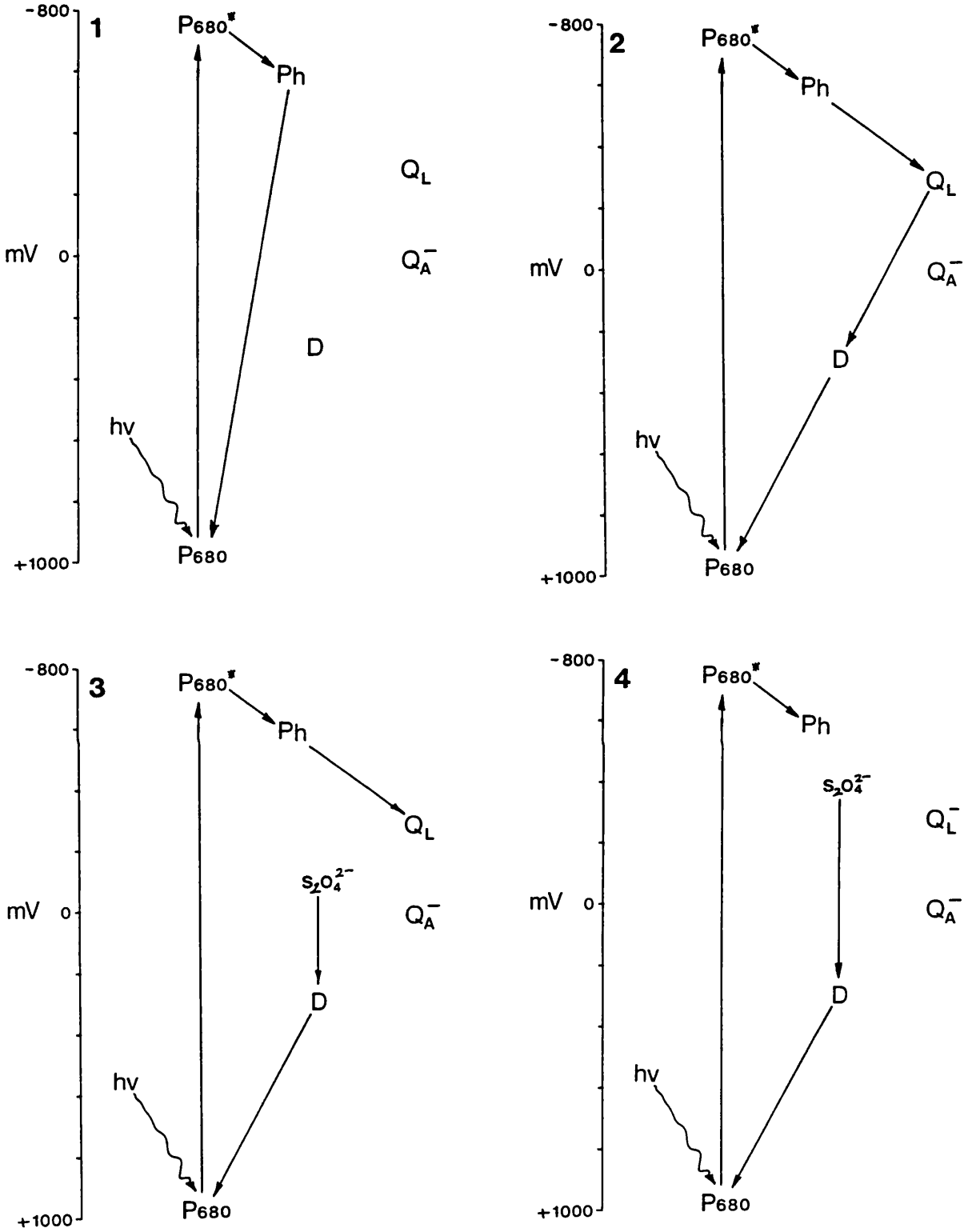

Figure 3.40 Model to explain the two steps observed in redox titrations of the split pheophytin signal. For a full explanation see section 3.4.4. The schemes 1-3 show possible electron transfer events in Tris-washed reaction centres when Q_A, but not Q_L, is chemically reduced. Scheme 4 is the situation when Q_L becomes reduced below ≈ -280 mV.

with the cyclic flow. Diner and Delosme (1983) noted that a sample poised at -185 mV gradually lost the Q_L fluorescence quenching capacity during illumination.

At potentials below ≈ -280 mV Q_L is reduced and the cyclic flow blocked so that the probability of Ph reduction, ultimately by dithionite, is increased (Fig.3.40 scheme 4). This is the low potential step and gives rise to the increase in split signal yield.

Cyclic electron flow involving PS2 has often been suggested, frequently these schemes include cytochrome b_{559} [Arnon and Tang, 1988; Thompson et al., 1988] but usually in conjunction with PQH_2. The number of cytochrome b_{559}s per reaction centre is still a matter of debate but there may only be one. If this is true then the observed heterogeneity in the cytochrome mid-point potential may play some role in the split signal phenomenon, possibly affecting the ability of the cytochrome to act as an electron donor.

As with all models there are problems with the one presented here. For instance Rutherford and Mathis (1983) found that split signal titrations illuminated at 5 K did not display the Q_L low potential step as the amplitude of the split signal did not rise above that associated with the Q_A step. This would be difficult to explain on the basis of the above model but Evans et al. (1982) also attempted to photoreduce Ph at 5 K and explained that low signal yield was due to inefficient electron donation at this temperature. This second interpretation appears more

likely.

One prediction that can be made from the model is that prolonged illumination of samples taken either side of the Q_L step should increase the split signal yield in the high potential sample relative to the low potential sample. However, Fig.3.38a shows that even after 40 mins illumination at 200 K this is not the case.

The split pheophytin signal titration phenomenon is now known not to be related to the mid-point potential of Q_A or to the bicarbonate effect. However, I argue here that it is related to the low potential fluorescence quencher Q_L, a definite component with an $E_{m7} \approx -280$ mV that, when reduced, increases the yield of reduced pheophytin. The split signal titrations will not be explained until the function and identity of Q_L are known.

3.5 Summary Of Results

1. By studying the PS2 primary quinone EPR signal I have shown that not only the lineshape but also the temperature dependent behaviour and microwave power saturation characteristics of the observed signal are dependent on the presence or absence of bicarbonate.

2. The PS2 quinone binding region EPR signals have all been found to be susceptible to trypsin treatment. The protective effect of calcium ions against trypsin treatment has been used to demonstrate the existence of a Ca^{2+} binding site in this region.

3. It was shown that LHCII removal from PS2 particles, with the detergent octylglucopyranoside at pH 6.0, caused the loss of bicarbonate binding. I have described a new OGP PS2 core preparation that retains the bicarbonate bound native state in the electron acceptor region and a dodecylmaltoside prepared CP47, CP43, D1, D2, cytochrome b_{559} complex, that displays the g=1.9 Q_A iron-semiquinone signal. The OGP preparations are a new system for studies into the "bicarbonate effect" because true bicarbonate depletion can be achieved without the need for displacement by another anion.

4. Analysis of the split pheophytin signal in +/- HCO_3^- OGP PS2 has identified a possible structural role for bicarbonate in maintaining reaction centre conformation. It is proposed that bicarbonate depletion may increase the distance between Q_A and pheophytin.

5. The two step titration of the split pheophytin EPR signal is not related to heterogeneity of the primary quinone mid-point potential, as Q_A always titrated in a single step. However, it was found to be related to the redox potential dependent ability to photoreduce pheophytin. The low potential component ($E_m \approx -280$ mV) in the split signal titration is suggested to be Q_L, the low potential PS2 fluorescence quencher; Q_L reduction increased the yield of reduced pheophytin.

REFERENCES

Aasa, R., Andréasson, L-E., Styring, S. and Vänngård, T. (1989) FEBS. Lett, 243, 156-160.

Akabori, K., Tsukamoto, H., Tsukihara, J., Nagatsuka, T., Motokawa, O. and Toyoshima, Y. (1988) Biochim. Biophys. Acta, 932, 345-357.

Anderson, J.M. and Andersson, B. (1982) TIBS, 7, 288-292.

Anderson, J.M. and Andersson, B. (1988) TIBS, 13, 351-355.

Arnon, D.I. (1949) Plant Physiol., 24, 1-15.

Arnon, D.I. and Tang, G.M.-S. (1988) Proc. Natl. Acad. Sci. USA, 85, 9524-9528.

Aro, E.-M., Hundal, T., Carlberg, I. and Andersson, B. (1990) Biochim. Biophys. Acta, 1019, 269-275.

Babcock, G.T., Ghanotakis, D.F., Bacon, K.E. and Diner, B.A. (1983) Biochim. Biophys. Acta, 723, 276-286.

Babcock, G.T., Widger, W.R., Cramer, W.A., Oertling, W.A. and Metz, J,G. (1985) Biochemistry, 24, 3638-3645.

Babcock, G.T., Barry, B.A., Debus, R.J., Hoganson, C.W., Atamian, M., McIntosh, L., Sithole, I. and Yocum, C.F. (1989) Biochemistry, 28, 9557-9565.

Barbato, R., Rigoni, F., Giardi, M.T. and Giacometti, G.M. (1989) FEBS Lett., 251, 147-154.

Barr, R., Troxel, K.S. and Crane, F.L. (1983) Plant Physiol., 73, 309-315.

Barry, B.A. and Babcock, G.T. (1987) Proc. Natl. Acad. Sci. USA, 84, 7099-7103.

Barry, B.A. and Babcock, G.T. (1988) Chemica Scripta, 28A, 117-122.

Barry, B.A., El-Deeb, M.K., Sandusky, P.O. and Babcock, G.T. (1990) J. Biol. Chem., 265, 20139-20143.

Bassi, R. and Dainese, P. (1990) In: Current Research in Photosynthesis, vol II 5.209 (Baltscheffsky, M. ed.), Kluwer Academic Publishers, Dordrecht.

Berthold, D.A., Babcock, G.T. and Yocum, F. (1981) FEBS Lett., 134, 231-234.

Blubaugh, D.J. and Govindjee (1988a) Photosynth. Res., 19, 85-128.

Blubaugh, D.J. and Govindjee (1988b) Biochim. Biophys. Acta, 936, 208-214.

Boussac, A., Zimmermann, J.-L. and Rutherford, A.W. (1989) Biochemistry, 28, 8984-8989.

Boussac, A., Zimmermann, J.-L., Rutherford, A.W. and Lavergne, J. (1990) Nature, 347, 303-306.

Bowden, S.J., Hallahan, B.J., Ruffle, S.V., Evans, M.C.W. and Nugent, J.H.A. (1991) Biochim. Biophys. Acta, in press.

Bowes, J.M., Crofts, A.R. and Shigeru, I. (1979) Biochim. Biophys. Acta, 547, 320-335.

Bowes, J.M., Horton, P. and Bendall, D.S. (1981) FEBS Lett., 135, 261-264.

Bowlby, N.R., Ghanotakis, D.F., Yocum, C.F., Petersen, J. and Babcock, G.T. (1988) In: Light-Energy Transduction in Photosynthesis: Higher Plants and Bacterial Models (Stevens, S.E., Jr. and Bryant, D.A., eds.) 215-226, The American Society of Plant Physiologists, Rockville, MD.

Butler, P.J.G. and Kühlbrandt, W. (1988) Proc. Natl. Acad. Sci. USA, 85, 3797-3801.

Butler, W.F., Calvo, R., Fredkin, D.R., Isaacson, R.A., Okamura, M.Y. and Feher, G. (1984) Biophys. J., 45, 947-973.

Chapman, D.J., Vass, I. and Barber, J. (1991) Biochim. Biophys. Acta, 1057, 391-398.

Chua, N.M. (1980) In: Methods in Enzymology, 69, 434-446, Academic Press, Inc.

Coleman, W.J. (1990) Photosynth. Res., 23, 1-27.

Coleman, W.J. and Govindjee (1987) Photosynth. Res., 13, 199-223.

Corrie, A.R. (1991) Ph.D. Thesis, University College London.

Corrie, A.R., Nugent, J.H.A. and Evans, M.C.W. (1991) Biochim. Biophys. Acta, 1057, 384-390.

Cox, R.P. and Bendall, D.S. (1974) Biochim. Biophys. Acta, 347, 49-59.

Crofts, A.R. and Wraight, C.A. (1983) Biochim. Biophys. Acta, 726, 149-185.

Crofts, A.R., Robinson, H.H. and Snozzi, M. (1984) In: Advances in Photosynthesis Research 1, 461-468 (Ed. Sybesma, C.) Martinus Nijhoff/Dr W.Junk publishers, The Netherlands.

Dainese, P. and Bassi R. (1991) J. Biol. Chem., 266, 8136-8142.

Debus, R.J., Barry, B.A., Babcock, G.T. and McIntosh, L. (1988a) Proc. Natl. Acad. Sci. USA, 85, 427-430.

Debus, R.J., Barry, B.A., Sithole, I., Babcock, G.T. and McIntosh, L. (1988b) Biochemistry, 27, 9071-9074.

Deisenhofer, J. and Michel, H. (1989) EMBO J., 8, 2149-2170.

Deisenhofer, J., Epp, O., Miki, K., Huber, R. and Michel, H. (1984) J. Mol. Biol., 180, 385-398.

Deisenhofer, J., Epp, O., Miki, K., Huber, R. and Michel, H. (1985) Nature, 318, 618-624.

Dekker, J.P., van Gorkom, H.J., Wensink, J. and Ouwehand, L. (1984) Biochim. Biophys. Acta, 767, 1-9.

Dekker, J.P., Bowlby, N.R. and Yocum, C.F. (1989) FEBS Lett., 254, 150-154.

de Paula, J.C., Innes, J.B. and Brudvig, G.W. (1985) Biochemistry, 24, 8114-8120.

de Vitry, C., Carles, C. and Diner, B.A. (1986) FEBS Lett., 196, 203-206.

Diner, B.A. (1988) Abstract from the Roussel-Uclaf meeting, Paris.

Diner, B.A. and Delosme, R. (1983) Biochim. Biophys. Acta, 722, 443-451.

Diner, B.A. and Petrouleas, V. (1987a) Biochim. Biophys. Acta, 893, 138-148.

Diner, B.A. and Petrouleas, V. (1987b) Biochim. Biophys. Acta, 895, 107-125.

Diner, B.A. and Petrouleas, V. (1990) Biochim. Biophys. Acta, 1015, 141-149.

Diner, B.A., de Vitry, C. and Popot, J. (1988) Biochim. Biophys. Acta, 934, 47-54.

Dismukes, G.C. (1988) Chemica Scripta, 28A, 99-104.

Dismukes, G.C. and Siderer, Y. (1981) Proc. Natl. Acad. Sci. USA, 78, 274-278.

Doring, G., Renger, G., Vater, J. and Witt, H.T. (1969) Z. Naturforsch, 24b, 1139-1143.

Dutton, P.L. (1978) In: Methods in Enzymology, LIV, 411-435, Academic Press, Inc.

Duysens, L.N.M. and Sweers, H.E. (1963) In: Studies on Microalgae and Photosynthetic Bacteria (Miyachi, S., ed.), Univ. Tokyo Press, Tokyo, 353-372.

Eckert, H.J., Wiese, N., Bernarding, J., Eichler, H.J. and Renger, G. (1988) FEBS Lett., 240, 153-158.

Eckert, H.J., Geiken, B., Bernarding, J., Napiwotzki, A., Eichler, H.-J. and Renger, G. (1991) Photosynth. Res., 27, 97-108.

El-Shintinawy, F. and Govindjee (1990) Photosynth. Res., 24, 189-200.

Enami, I., Kamino, K., Shen, J-R., Satoh, K. and Katoh, S. (1989) Biochim. Biophys. Acta, 977, 33-39.

Evans, M.C.W. and Ford, R.C. (1986) FEBS Lett., 195, 290-294.

Evans, M.C.W., Lord, A.V. and Reeves, S.G. (1974) Biochem. J., 138, 177-183.

Evans, M.C.W., Diner, B.A. and Nugent, J.H.A. (1982) Biochim. Biophys. Acta, 682, 97-105.

Evans, M.C.W., Atkinson, Y.E. and Ford, R.C. (1985) Biochim. Biophys. Acta, 806, 247-254.

Feher, G., Allen, J.P., Okamura, M.Y. and Rees, D.C. (1989) Nature, 339, 111-116.

Ford, R.C. and Evans, M.C.W. (1983) FEBS Lett., 160, 159-163.

Fotinou, C. and Ghanotakis, D.F. (1990) Photosynth. Res., 25, 141-145.

Fromme, R. and Renger, G. (1990) Z. Naturforsch., 45c, 373-378.

Gaba, V., Marder, J.B., Greenberg, B.M., Mattoo, A.K. and Edelman, M. (1987) Plant Physiol., 84, 348-352.

Gerken, S., Brettel, K., Schlodder, E. and Witt, H.T. (1988) FEBS Lett., 237, 69-75.

Ghanotakis, D.F. and Yocum, C.F. (1986) FEBS Lett., 197, 244-248.

Ghanotakis, D.F., Demetriou, D.M. and Yocum, C.F. (1987) Biochim. Biophys. Acta, 891, 15-21.

Good, N.E. (1963) Plant Physiol., 38, 298-304.

Gounaris, K., Chapman, D.J., Booth, P., Crystall, B., Giorgi, L.B., Klug, D.R., Porter, G. and Barber, J. (1990) FEBS Lett., 265, 88-92.

Govindjee (1990) Photosynth. Res., 25, 151-160.

Govindjee, Pulles, R., Govindjee, R., van Gorkom, H.J. and Duysens, L.N.M. (1976) Biochim. Biophys. Acta, 449, 602-605.

Govindjee, Weger, H.G., Turpin, D.H., van Rensen, J.J.S., de Vos, O.J. and Snel, J.F.H. (1991) Naturwissenschaften, 78, 168-170.

Green, B.R., Pichersky, E. and Kloppstech, K. (1991) TIBS, 16, 181-186.

Greenberg, B.M., Gaba, V., Mattoo, A.K. and Edelman, M. (1987) EMBO J., 6, 2865-2869.

Guiles, R.D., Zimmermann, J.-L., McDermott, A.E., Yachandra, V.K., Cole, J.L., Dexheimer, S.L., Britt, R.D., Weighardt, K., Bossek, U., Sauer, K. and Klein, M.P. (1990) Biochemistry, 29, 471-485.

Hallahan, B.J., Ruffle, S.V., Bowden, S.J. and Nugent, J.H.A. (1991) Biochim. Biophys. Acta, 1059, 181-188.

Hansson, Ö and Wydrzynski, T. (1990) Photosynth. Res., 23, 131-162.

Hansson, Ö, Aasa, R. and Vänngård, T. (1987) Biophys. J., 51, 825-832.

Herrmann, R.G., Alt, J., Schiller, B., Widger, W.R. and Cramer, W.A. (1984) FEBS Lett., 176, 239-244.

Hoganson, C.W. and Babcock, G.T. (1988) Biochemistry, 27, 5848-5855.

Hoganson, C.W. and Babcock, G.T. (1989) Biochemistry, 28, 1448-1454.

Holzapfel, W., Finkele, U., Kaiser, W., Oesterhelt, D., Scheer, H., Stilz, H.U. and Zinth, W. (1990) Proc. Natl. Acad. Sci. USA, 87, 5168-5172.

Horton, P.H. and Croze, E. (1977) Biochim. Biophys. Acta, 462, 86-101.

Horton, P.H. and Croze, E. (1979) Biochim. Biophys. Acta, 545, 188-201.

Hundal, T., Virgin, I., Styring, S. and Andersson, B. (1990) Biochim. Biophys. Acta, 1017, 235-241.

Ikeuchi, M., Yuasa, M. and Inoue, Y. (1985) FEBS Lett., 185, 316-322.

Inui, T., Kawamori, A., Kuroda, G., Ono, T. and Inoue, Y. (1989) Biochim. Biophys. Acta, 973, 147-152.

Jegerschöld, C. and Styring, S. (1991) FEBS Lett., 280, 87-90.

Jegerschöld, C., Virgin, I. and Styring, S. (1990) Biochemistry, 29, 6179-6186.

Joliot, P. and Joliot, A. (1979) Biochim. Biophys. Acta, 546, 93-105.

Joliot, P. and Joliot, A. (1981) FEBS Lett., 134, 155-158.

Jursinic, P., Warden, J. and Govindjee (1976) Biochim. Biophys. Acta, 440, 322-330.

Kawamori, A., Satoh, J., Inui, T. and Satoh, K. (1987) FEBS Lett., 217, 134-138.

Kim, H.D., Britt, R.D., Klein, M.P. and Sauer, K. (1990) J. Am. Chem. Soc., 112, 9389-9391.

Kirmaier, C., Gaul, D., DeBey, R., Holten, D. and Schenck, C.C. (1991) Science, 251, 922-927.

Klimov, V.V., Klevanick, A.V., Shuvalov, V.A. and Krasnovskii, A.A. (1977) FEBS Lett., 82, 183-186.

Klimov, V.V., Dolan, E. and Ke, B. (1980a) FEBS Lett., 112, 97-100.

Klimov, V.V., Dolan, E.D., Shaw, E.R. and Ke, B. (1980b) Proc. Natl. Acad. Sci. USA, 77, 7227-7231.

Kobayashi, M., Maeda, H., Watanabe, T., Nakane, H. and Satoh, K. (1990) FEBS Lett., 260, 138-140.

Kok, B., Forbush, B. and McGloin, M. (1970) Photochem. Photobiol., 11, 457-475.

Knaff, D.B. and Arnon, D.I. (1969) Proc. Natl. Acad. Sci. USA, 63, 956-962.

Kretschmann, H., Dekker, J.P., Saygin, O. and Witt, H.T. (1988) Biochim. Biophys. Acta, 932, 358-361.

Kretsinger, R.H. and Nockolds, C.E. (1973) J. Mol. Biol., 248, 3313-3326.

Kühlbrandt, W. and Wang, D.N. (1991) Nature, 350, 130-134.

Lavergne, J. (1987) Biochim. Biophys. Acta, 894, 91-107.

MacKinney, G. (1941) J. Biol. Chem., 140, 315-322.

Malkin, R. and Vänngård, T. (1980) FEBS Lett., 111, 228-231.

Mathis, P. (1990) Biochim. Biophys. Acta, 1018, 163-167.

Mathur, P., Crowder, M. and Dismukes, G.C. (1987) J. Am. Chem. Soc., 109, 5227-5233.

McDermott, A.E., Yachandra, V.K., Guiles, R.D., Cole, J.L., Dexheimer, S.L., Britt, R.D., Sauer, K. and Klein, M.P. (1988) Biochemistry, 27, 4021-4031.

McTavish, H., Picorel, R., and Seibert, M. (1989) Plant. Physiol., 89, 452-456.

Metz, J.G., Nixon, P.J., Rögner, M., Brudvig, G.W. and Diner, B.A. (1989) Biochemistry, 28, 6960-6969.

Meyer, B., Schlodder, E., Dekker, J.P. and Witt, H.T. (1989) Biochim. Biophys. Acta, 974, 36-43.

Michel, H. and Deisenhofer, J. (1988) Biochemistry, 27, 1-7.

Michel, H., Epp, O. and Deisenhofer, J. (1986) EMBO J., 5, 2445-2451.

Miyao, M., Murata, N., Lavorel, J., Maison-Peteri, B., Boussac, A. and Etienne, A.L. (1987) Biochim. Biophys. Acta, 890, 151-159.

Morden, C.W. and Golden, S.S. (1989) Nature, 337, 382-385.

Nagatsuka, T., Fukuhara, S., Akabori, K. and Toyoshima, Y. (1991) Biochim. Biophys. Acta, 1057, 223-231.

Nakatani, H.Y. (1984) Biochem. Biophys. Res. Comm., 120, 299-304.

Nakatani, H.Y., Ke, B., Dolan, E. and Arntzen, C.J. (1984) Biochim. Biophys. Acta, 765, 370-379.

Nanba, O. and Satoh, K. (1987) Proc. Natl. Acad. Sci. USA, 84, 109-112.

Nitschke, W. and Rutherford A.W. (1991) TIBS, 16, 241-245.

Nugent, J.H.A. and Evans, M.C.W. (1980) FEBS Lett., 112, 1-4.

Nugent, J.H.A., Diner, B.A. and Evans, M.C.W. (1981) FEBS Lett., 124, 241-244.

Nugent, J.H.A., Demetriou, C. and Lockett, C.J. (1987) Biochim. Biophys. Acta, 894, 534-542.

Nugent, J.H.A., Corrie, A.R., Demetriou, C., Evans, M.C.W. and Lockett, C.J. (1988) FEBS Lett., 235, 71-75.

Nugent, J.H.A., Telfer, A., Demetriou, C. and Barber, J. (1989) FEBS Lett., 255, 53-58.

Nugent, J.H.A., Doetschman, D. and MacLachlan, D.J. (1991) Biochemistry, submitted.

Ohad, I., Adir, N., Koike, H., Kyle, D.J. and Inoue, Y. (1990) J. Biol. Chem., 265, 1972-1979.

Okamura, M.Y., Isaacson, R.A. and Feher, G. (1979) Biochim. Biophys. Acta, 546, 394-417.

Okamura, M.Y., Satoh, K., Isaacson, R.A. and Feher, G. (1987) In: Progress in Photosynthesis Research (Biggins, J. ed.) 1, 379-381, Martinus Nijhoff, Dordrecht.

O'Malley, P. and Babcock, G.T. (1984) Biochim. Biophys. Acta, 765, 370-379.

Ort, D.R. and Good, N.E. (1988) TIBS, 13, 467-469.

Ottmeier, W., Masson, K. and Donner, A. (1988) FEBS Lett., 231, 259-262.

Pace, R.J., Smith, P., Bramley, R. and Stehlik, D. (1991) Biochim. Biophys. Acta, 1058, 161-170.

Paddock, M.L., Rongey, S.H., Feher, G. and Okamura, M.Y. (1989) Proc. Natl. Acad. Sci. USA, 86, 6602-6606.

Paddock, M.L., McPherson, P.H., Feher, G. and Okamura, M.Y. (1990) Proc. Natl. Acad. Sci. USA, 87, 6803-6807.

Petersen, J., Dekker, J.P., Bowlby, N.R., Ghanotakis, D.F., Yocum, C.F. and Babcock, G.T. (1990) Biochemistry, 29, 3226-3231.

Petrouleas, V. and Diner B.A. (1986) Biochim. Biophys. Acta, 849, 264-275.

Petrouleas, V. and Diner B.A. (1987) Biochim. Biophys. Acta, 893, 126-137.

Pfister, K., Steinback, K.E., Gardner, G. and Arntzen, C.J. (1981) Proc, Natl. Acad. Sci., 78, 981-985.

Prince, R.C., Tiede, D.M., Thornber, J.P. and Dutton, P.L. (1977) Biochim. Biophys. Acta, 462, 467-490.

Regitz, G. and Ohad, I. (1976) J. Biol. Chem., 251, 247-252.

Renger, G. (1976) FEBS Lett., 69, 225-230.

Renger, G. (1977) In: Bioenergetics of Membranes, 339-350, (Ed. Packer, L. et al.) Elsevier/North-Holland Biomedical Press.

Renger, G., Rutherford, A.W. and Völker, M. (1985) FEBS Lett., 185, 243-247.

Renger, G., Hagemann, R. and Fromme, R. (1986) FEBS Lett., 203, 210-214.

Renger, G., Kayed, A. and Oettmeier, W. (1987) Z. Naturforsch., 42c, 698-703.

Renger, G., Fromme, R. and Hagemann, R. (1988) Biochim. Biophys. Acta, 935, 173-183.

Renger, G., Messinger, J. and Fromme, R. (1989) Z. Naturforsch., 44c, 423-430.

Rögner, M., Nixon, P.J. and Diner, B.A. (1990) J. Biol. Chem., 265, 6189-6196.

Rögner, M., Chisholm, D.A. and Diner, B.A. (1991) Biochemistry, 30, 5387-5395.

Rutherford, A.W. (1989) TIBS, 14, 227-232.

Rutherford, A.W. and Mathis, P. (1983) FEBS Lett., 154, 328-334.

Rutherford, A.W. and Zimmermann, J.-L. (1984) Biochim. Biophys. Acta, 767, 168-175.

Rutherford, A.W., Heathcote, P. and Evans, M.C.W. (1979) Biochem. J., 182, 515-523.

Rutherford, A.W., Paterson, D.R. and Mullet, J.E. (1981a) Biochim. Biophys. Acta, 635, 205-214.

Rutherford, A.W., Mullet, J.E. and Crofts, A.R. (1981b) FEBS Lett., 123, 235-237.

Rutherford, A.W., Zimmermann, J.-L. and Mathis, P. (1984) In: Advances in Photosynthesis Research 1, 445-448 (Ed. Sybesma, C.) Martinus Nijhoff/Dr W.Junk publishers, The Netherlands.

Rutherford, A.W., Boussac, A. and Zimmermann, J.-L. (1991) New J. Chem., 15, 491-500.

Satoh, K., Hansson, Ö. and Mathis, P. (1990) Biochim. Biophys. Acta, 1016, 121-126.

Schatz, G.H., Brock, H. and Holzwarth, A.R. (1988) Biophys. J., 54, 397-405.

Schepler, K.L., Dunham, W.R., Sands, R.H., Fee, J.H. and Abeles, R.H. (1975) Biochim. Biophys. Acta, 397, 510-518.

Semin, B.K., Loviagina, E.R., Aleksandrov, A.Yu., Kaurov, Yu.N. and Novakova, A.A. (1990) FEBS Lett., 270, 184-186.

Shipton, C.A. and Barber, J. (1991) Proc. Natl. Acad. Sci. USA, 88, 6691-6695.

Sipos, T. and Merkel, R. (1970) Biochemistry, 9, 2766-2775.

Sopory, S.K., Greenberg, B.M., Mehta, R.A., Edelman, M. and Mattoo, A.K. (1990) Z. Naturforsch., 45c, 412-417.

Stemler, A. (1977) Biochim. Biophys. Acta, 460, 511-522.

Stemler, A. (1989) Plant Physiol., 91, 287-290.

Stemler, A. and Murphy, J.B. (1985) Plant Physiol., 77, 974-977.

Styring, S. and Rutherford, A.W. (1987) Biochemistry, 26, 2401-2405.

Styring, S. and Rutherford, A.W. (1988) Biochemistry, 27, 4915-4923.

Styring, S., Virgin, I., Ehrenberg, A. and Andersson, B. (1990) Biochim. Biophys. Acta, 1015, 269-278.

Sundby, C. (1990) FEBS Lett., 274, 77-81.

Sundby, C., Larsson, U.K. and Henrysson, T. (1989) Biochim. Biophys. Acta, 975, 277-282.

Svensson, B., Vass, I., Cedergren, E. and Styring, S. (1990) EMBO J., 9, 2051-2059.

Tae, G.-S., Black, M.T., Cramer, W.A., Vallon, O. and Bogorad, L. (1988) Biochemistry, 27, 9075-9080.

Takahashi, E. and Wraight, C.A. (1990) Biochim. Biophys. Acta, 1020, 107-111.

Takahashi, E. and Wraight, C.A. (1991) FEBS Lett., 283, 140-144.

Takahashi, Y. and Katoh, S. (1986) Biochim. Biophys. Acta, 848, 183-192.

Tamura, N. and Cheniae, G.M. (1987) Biochim. Biophys. Acta, 890, 179-194.

Tang, X-S. and Satoh, K. (1985) FEBS Lett., 179, 60-64.

Tang, X-S., Fushimi, K. and Satoh, K. (1990) FEBS Lett., 273, 257-260.

Thompson, L.K. and Brudvig, G.W. (1988) Biochemistry, 27, 6653-6658.

Thompson, L.K., Miller, A.-F, de Paula, J.C. and Brudvig, G.W. (1988) Israel J. Chem., 28, 121-128.

Thompson, L.K., Miller, A.-F., Buser, C.A., de Paula, J.C. and Brudvig, G.W. (1989a) Biochemistry, 28, 8048-8056.

Thompson, L.K., Blaylock, R., Sturtevant, J.M. and Brudvig, G.W. (1989b) Biochemistry, 28, 6686-6695.

Tiede, D.M., Prince, R.C. and Dutton, P.L. (1976) Biochim. Biophys. Acta, 449, 447-467.

Trebst, A. (1986) Z. Naturforsch, 41c, 240-245.

Trebst, A. and Draber, W. (1986) Photosynth. Res., 10, 381-392.

Trebst, A., Depka, B., Kraft, B. and Johanningmeier, U. (1988) Photosynth. Res., 18, 163-177.

Trebst, A., Depka, B. and Kipper, M. (1990) In: Current Research in Photosynthesis, vol I 2.217 (Baltscheffsky, M. ed.), Kluwer Academic Publishers, Dordrecht.

Turner, S., Burger-Wiersma, T., Giovannoni, S.J., Mur, L.R. and Pace, N.R. (1989) Nature, 337, 380-382.

van Gorkom, H.J. (1974) Biochim. Biophys. Acta, 347, 439-442.

van Mieghem, F.J.E., Nitschke, W., Mathis, P. and Rutherford, A.W. (1989) Biochim. Biophys. Acta, 977, 207-214.

van Mieghem, F.J.E., Satoh, K. and Rutherford, A.W. (1991) Biochim. Biophys. Acta, 1058, 379-385.

van Rensen, J.J.S., Tonk, W.J.M., and de Bruijn, S.M. (1988) FEBS Lett., 226, 347-351.

Vass, I and Styring, S. (1991) Biochemistry, 30, 830-839.

Vermaas, W.F.J. and Rutherford, A.W. (1984) FEBS Lett., 175, 243-248.

Vermaas, W.F.J., Rutherford, A.W. and Hansson, Ö. (1988) Proc. Natl. Acad. Sci. USA, 85, 8477-8481.

Virgin, I., Salter, H., Ghanotakis, D.F. and Andersson, B. (1991) FEBS Lett., 287, 125-128.

Völker, M., Renger, G. and Rutherford, A.W. (1986) Biochim. Biophys. Acta, 851, 424-430.

Warden, J.T., Blankenship, R.E. and Sauer, K. (1976) Biochim. Biophys. Acta, 423, 462-478.

Wasielewski, M.R., Johnson, D.G., Seibert, M. and Govindjee (1989) Proc. Natl. Acad. Sci. USA, 86, 524-528.

Whitmarsh, J. and Cramer, W.A. (1978) Biochim. Biophys. Acta, 501, 83-93.

Widger, W.R., Cramer, W.A., Hermondson, M., Meyer, D. and Gullifor, M. (1984) J. Biol. Chem., 259, 3870-3876.

Widger, W.R., Cramer, W.A., Hermondson, M. and Herrmann, R.G. (1985) FEBS Lett., 191, 186-190.

Williams, J.C., Steiner, L.A., Ogden, R.C., Simon, M.I. and Feher, G. (1983) Proc. Natl. Acad. Sci. USA, 80, 6505-6509.

Witt, H.T. (1991) Abstract, The Biochemical Society 37th Harden Conference: The Molecular And Structural Basis Of Regulation In Photosynthesis.

Woese, C.R. (1987) Microbiol. Rev., 51, 221-271.

Wraight, C.A. (1978) FEBS Lett., 93, 283-288.

Yamaguchi, N., Takahashi, Y. and Satoh, K. (1988) Plant Cell Physiol., 29, 123-129.

Yocum, C.F. (1991) Biochim. Biophys. Acta, 1059, 1-15.

Yocum, C.F., Yerkes, C.T., Blankenship, R.E., Sharp, R.R. and Babcock, G.T. (1981) Proc. Natl. Acad. Sci. USA, 78, 7507-7511.

Zimmermann, J.-L. and Rutherford, A.W. (1984) Biochim. Biophys. Acta, 767, 160-167.

Zimmermann, J.-L. and Rutherford, A.W. (1986a) Biochim. Biophys. Acta, 851, 416-423.

Zimmermann, J.-L. and Rutherford, A.W. (1986b) Biochemistry, 25, 4609-4615.